Hierarchical Decentralized Control for Enhanced Stability of Large-Scale Power Systems

Srivats Shukla

Dissertation submitted to the Faculty of the
Virginia Polytechnic Institute and State University
in partial fulfillment of the requirements for the degree of

Doctor of Philosophy
in
Electrical Engineering

Lamine Mili, Chair
Robert Broadwater
A.A.(Louis) Beex
Daniel Stilwell
Michael von Spakovsky

Dec 12, 2016
Falls Church, Virginia

Keywords: Power Systems, Decentralized Control, Voltage Stability, Rotor Angle Stability, Lyapunov's Second Method, Stochastic Regression

Hierarchical Decentralized Control for Enhanced Stability of Large-Scale Power Systems

Srivats Shukla

ABSTRACT

Due to the ever-increasing penetration of distributed generation units connected to the power distribution system, electric power systems, worldwide, are undergoing a paradigm shift with regards to system monitoring, operation and control. We envision that with the emergence of 'active' distribution systems consisting of 'prosumers' and localized energy markets, decentralized control methods in power systems are gaining a growing attention among power researchers. Traditionally, two main types of control schemes have been implemented in power systems: (a) wide-area monitoring based centralized control, and (b) local measurement based primary (machine) level control. By contrast, decentralized control schemes based on local monitoring and control of strategically-determined subsystems (or 'areas') of a large-scale power system are not used. The latter control schemes offer several advantages over the former, which include more flexibility, simplicity, economy and scalability for large-scale systems. In this dissertation, we summarize our research work on hierarchical and decentralized control techniques for the enhancement in a unified manner of voltage and rotor angle stability in large-scale power systems subject to large (e.g., short circuits) and small (e.g., small load changes) disturbances. We study system robustness by calculating local stability margins. We derive decentralized control laws that guaranty global asymptotic stability by applying Lyapunov's second method for interconnected systems. Furthermore, we argue that the current centralized control structure must only play a supervisory control role at a higher (tertiary) hierarchical level by processing the decisions taken by the regional control entities regarding the stability/instability of the system. This ensures system-wide situational awareness while minimizing the communication bandwidth requirements. We also develop a multi-agent based framework for this hierarchical control scheme. Finally, we compare different communication protocols using simulation models and propose an efficient communication network design for decentralized control schemes. This work, in principle, motivates the development of fast stability analysis which, in the future, may also account for the non-linear coupling that exist between machine rotor angles and bus voltages in power system models. As a future work, we propose the use of statistical techniques like random-effects regression and saddlepoint approximation method to reliably estimate the type-I and type-II probability errors in the proposed hierarchical, decentralized control decision process.

Hierarchical Decentralized Control for Enhanced Stability of Large-Scale Power Systems

Srivats Shukla

GENERAL AUDIENCE ABSTRACT

In the present research work, we have proposed a decentralized, hierarchical control scheme for large-scale, interconnected power systems. Using Lyapunov's second method for interconnected systems, we have derived *decentralized* control laws for control devices which ensure global asymptotic stability of weakly interconnected power systems. The decentralized control schemes have several advantages over centralized ones. For instance, the former approaches lead to a reduction of dimensionality in terms of both modeling and controlling the state variables of a system. One of the major contributions of this research work is the reduction of the dimensionality of the energy function and of the regression models used to determine the control laws, which results from the non requirement of exchanging information between control areas or of sending all the measurements to a central controller. Hence, the proposed scheme also yields smaller communication requirements than those of completely centralized wide-area controllers, while offering a better situational awareness. Similar decentralized control schemes are commonly used in robotic, transportation and surveillance systems.

To Amma, Papa and Supriya

Acknowledgments

As a graduate student working on my assignments and writing research papers, my faculty members, friends, and family gave immense technical and moral support. The one person who is actually responsible for any and all of my success as a researcher is my thesis adviser, Professor Lamine Mili. He constantly 'raised the bar' to make me a better researcher. Not only did Prof. Mili inculcate in me the habit of hunting for challenging, new research ideas, but also, he made me improve the way I would communicate my ideas, both in written and oral expressions. I am highly indebted to him in bringing forth the idea of 'decentralization' at the beginning of my research, by giving practical examples about the *modus operandi* of soldiers in a military. I would also like to acknowledge the feedback of Dr. Robert Broadwater, Dr. A.A. (Louis) Beex, Dr. Michael von Spakovsky and Dr. Daniel Stilwell during the committee meetings. Their rigorous questioning of this research work helped to strengthen the ideas presented in this dissertation. The feedback of anonymous reviewers of the conference and transactions papers was another great source of improvement of our research ideas.

I also had the chance to work closely with Dr. Sandeep Shukla's group on Cyber Physical Systems' Security, and would like to acknowledge the support of his group on the work related to microgrid communications. The Smarter Energy Group at IBM Watson where I have interned for more than a year, helped me rediscover my strengths as a researcher, without which crossing the finishing line would have been very hard. I would also like to specifically mention the names of some other PhD students at Virginia Tech, namely Marcos Netto, Chetan Mishra, Ahmad Tbaileh, Junbo Zhao, Quinny Chen, and Ibrahima Diagne, who have helped me in carrying out simulations, changing the diagrams in my research papers, or even helped me to obtain a copy of a software or a book. Last but not the least, a special acknowledgment for the great administrative staff members who have been helping all the students enrolled in the NCR to succeed in their course of study. Special thanks go to Cindy and Roxanne (NCR ECE/CS Administrative & Program Specialists), Jeny (CGEP), Debbie (Library), Jim (VBS), Neil (IT), Barbara (Facilities), Bronwen, Debbie, Corinne and Jessica (GSSO).

Contents

List of Figures

List of Tables

Chapter 1

Introduction

Power system static security analysis has traditionally been carried out in an offline mode, under the assumption that future operating conditions along with probable contingencies such as line and generator outages could be forecasted reasonably well. This analysis supposes the availability of reliable load forecasting tools, dispatchable generation, and an exhaustive list of credible contingencies. But with the increasing penetration of intermittent resources connected to the power distribution systems, making the latter active (responsive) systems, the prediction of net demand and circuit reconfigurations has become more uncertain. As a result, online dynamic security assessment techniques are being developed, which rely on the availability of (1) high speed, time-stamped measurements of the state variables, and (2) accurate model of the interconnected system, to correctly compute system stability margins for overall security assessment. The online security/stability analysis schemes reduce the dependency on accurate forecasting of system operating conditions, due to the reliance on real-time measurements, but introduce another challenge of accurately predicting system stability margins in near-real time, giving the operator (or an automated agent) enough time to trigger appropriate control actions [1]. Refer to Fig. 1.1. Clearly, the online stability assessment approach is of a centralized nature, since it is conducted by a single piece of software processing all the measurements at a single location. Such centralized processing necessitates complex, fast and accurate computational capabilities, even when the distinct contingency scenarios are parallelized. Furthermore, a centralized stability assessment scheme requires highly reliable software/hardware infrastructure due to a single point of failure.

Evidently, power system dynamic security analysis involves at its core the stability analysis of an interconnected (or global) power system. Hence, any control scheme, whether centralized or decentralized, aims at enhancing the global stability of the system. It should be noted that power system stability has been classified as frequency, voltage and rotor angle stability [2]. Global stability in this context essentially stands for asymptotic stability of the three aforementioned types. As a standard practice, hierarchical, decentralized methods have been implemented for frequency instability detection and control [3]. By contrast, rotor angle

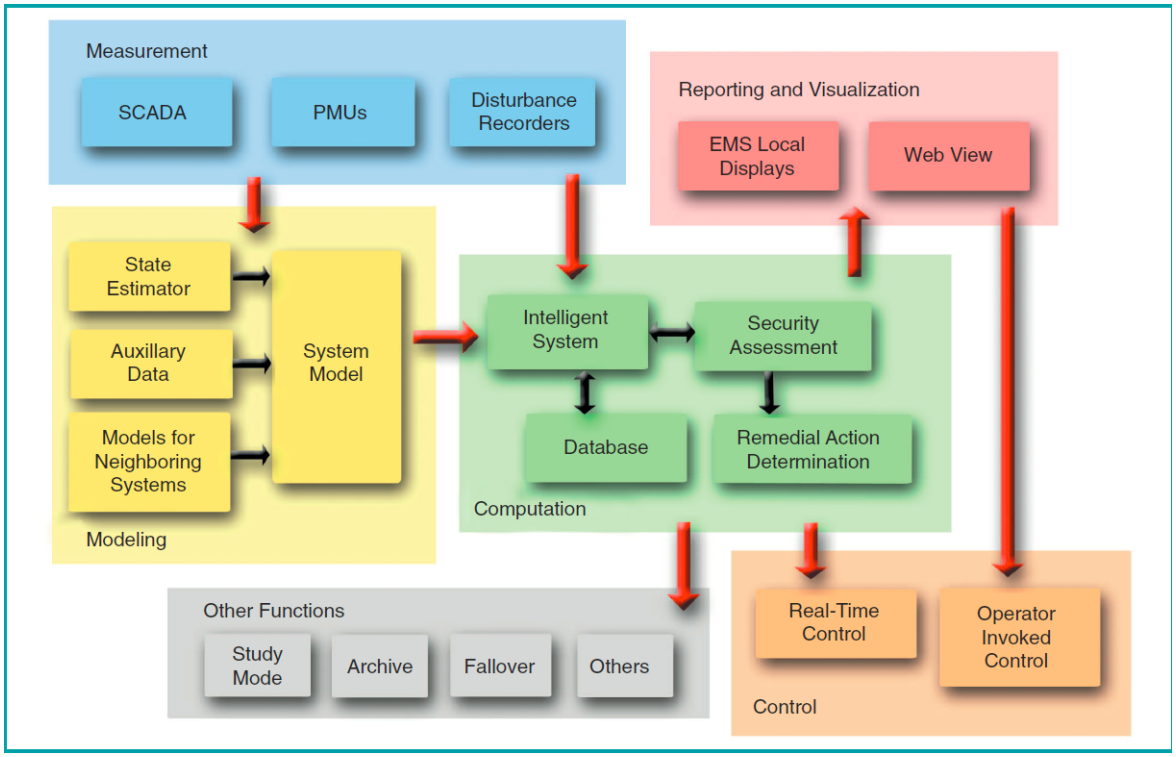

Figure 1.1: Block Diagram of an Online Security Assessment Tool. Taken from : [1]

and voltage instability detection and control schemes are implemented either at the local machine level (i.e., primary control) or centralized at the global system level (i.e., secondary and tertiary control) depending on the measurement configuration [4]. The primary level control methods are designed to respond quickly, for instance in voltage stability, to a local state variable exceeding thresholds, and not for managing system level stability margins. On the other hand, centralized methods are responsible for controlling system stability margins; hence, they are complex and uneconomical. This motivates us to explore the application of decentralized methods for rotor angle and voltage stability.

Decentralized and hierarchical control schemes, which have found application in large-scale dynamical systems such as urban traffic networks and robotic systems, provide many advantages, including enhanced reliability, decreased computational complexity, and economic efficiency [5]. In contrast to the aforementioned centralized control schemes, they are applied in large-scale systems, which typically consist of multiple interconnected dynamical sub-systems, wherein each subsystem is capable of taking its control decisions locally, based on local measurements [Ch.6, 6]. Electrical power grids are also composed of coupled subsystems due to the presence of localized generation and loads in certain subregions of the network. These subregions are typically interconnected with each other via high impedance transmission tielines. Therefore, we can conceptualize a decentralized, hierarchical stability analysis and control structure, wherein, different weakly-coupled subsystems are moni-

tored and controlled independently using secondary controls; coordination between them are achieved at a central, tertiary level based on the decisions taken by regional controllers and telemetered to higher level. Note that this hierarchical control may result in the increase of investment made by utilities to maintain area-wise operating centers and supervising operators. Hence, decentralized control schemes for such large-scale system are usually implemented via a Multi-Agent System (MAS) framework [7],[8]. Bearing this in mind, we outline the objectives of this research next.

1.1 Research objectives

Decentralized control methods have been discussed with regard to large-scale dynamic systems in general, but there is a lack of studies specifically on their applications in power systems. Hence, the goal of the present research work is to develop a hierarchical, decentralized scheme for voltage and rotor angle stability enhancement in power systems. To that end, we address key issues related to the system characteristics (e.g. weak or strong coupling amongst subsystems), and the sufficiency of these schemes under specific disturbances.

The first objective of this research is to develop a new process that allows us to identify coupled subsystems of a large-scale power system, which can be monitored and controlled independently. The basis of this process lies in the theory of perturbation methods [5],[9], which is discussed briefly here. A large-scale dynamical system ($\mathbf{X}$) is assumed to be composed of N dynamical subsystems with state vectors ($\underline{x}_1, \underline{x}_2 ... \underline{x}_N$), each of which may be controlled independently. This can be mathematically represented as,

$$\begin{bmatrix} \dot{\underline{x}}_1 \\ \dot{\underline{x}}_2 \\ \vdots \\ \dot{\underline{x}}_N \end{bmatrix} = \begin{bmatrix} \mathbf{A}_{11} & \epsilon\mathbf{A}_{12} & ...\epsilon\mathbf{A}_{1N} \\ \epsilon\mathbf{A}_{21} & \mathbf{A}_{22} & ...\epsilon\mathbf{A}_{2N} \\ \vdots & & \\ \epsilon\mathbf{A}_{N1} & \epsilon\mathbf{A}_{N2} & ...\mathbf{A}_{NN} \end{bmatrix} \begin{bmatrix} \underline{x}_1 \\ \underline{x}_2 \\ \vdots \\ \underline{x}_N \end{bmatrix} + \begin{bmatrix} \mathbf{B}_{11} & \mathbf{0} & ...\mathbf{0} \\ \mathbf{0} & \mathbf{B}_{22} & ...\mathbf{0} \\ \vdots & & \\ \mathbf{0} & \mathbf{0} & ...\mathbf{B}_{NN} \end{bmatrix} \begin{bmatrix} \mathbf{u}_1 \\ \mathbf{u}_2 \\ \vdots \\ \mathbf{u}_N \end{bmatrix} \tag{1.1}$$

where ϵ denotes the strength of coupling between the individual groups of state variables (or subsystems). These subsystems will also be denoted as 'control areas' in this dissertation. One of the objectives of this research is to determine these independently controllable subsystems. Furthermore, we identify the scenarios under which the coupling parameter, ϵ, although small, is significant, and under which scenarios it will tend to zero ($\epsilon \to 0$), as it is done in regular perturbation methods.

The second objective of this research is to investigate various models for estimating the local rotor angle and voltage stability margins from local measurements. Here the term 'local' indicates that the stability margin of a control area k is estimated based on the measurements of the state variables that are available in that area $\underline{x}_k$. We implement two different models for estimating rotor angle and voltage stability margins (subsequently, two different decentralized control laws), even though there is a strong coupling in the voltage

and rotor angles within each subsystem. This distinction is made on the basis that these instabilities are triggered by different types of disturbances, and the consequent instability can be controlled by affecting one or the other principal system variable [2].

The third objective of this research is to derive decentralized control laws, that ensure the global asymptotic stability under small or large disturbances. These control laws are based on the local stability margins and they are applied to different control devices (capacitor banks, FACTS based TCSCs) which are assumed to have been pre-installed in each control area. These control laws determined for local control devices must ensure global asymptotic stability. As mentioned before, each of the control areas shall be managed by a group of separate software agents. As a part of this research, we describe the control-agent behaviors, their coordination and communication requirements at the regional and global levels.

The fourth objective of this research is to address the detrimental impact that the various uncertainties may have on the decentralized control decision process, and hence, on the control decisions. The uncertainities may originate from (i) the control area boundaries under different operating conditions, and (ii) the models of stability margins based on the noisy sensor measurements. These uncertainties may lead to inadvertent erroneous control decisions; for instance, certain control devices may act even when there is no instability (false-alarms) and certain devices may fail to act when the system is unstable (mis-detection). The detrimental effect of these uncertaintites may be intensified by the fact that most of the decisions are taken by automated software agents, without any interference of human operators. Thus one of the aims of this research is to quantify the probabilities of errors in control decisions at both local and global system levels.

In the next section, we carry out a brief literature review related to the subject matter addressed in this dissertation.

1.2 Literature review

In the present research work we have proposed a decentralized control scheme to enhance the stability of large scale power systems. In our work, we have taken advantage of several techniques and tools discussed in the literature in automatic control, signal processing, software agent systems, and Bayesian statistics. We provide a brief glossary of some key references from these diverse fields.

1.2.1 Decentralized control methods for large scale dynamical systems

Sandell *et.al.* [5] surveyed the literature in the early 80s, wherein they discussed some fundamental methods for model simplification and stability of large-scale dynamical systems.

They highlighted perturbation methods for simplifying the system model in case of strongly and weakly coupled systems. Furthermore, they provided a survey of the decentralized control methods based on the Lyapunov method for interconnected systems, the input-output methods and certain decentralized stochastic control methods. The Lyapunov method for interconnected systems, which is one of the methods we have leveraged in this research, was introduced by Bailey in 1965 [10]. Bailey proved sufficient conditions for asymptotic stability of interconnected systems using the Lyapunov's energy function approach. However, the authors in [5] and [10] discuss stability of interconnected systems without describing any methods for determining the coupling parameters in strongly or weakly coupled systems. This is precisely what Kokotović *et.al.*. [9],[11] have done; indeed, they introduced various singular perturbation methods that account for the coupling parameter in interconnected systems. The researchers also discussed the aggregation and control when these dynamical subsystems exhibit strong coupling and a phenomena called *time-scale decomposition* occurs, to account for the existence of fast and slow modes.

The topic of decentralized data fusion or decentralized inference has been discussed extensively in the signal processing literature [12]-[17], and has found applications in radar systems and wireless sensor networks. The latter research has been focused on enhancing the efficiency and reliability of a detection process using decentralized decision fusion. Researchers have discussed the reduction of the communication bandwidth and the optimization of the accuracy of a decision rule under noisy information channels [12]-[14]. Bayesian approaches have been used for optimizing the global error probabilities, assuming a priori knowledge of local sensor error probabilities [15] under different types of configuration of sensor networks (parallel, series, hybrid). Kassam and Poor [16] have outlined robust approaches for optimizing global error probabilities under absence of a priori information. Statistical approaches have been used to accurately quantify the probabilities of the decision errors at different hierarchical levels. Aldosari and Moura [17] survey the literature for existing approaches and propose saddlepoint approximation methods for estimating the decision error. They show that the latter technique, based on Edgeworth expansion, is superior to the existing techniques like normal approximation when it comes to estimating tail probabilities for thick-tailed probability distributions.

Decentralized control of dynamical systems using a Multi-Agent system framework has been studied by computer scientists. For instance, Jennings in [18] proposed a theoretical model under which software agents can cooperate under the notion of 'shared responsibility' to achieve a shared goal. Another example comes from the robotics and automation literature. For instance Feddema *et.al.* [19] used decentralized Lyapunov control for stability of formation and motion in cooperative robotic vehicles. Although several stability assessment and control methods have been discussed for large- scale power systems (which is discussed next), a direct implementation of decentralized control schemes like in [19] is missing. This will constitute precisely the central theme of this research.

1.2.2 Stability assessment and control methods in power systems

Power system voltage and dynamic stability assessment is a critical component of online security assessment. Morison et.al. [1] reviewed online security assessment in power systems while the joint IEEE/CIGRE task force on stability [2] compared power system security assessment with system reliability and stability. Santo et. al. [20] explored the application of distributed architectures for security assessment of power systems. But the latter study is limited to the parallelization of the algorithms that implements different contingency scenarios and data collection; it does not address the decentralization of system stability monitoring and control itself. Under the purview of online security assessment, several methods have been proposed for centralized stability monitoring and control.

Glavic and Van Cutsem [4] provided a literature review on different voltage instability detection schemes and classified them according to the required measurement configuration. They highlighted several 'wide-area' monitoring schemes that rely on synchronized (e.g. [21],[22]) or non-synchronized (e.g. [23],[24]) measurements collected from the entire system and processed at a central location to assess the system voltage stability. A class of centralized online voltage stability methods is dedicated to monitoring the available reactive reserves in the system to estimate the voltage stability margin [24]-[26]. Van Cutsem [25] gave a practical definition of *reactive power margins* in terms of the difference of maximum reactive load consumption in an area with respect to the current operating point. Based on these principles, Bao *et. al.* [24] and later Leonardi and Ajjarapu [26] proposed regression-based models that relate the voltage stability margins to the reactive power reserves. All the wide-area stability assessment and control schemes discussed in [21]-[26] focused only on centralized schemes, which require a large communication bandwidth; they are designed to address long-term voltage stability problems.

Decentralized assessment and control of voltage instabilities has received the attention of power utilities fairly recently. As of now, only few implementations of such schemes have been performed around the world. For instance, hierarchical voltage control schemes have been adopted by the French and the Italian utilities [27],[28], and very recently contemplated by Spanish utilities [29] and Southern California Edison (SCE) in the US [30]. They are primarily dedicated to monitoring and controlling voltage violations, instead of methodically assessing the local stability margins; consequently, they hence do not guarantee system security. Very recently, Mehrjerdi *et. al.* [31],[32] proposed a design of fuzzy logic controllers for decentralized coordinated control of 'partitioned' power systems. The partitions are found using a graph-theoretic analysis while each of them is controlled by a local fuzzy logic controller, coordinating their actions with other area controllers. These partitions are derived on the basis of graph theoretic principles, without considering the reactance of long transmission lines between them. It should be noted here that the reactance of transmission lines directly effects the ability to transmit the reactive power between two areas and hence the regional voltage stability. Moreover, in the latter scheme, the fuzzy logic controllers take actions depending on the sensitivity of voltage to change in load (or disturbance) without

focusing on stability margins or availability of reactive power in a partition.

Wide-area security and stability assessment schemes have also been implemented for rotor angle instabilities. For instance, Kamwa *et. al.* [33] developed a dynamic security assessment method for the Hydro-Québec system, which is composed of 9 control areas. Following a dynamic disturbance, the deviation of the state variables of each of these control areas from the system's Center of Inertia (CoI) is estimated and then utilized to calculate a wide-area stability index (WASI). The proposed stability index (WASI) is a centralized metric for system security. In the discussed voltage and rotor angle control schemes, no mechanisms were proposed to damp in a unified way both transient rotor angle and voltage instabilities. One exception is the work of Guo *et al.* [33], who proposed a global control using energy functions to damp transient angle and voltage instabilities at an individual synchronous machine level, not at the system level. Similarly, Ghandhari [47] and Noroozian *et al.* [35] derived control laws on FACTS devices to damp transient oscillations in power systems using an energy function approach. The latter work does not consider decentralized control schemes as proposed by Bailey in [10].

As explained in the research objectives section, in the present research work we leverage the research work in decentralized control of large scale dynamical systems to propose decentralized control of voltage and rotor angle stability in power systems.

1.3 Key results

In this dissertation we present our results related to the implementation of a decentralized, hierarchical control scheme for the improvement of rotor angle and voltage stability, following a disturbance in a large-scale interconnected power system. Firstly, we show that the state variables related to rotor angles and bus voltages in a large-scale power system can be grouped together as interconnected subsystems based on time-scale decomposition or singular-perturbation methods. The interconnection or 'coupling' amongst subsystems is determined via the relative electrical distance between different buses in the power system. Based on the singular perturbation approach, we show that the control area determination technique as proposed by Schlueter *et.al.*[52] for voltage controllability analysis is equivalent to the coherent group analysis in the case of dynamic state variables like rotor angles proposed by Chow [36].

Secondly, we use the Lyapunov's second method for interconnected systems to derive control laws of control devices that ensure the global asymptotic stability after large disturbances. The control laws derived using this method ensure the damping of local oscillations as well as the oscillations caused by the disturbances in the interconnected subsystems. One of the important contributions of this work is that the proposed control schemes achieve global asymptotic stability using the measurements of only the local state variables in the respective control area. This is advantageous because the prior schemes are based on the measurements

taken from all the interconnected areas. Hence, the proposed scheme requires less overall infrastructure investment, since the increase in the number of local measurement units is compensated by the decrease in the communication bandwidth that is required for the prior schemes. We also found in our simulations that the rate of damping of oscillations is effected by the proximity of a control device to the control area boundary. The derived control laws can be easily implemented on a FACTS based control device. We take a specific example of Thyristor Controlled Series Capacitors to perform simulations on a standard 9-bus system.

Thirdly, we propose decentralized enhancement of voltage stability, following a small disturbance, by online estimation of voltage stability margins (VSM) based on reactive power reserve (RPR) monitoring in each control area. The relationship between VSM and RPRs in each control area is modeled using multi-linear regression models. Later, use of random coefficient regression models is suggested for accurately quantifying uncertainty in control decisions. The decentralized, hierarchical control scheme is implemented under a Multi-Agent System (MAS) framework.

Fourthly, we compare different communication protocols using simulation based models for the discussed framework. We propose a communication network design which is efficient under normal and stressed conditions of power system operation. In our research, we compared various communication protocols for certain performance metrics like throughput rate, retransmission attempts, and packet drops under stressed conditions and suggest the protocols which are most suited under such 'harsh' environments.

1.4 Organization of thesis

This dissertation is organized in two parts. Chapter 2 discusses the state-of-the-art methods in decentralized control and power system stability assessment while Chapters 3 to 5 provides a summary of three research papers on the implementation of multi-agent based decentralized control for stability enhancement of power systems.

In the first part of the second chapter we discuss methods from the existing literature on decentralized control methods for dynamical systems. We also highlight the principles behind hierarchical decentralized control and data fusion, and related probability of errors in control decisions at different hierarchical levels. In addition, we highlight some techniques for estimation of those errors. Subsequently, in the second part of this chapter we give a general background on the power system stability problem. We highlight two types of instabilities that have been studied during the course of this research, namely the transient (rotor angle) instability and the voltage instability. Some methods used to evaluate these instabilities are discussed. A review of two important methods is outlined next: 1. The energy (Lyapunov) function based approaches for estimating transient stability margins and the control laws for FACTS devices for damping transient oscillations. 2. A regression based method for modeling voltage stability margins as a function of the reactive reserves in the system and

related sensitivity based control actions.

In the third chapter, we briefly discuss some methods to accurately approximate the uncertainty in control decisions in a hierarchical control scheme. We outline statistical methods like random coefficient regression and saddlepoint approximations to accurately approximate the distributions of certain random variables. These distributions can be used to identify the error probabilities of first and second kind in control decisions.

In the fourth chapter, we discuss the implementation of decentralized, hierarchical scheme for voltage and rotor angle stability enhancement in large scale power systems. We present a technique aimed at determining weakly coupled coherent areas in power systems. Subsequently, we propose a technique for decentralized secondary voltage instability control scheme based on monitoring reactive power reserves, and decentralized rotor angle instability control based on the Lyapunov's second method for interconnected systems. We derive control laws for FACTS devices. Moreover, we highlight a tertiary control technique based on the 'fusion' of partial information received from the secondary controllers.

In the fifth chapter, we highlight various applications of Multi-Agent Systems (MAS) in power engineering. We study the specific advantages that MAS bring to power engineering control applications. Subsequently, we outline the recommended FIPA standards on Agent Management Systems and Agent Communication Languages (ACLs). In a latter part of the chapter we summarize a case study on communication infrastructure issues in MAS applications for control of stressed power systems.

In the sixth chapter, we address another direction of research, wherein we use statistical techniques to determine the error probabilities in hierarchical control decisions. For the secondary (or local) control decisions we use the well established technique of stochastic parameter regression for deriving the distributions of local stability margins, and subsequently for calculating local error probabilities. For the tertiary (or the global) control decisions, we describe the Saddlepoint approximation technique, which is an accurate method for approximating the tail probabilities of distributions whose first and second moments exist.

In the seventh chapter, we discuss the main simulation results of the proposed decentralized, hierarchical control schemes on IEEE test-beds. We also describe some of the inferences that we derived from these simulations. Furthermore, we conclude by highlighting the advantages of the proposed methods, and suggesting scope of future research work.

Chapter 2

Stability of Large Scale Dynamical Systems.

2.1 Introduction

In the following chapter, we review some of the techniques that have been implemented for decentralized control of large scale dynamical systems. This chapter is divided into two parts; the first part discusses the concepts underlying strong and weak coupling in the interconnected systems, and the necessary and sufficient conditions for asymptotic stability, post a disturbance. The second part of the chapter discusses some of the existing methods for stability enhancement in power systems, which are a specific type of large-scale interconnected systems. The latter part of the chapter highlights the theoretical reasoning behind classifying power systems as weakly coupled (or loosely interconnected) systems, based on the reactance of transmission lines. Furthermore, it outlines some of the existing control methods for mitigating instabilities, which are essentially centralized.

2.2 Decentralized techniques for control of interconnected dynamical systems

As mentioned before, in this part of the chapter we first discuss the *perturbation* methods [9],[11] to classify interconnected dynamical systems into strongly or weakly coupled systems. Subsequently, we outline (a) energy-function and (b) input-output type approaches for ensuring their asymptotic global stability.

2.2.1 Perturbation methods in large-scale interconnected systems

Perturbation theory in mathematics deals with the solution of a problem, which can be approximated by a structurally simpler problem; where an exact solution of the latter exists. The structurally simpler problem may be solvable, for instance, because it is linear or easily integrable. In the control theory, perturbation methods have been often used to model complex dynamical systems. Assume that the dynamical model of the actual system represents a more complex structure but it can be be modeled as a perturbation on a system of a simpler structure. Here the perturbation term, say ϵ, is used to model the difference between the two systems. Furthermore, perturbation methods have been also used to represent aggregation in large-scale, interconnected, dynamical systems by Sandell *et.al.* in [5]. In the latter research work, the authors have classified the large-scale dynamical systems as *weakly* and *strongly* coupled systems based on the role of the perturbation term in the system model. Here coupling can be roughly understood as the *strength* of interconnection between two subsystems.

2.2.1.1 Weakly Coupled Dynamical Systems

Lets consider the system illustrated in Fig. 2.1, which is composed of two coupled subsystems ($\underline{x}_1$ and $\underline{x}_2$). Also assume that the system model is represented by,

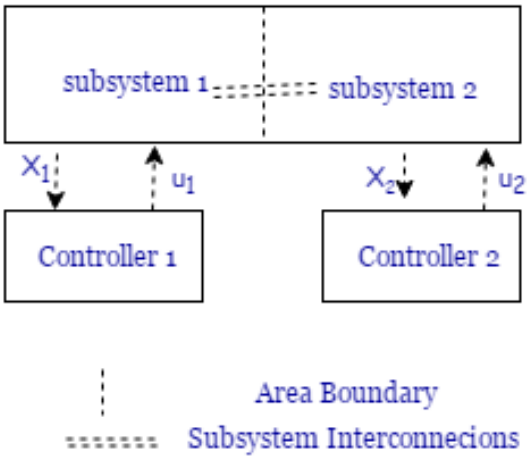

Figure 2.1: Decentralized control of a system with two weakly coupled subsystems

$$\begin{bmatrix} \dot{\underline{x}}_1 \\ \dot{\underline{x}}_2 \end{bmatrix} = \begin{bmatrix} \mathbf{A}_{11} & \epsilon\mathbf{A}_{12} \\ \epsilon\mathbf{A}_{21} & \mathbf{A}_{22} \end{bmatrix} \begin{bmatrix} \underline{x}_1 \\ \underline{x}_2 \end{bmatrix} + \begin{bmatrix} \mathbf{B}_{11} & \mathbf{0} \\ \mathbf{0} & \mathbf{B}_{22} \end{bmatrix} \begin{bmatrix} \mathbf{u}_1 \\ \mathbf{u}_2 \end{bmatrix} \tag{2.1}$$

wheer $\epsilon \geq 0$ is a perturbation or 'coupling' parameter, and $\mathbf{u}_1$, $\mathbf{u}_2$ are the external inputs to these subsystems. The state transition matrix $\mathbf{A}$ is composed of (a) $\mathbf{A}_{11}$ and $\mathbf{A}_{22}$, the block diagonal matrices representing the state transition matrices of individual subsystems, and

(b) $\mathbf{A}_{11}$ and $\mathbf{A}_{12}$ are the off-diagonal matrices representing the interconnections. Sandell *et.al.* [5] observe that the weak coupling is a case of *non-singular perturbation* where ϵ shows up in the right hand side of the system differential equation. In such a case the two subsystems have relatively closer time constants. It can also be seen that ϵ multiplied by the off-diagonal terms of the system matrix determine how the trajectory of state variables in the vector $\underline{x}_1$ are effected by those of $\underline{x}_2$ and vice-versa. It is obvious, that for $\epsilon = 0$ the system decouples into independent subsystems, each of which represents an approximate aggregated model of a group of state variables. There are two direct consequences of this assumption: (a) the dimensionality of the system is decreased which reduces the computations associated with control system design, and system simulations, and (b) a completely decentralized control structure can be designed for this type of system. But care should be taken that a decentralized control design by assuming complete decoupling, while the ϵ parameter is not insignificant, leads to a loss in the performance of controllers. The latter situation arises when one subsystems' output effect the other via the interconnections. If the loss of performance is known to be significant, then it is best to design control laws using Lyapunov's second law for interconnected systems as discussed in a later subsection. Chow [36, Chap.3] outlines a method to determine the coupling parameter for interconnected power systems, which will be discussed in detail later.

2.2.1.2 Strongly Coupled Systems

Strong coupling indicates that the subsystems may not be decoupled, as there is a direct relationship between the sets of state variables corresponding to different subsystems. The coupling parameter may show up on the left hand side in the system model, as depicted in (2.2). Assume a system composed of two subsystems whose model is given as,

$$\begin{bmatrix} \dot{\underline{x}_1} \\ \epsilon\dot{\underline{x}_2} \end{bmatrix} = \begin{bmatrix} \mathbf{A}_{11} & \mathbf{A}_{12} \\ \mathbf{A}_{21} & \mathbf{A}_{22} \end{bmatrix} \begin{bmatrix} \underline{x}_1 \\ \underline{x}_2 \end{bmatrix} \tag{2.2}$$

where $\epsilon \geq 0$ is the perturbation parameter, which represents the time-constant of the subsystem $\underline{x}_2$, and rest of the symbols are same as in (2.1). In the above representation, the subsystem $\underline{x}_1$ is assumed to exhibit slower dynamics and $\underline{x}_2$ exhibits relatively faster dynamics. Under the condition that dynamics of $\underline{x}_2$ are fast enough, and that the evolution of the state variables of this subsystem can be approximated as a transient as compared to the time-scales of the subsystem $\underline{x}_1$, we can approximate the perturbation parameter as $\epsilon = 0$. The latter obviously requires the assumption of the stability of matrix $\mathbf{A}_{22}$. Under such assumptions the dynamical system equations can be reduced in the form,

$$\underline{x}_2 = -\mathbf{A}_{22}^{-1}\mathbf{A}_{21}\underline{x}_1 \tag{2.3}$$

and by substitution,

$$\dot{\underline{x}_1} = (\mathbf{A}_{11} - \mathbf{A}_{22}^{-1}\mathbf{A}_{21}\underline{x}_1)\underline{x}_1 \tag{2.4}$$

This approach is known as *singular perturbation* approach, and leads to *time-scale decomposition* amongst subsystems, which are strongly coupled. To interpret this mathematically, the singular perturbation approach followed by substitution of (2.3) into (2.4) led to the reduction of system order, and approximated the dynamical equation of the subsystem $\underline{x}_2$ into an algebraic equation. This is also known as the zeroth order, or strong coupling approximation in the singular perturbation theory. However, it should be noted that it is a complex exercise to model a system in the form (2.2). As stated in [5], it requires a 'considerable physical insight' for modeling the system as composed of slow and fast modes as desired by the framework. Fortunately, for power systems, some methods have been identified for the latter, for example see [38].

Such dynamical systems exhibiting time-scale decomposition are suitable candidates for the implementation of hierarchical control schemes. From (2.2), the dynamics of the faster subsystem are described by,

$$\epsilon \dot{\underline{x}}_2 = \mathbf{A}_{22}\underline{x}_2 + \mathbf{A}_{21}\underline{x}_1 \tag{2.5}$$

and dividing the equation by the perturbation parameter,

$$\dot{\underline{x}}_2 = \frac{\mathbf{A}_{22}}{\epsilon}\underline{x}_2 + \frac{\mathbf{A}_{21}}{\epsilon}\underline{x}_1 \tag{2.6}$$

where the second term on the right hand side can assumed to be algebraic (not showing any dynamics) because the dynamics of the subsystem $\underline{x}_1$ are too slow to change at the time-scale of $\underline{x}_2$. Hence, the dynamics of the faster subsystems are governed by the eigenvalues (or modes) of the matrix $\frac{\mathbf{A}_{22}}{\epsilon}$. A controller designed to stabilize subsystem $\underline{x}_2$ will damp out the fast modes of the latter matrix. The stabilized state variables of the subsystem $\underline{x}_2$ will then act as algebraic state variables in the time-scales of slower subsystem $\underline{x}_1$. Refer to Fig.2.2. It depicts the situation where two sets of state variables in a strongly coupled system exhibit a time-scale decomposition phenomena. This theme is exploited in power systems literature by researchers like Chow [36], to identify groups of state variables which are strongly coupled with others in its own sub-group but loosely coupled with all the other state variables. The latter phenomena, termed coherency is discussed in the next section.

2.2.2 Stability of interconnected dynamical systems

One of the qualitative properties of large, interconnected systems is their stability under small or large, internal or external disturbances. To that end, it is important to determine the necessary and sufficient conditions for stability for the entire system asymptotically. Special attention needs to be given to the effect that disturbances in one group of state variables (or one subsystem) causes on the other interconnected systems. In this section we first give a brief overview of the Lyapunov method for stability of dynamical systems. Then, we list the assumptions regarding the system model, followed by a discussion on methods for interconnected system asymptotic stability.

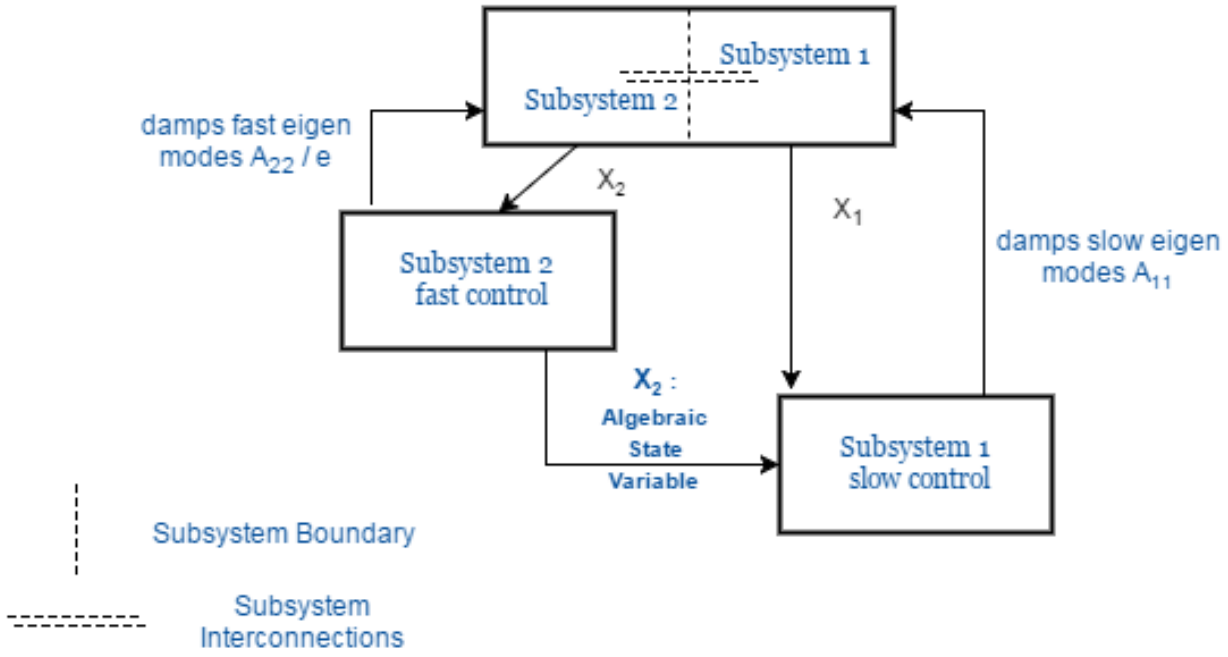

Figure 2.2: Hierarchical control of a system with two strongly coupled subsystems exhibiting time-scale decomposition

2.2.2.1 Lyapunov's second method for stability of dynamical systems

In 1892, A.M. Lyapunov, proposed [37], that the stability of an equilibrium point of a n -dimensional dynamical system

$$\dot{\mathbf{x}} = f(\mathbf{x}), \quad f(\mathbf{0}) = \mathbf{0} \tag{2.7}$$

can be ascertained without numerical integration. He stated that if there exists a scalar function $V(\mathbf{x})$ for (2.7) that is positive definite, i.e., $V(\mathbf{x}) > 0$ around the equilibrium point $\mathbf{0}$ and the derivative $\dot{V}(\mathbf{x}) < 0$, then the equilibrium is asymptotically stable. $\dot{V}(\mathbf{x})$ is obtained as

$$\dot{V}(\mathbf{x}) = \sum_{i=1}^{n} \frac{\partial V}{\partial x_i} \dot{x}_i = \sum_{i=1}^{n} \frac{\partial V}{\partial x_i} f_i(\mathbf{x}) = \nabla V^T f(\mathbf{x}) \tag{2.8}$$

where n is the dimension of the system in (2.7). Hence, the existence of a Lyapunov function $V(\mathbf{x})$ and a negative definite derivative of that function $\dot{V}(\mathbf{x}) < 0$ are regarded as the necessary and sufficient conditions for the asymptotic stability of a dynamical system under disturbance, in general. This method is known as Lyapunov's second method and was later expanded to address the stability of an interconnected system, as discussed in the next subsections.

2.2.2.2 Assumptions for interconnected system stability

- The dynamical system under study is composed of interconnected subsystems, whose boundaries are pre-specified. Furthermore, the system model and dynamical models of each of the subsystems is available.
- Each of the subsystems, when considered in isolation from the others, is stable (for instance, in the Lyapunov sense). Also, some quantitative measure of this stability, like the rate of decrease of the Lyapunov function, $\dot{V}(\mathbf{x}_i)$ is given for each subsystem.
- Control devices, if any, are also pre-installed in the system at strategic locations.

The focus here is to find the necessary and sufficient condition for the stability of interconnected system in terms of the aforementioned quantitative measure of stability and some quantitative measure of strength of interconnection (for e.g. ϵ). It should be noted that if the system is sufficiently weakly coupled, the set of isolated subsystems will be stable due to the second assumption above. This conclusion is of important consequence in the assumptions regarding voltage stability enhancement. In case the systems are rather strongly coupled, the following stability analysis techniques may be adopted.

2.2.2.3 Lyapunov's second method for interconnected systems

In this section we describe the necessary and sufficient conditions for stability of an interconnected system in the Lyapunov sense, under the aforementioned assumptions. These theorems are stated without proof. The reader is encouraged to read the work by Bailey [10], which consists of detailed proof and examples of application of Lyapunov's second method for the stability of interconnected systems. The framework discussed below closely follows the review in [5].

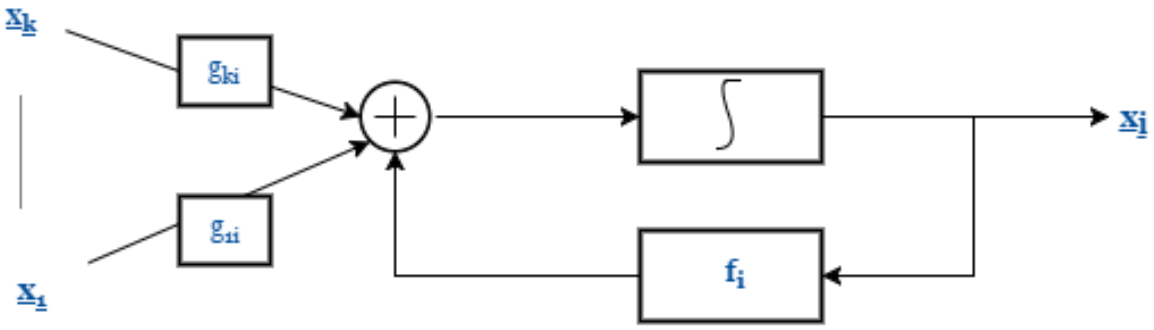

Figure 2.3: Seperable interaction terms of an interconnected system.

Assume that the dynamical model of the coupled system can be stated as

$$\dot{\mathbf{x}} = \mathbf{F}(\mathbf{x}, t) \tag{2.9}$$

which is assumed to be composed of weakly coupled subsystems whose dynamic model is given by

$$\dot{\mathbf{x}}_i = \mathbf{f}_i(\mathbf{x}_i, t) + \mathbf{g}_i(\mathbf{u}, t), \qquad i = 1, ..., N \tag{2.10}$$

where $\mathbf{x}_i$ represents the state vector of the i_{th} subsystem and second term on the right hand side represents the input to this subsystem. Furthermore, suppose that $\mathbf{u}$ represents the state feedback of the form,

$$\mathbf{u}(t) = \mathbf{x}(t) \tag{2.11}$$

Here, $\mathbf{x} \in R^n$, $\mathbf{x}_i \in R^{n_i}$, and the transposes of the global and subsystem state vectors are related by,

$$\mathbf{x}^{'}(t) = (\mathbf{x}_1^{'}(t), ..., \mathbf{x}_N^{'}(t)) \tag{2.12}$$

As we find in the case of power systems, the input or the interaction term g_i is separable in the sense that it is composed of input terms from the individual subsystems, e.g. in Fig. 2.3,

$$\mathbf{g}_i(\mathbf{x}, t) = \sum_{r=1, r\neq i}^{N} \mathbf{g}_{ir}(\mathbf{x}_i, t) \tag{2.13}$$

Finally, we assume the origin ($\mathbf{0}$) to be an equilibrium point, that is,

$$\mathbf{f}_i(\mathbf{0}, t) \equiv \mathbf{0}, \quad \mathbf{g}_i(\mathbf{0}, t) \equiv \mathbf{0}, \quad \mathbf{F}(\mathbf{0}, t) \equiv \mathbf{0} \tag{2.14}$$

Next, suppose that a continuously differentiable scalar function V_i may be defined along the trajectory of (2.10) such that it is positive definite and, similar to (2.8), its time derivative can shown to be,

$$\dot{V}_i = \frac{\partial V(\mathbf{x}_i(t), t)}{\partial t} + \frac{\partial V(\mathbf{x}_i(t), t)}{\partial \mathbf{x}_i} \dot{\mathbf{x}}_i(t) \tag{2.15}$$

and substituting (2.10) into (2.15) we have,

$$\dot{V}_i = \frac{\partial V(\mathbf{x}_i(t), t)}{\partial t} + \frac{\partial V(\mathbf{x}_i(t), t)}{\partial \mathbf{x}_i} \mathbf{f}_i(\mathbf{x}_i, t) + \frac{\partial V(\mathbf{x}_i(t), t)}{\partial \mathbf{x}_i} \mathbf{g}_i(\mathbf{u}_i, t) \tag{2.16}$$

Now if the rhs of (2.15) could be bounded by functions of $\mathbf{x}_i$ as,

$$\dot{V}_i(\mathbf{x}_i(t), t) \leq h_i(\gamma_1(\mathbf{x}_1(t), t), ..., \gamma_N(\mathbf{x}_N(t), t)) \tag{2.17}$$

where γ_i are also positive definite, then we can derive conditions on the h_i and γ_i such that $V(\mathbf{x}_i(t), t) \to 0$ as $t \to \infty$ for $i = 1, 2, ..N$.

Necessary and sufficient Condition

It can be shown (see [5] and references therein) that *if* (2.17) holds with $\gamma_i(\mathbf{x}_i(t), t) =$

$V_i(\mathbf{x}_i(t),t)$ and with $h_i(\gamma_1(\mathbf{x}_1(t),t),....,\gamma_N(\mathbf{x}_N(t),t))$ non-increasing in γ_j for $j \neq i$, and if the origin is an asymptotically stable equilibrium of the N-dimensional system,

$$\dot{V}_i = h_i(V_1,...,V_N,t), \quad i = 1,...,N, \tag{2.18}$$

then the overall system is stable. The N-vector $\mathbf{V}^{'}(\mathbf{x},t) = (V_1(\mathbf{x}_1,t),...,V_N(\mathbf{x}_N,t))$ is denominated a Vector Lyapunov Function.

Later, researchers like Bailey [10] extended the above result to represent it in the form matrix inequalities, and derive the necessary and sufficient conditions in terms of properties of that matrix. Specifically, Bailey showed that (2.17) takes form of the inequality

$$\dot{V}_i(\mathbf{x}_i(t),t) \leq -\sum_r \tilde{a}_{ir} V_r(\mathbf{x}_r,t) \tag{2.19}$$

or putting the same in matrix form,

$$\dot{\mathbf{V}} \leq \tilde{A}\mathbf{V} \tag{2.20}$$

where $\dot{\mathbf{V}}$ is the corresponding vector of the derivatives of Lyapunov functions of all the component subsystems and the matrix $\tilde{A}$ is the matrix of $\tilde{a}_{ir}$ in (2.19). Here $\tilde{A}$ is a matrix with positive diagonal and non-positive off diagonal entries. Also, it is obvious that $\tilde{a}_{ir}, \quad i \neq r$ give a bound on subsystem interactions. Bailey showed that (2.20) is stable if $\tilde{A}$ is a M-matrix. The conditions for the stability of (2.20) or precisely for $\tilde{A}$ being a M-matrix are:

- the inverse $\tilde{A}^{-1}$ exists and all its entries are non-negative,
- the leading principal minor determinants of $\tilde{A}$ are all positive,
- the eigenvalues of $\tilde{A}$ have positive real parts.

For example, if $\tilde{A}$ is diagonally dominant, that is, $\tilde{a}_{ii} > \sum_{r \neq i} |\tilde{a}_{ir}|$, then it is an M-matrix. This framework of decentralized stability of interconnected systems (2.9)-(2.20) has been used in the present research work to formulate control laws which guarantee asymptotic stability in interconnected power systems. Next, we discuss the rotor angle and voltage stability assessment methods in power systems.

2.3 Techniques for power system stability enhancement - Traditional centralized methods

2.3.1 Definition

Power system is a large-scale dynamical system, and its stability has been recognized as an important problem for secure system operation for over a century [38],[39]. Unlike many

other dynamical systems, the power system is a nonlinear system that operates in a constantly changing environment; loads, generator outputs and key operating parameters change continually. When subjected to a disturbance, the stability of the system depends on the initial operating condition as well as the nature of the disturbance. Hence, a rigorous effort was undertaken by several joint task forces, like the IEEE/CIGRE [2],[40], for precisely defining the term *Power System Stability*, and exhaustively classifying all practical instability scenarios. The definition of power system stability, proposed by the latter is as follows:

> Power system stability is the ability of an electric power system, for a given initial operating condition, to regain a state of operating equilibrium after being subjected to a physical disturbance, with most system variables bounded so that practically the entire system remains intact.

Thus, the stability of an electric power system, post a disturbance, is a characteristic of the movement of the system state variables around a (stable) equilibrium point, which is the normal operating condition. Because of the constant changes that occur in the power system (as in the case of small fluctuations in loads), the notion of a steady state or an equilibrium point essentially implies no net variation over a cycle. Power systems are continuously subjected to a variety of disturbances, small and large. Stability of an equilibrium point entails that the system must be able to adjust to the changing conditions and operate in the normal state, without violating any constraint. Furthermore, it is also desirable that due to large disturbances of severe nature, such as a short circuit on a transmission line or the loss of a large generator, the system state variables are not driven into sustained oscillations of increasing amplitude. Hence, a large disturbance often leads to topology changes in the network for removing the faulted equipment.

It is necessary to emphasize that the for an interconnected dynamic system like power system, a post disturbance stable equilibrium requires that the system integrity is preserved, i.e., practically all generators and loads remain connected through a single contiguous transmission circuit. Only if it is necessary for the sustaining operational continuity of the entire system, some generators and loads may be disconnected by intentional tripping or by relay operations. Due to non-linear interactions between groups of dynamic state variables or subsystems, following certain large disturbances, it might be advisable to intentionally isolate two or more "islands" (or subsystems) to preserve as much of the local demand-supply balance as possible. Subsequent to an emergency or an extremis condition, the system can be restored to the normal state by human or automatic control actions. Failure to perform any of the aforementioned actions will cause instability, resulting in a 'run-away' situation. For instance, the instability may cause a progressive increase in rotor angle separation of two coherent groups of generator rotors, or a progressive decrease in voltages in a control area. The latter may lead to a cascading failure scenario. For the purposes of assessment and efficient control of the complex instability phenomena in power systems, a classification of instabilities has been made by researchers, which is discussed next.

2.3.2 Classification

Power system stability is essentially a single, unified problem due to the non-linear interaction of different state variables, specially under stressed conditions. However, the different forms of instabilities that arise in a power system cannot be effectively controlled by treating them in a unified manner. Because of the 'curse of dimensionality' and the complexity of stability problems, it is easier to make simplifying assumptions for addressing specific types of instabilities. Making such assumptions enables us to ignore certain details in the system models (for e.g., ignoring fast dynamics to address slow dynamics), and relevant analytical techniques. Analysis of stability, including the identification of factors contributing to a specific type of instability and subsequently formulating techniques to enhance operational security, is better handled by classification of system stability into different categories.

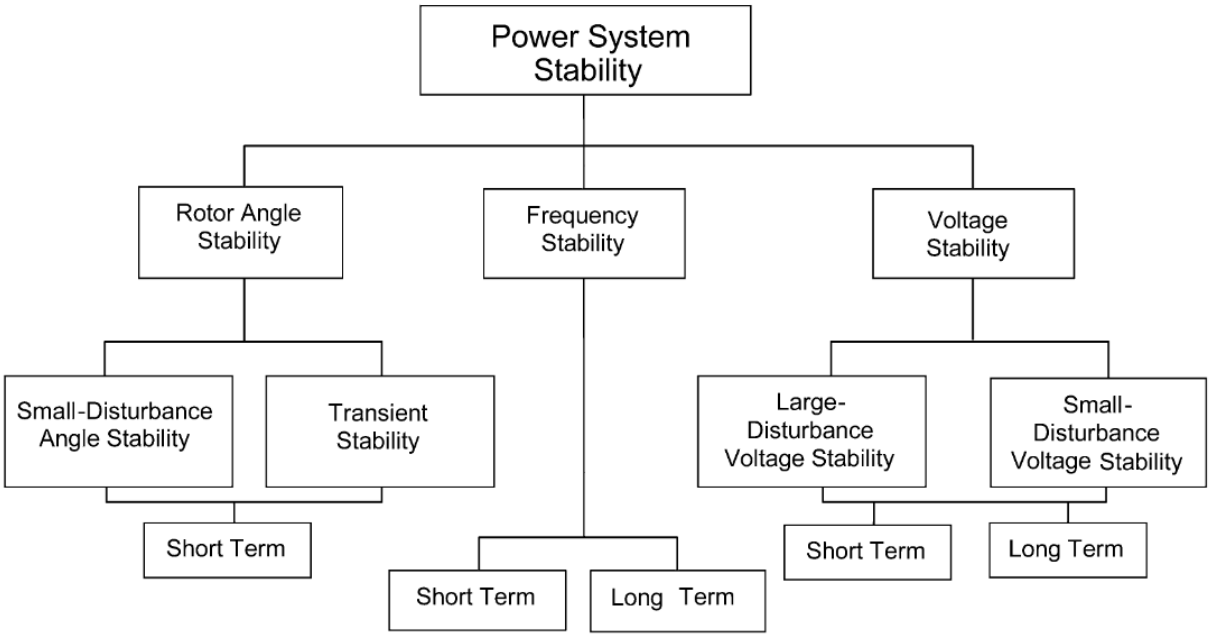

Figure 2.4: Classification of power systems stability. Source: [2].

Fig. 2.4 gives the classification of the power system stability problem, as proposed by the IEEE/CIGRE working group in [2]. The classification of power system stability proposed in [2] is based on the following factors:

- The physical nature of the resulting instability as indicated by the main system state variable in which instability can be observed (e.g. rotor, voltage).
- The size of the disturbance considered, which influences the method of calculation and prediction of stability (e.g. large, small).

- The devices, processes, and the time constants that must be taken into consideration in order to assess stability (e.g. short-term, long-term).

The current research work is focused on the transient instability of rotor angles and voltages (caused by large disturbances, like short circuits), and long-term voltage instabilities (caused by small disturbances, like slow increase in load). Hence, in the subsequent sections we describe both of these instabilities in further detail.

2.3.3 Large-Disturbance (Transient) Stability

2.3.3.1 Preliminaries

Rotor angle stability or transient stability, as it is commonly referred to, is concerned with the ability of the power system to maintain coherency in the dynamic state variables, post a large disturbance, such as a short circuit on a transmission line. The resulting system response is influenced by a nonlinear power-angle relationship and may lead to a large deviation of generator rotor angles from a common reference frame. Transient stability depends on (a) the initial operating state, which relates to the potential energy of the equilibrium point, and (b) the amount of kinetic energy pushed into the system by the disturbance. Instability may present itself in the form of aperiodic separation of the rotor angles, due to insufficient synchronizing torque, resulting in a 'first swing instability'. However, in large power systems, first swing instability is rarely observed, due to a superimposition of several modes like slow inter-area and fast local-plant swing modes causing rotor angle instability beyond the first swing [41].

The transient instability may be observed, for example, in the evolution of rotor angles as the time elapses after a disturbance. If the deviation in rotor angle $\Delta\delta_i$ of a machine or a group of machines increases continually with respect to the rest of the system, the system is unstable. The rotor angles of each of the machines are measured with respect to a synchronously rotating reference frame. Thus, relative rotor angles rather than a absolute rotor angles must be monitored to assess the stability margins. The time frame of interest in transient stability studies is usually 3 to 5 seconds following the disturbance, which may extend unto 10 – 20 seconds for very large systems with dominant inter-area swings. Next, we describe a modeling framework for transient stability assessment in power systems.

In the simplest form, a power system undergoing a disturbance can be described by a set of three differential equations:

1. **Prefault State**
$$\dot{\underline{x}}(t) = f^I(\underline{x}(t)) \qquad -\infty < t \leq 0 \tag{2.21}$$
2. **During Fault State**
$$\dot{\underline{x}}(t) = f^F(\underline{x}(t)) \qquad 0 < t \leq t_{cl} \tag{2.22}$$

3. **Post fault state**

$$\dot{\underline{x}}(t) = f(\underline{x}(t)) \qquad t_{cl} < t < \infty \tag{2.23}$$

where $\underline{x}(t)$ is the vector of state variables of the system at time t. At $t = 0$, a fault occurs in the system and the system trajectory changes from f^I to f^F. During $0 < t \leq t_{cl}$ (called the *faulted* period), the system is governed by the 'fault-on' trajectory f^F. In real time system operation, before the fault is cleared at $t = t_{cl}$, we may have several switchings in the network, each giving rise to a different trajectory f^F. Another assumption that we make for the sake of reducing the complexity is that the fault causes the dynamics to evolve along a single trajectory f^F, indicating that there are no changes in the topology of the system between $t = 0$ and $t = t_{cl}$. When the fault is cleared at $t = t_{cl}$, we have a postfault system with its dynamics $f(x(t))$. In the prefault period $-\infty < t \leq 0$, the system would have settled down to a steady state, so that $\underline{x}(0) = \underline{x}_0$ is known. Therefore, (2.21) can be removed by adding the initial conditions in (2.22), resulting in the above system of equations written as

$$\begin{aligned} \dot{\underline{x}}(t) = f^F(\underline{x}(t)) \quad & 0 < t \leq t_{cl} \\ \underline{x}(0) = \underline{x}_0 & \end{aligned} \tag{2.24}$$

and

$$\dot{\underline{x}}(t) = f(\underline{x}(t)) \qquad t > t_{cl} \tag{2.25}$$

where the initial condition $\underline{x}(t_{cl})$ can be determined by solving the dynamical equations of the faulted system (2.24) evaluated at $t = t_{cl}$. Let us assume that (2.25) has a stable equilibrium point $\underline{x}_s$. The stability problem is to find whether the trajectory $\underline{x_s}(t)$ for (2.25) with the initial condition $\underline{x}(t_{cl})$ will converge to $\underline{x}_s$ as $t \to \infty$. The largest value of t_{cl} for which this holds true is called the critical clearing time t_{cr}.

Later in the chapter, we discuss a method to determine t_{cr} by analyzing the evolution of the dynamical system (2.24) along its trajectory. If a lyapunov function can be formulated for the power system under study, then a 'stability boundary' around the equilibrium point $\underline{x}_s$ can be determined. Then, t_{cr} is the point where the system of (2.24) exists the stability region of the equilibrium point in (2.25). Next, we discuss a dynamic model of power system for formulation of a lyapunov function. Power system researchers denominate the latter as a Transient Energy Function (TEF) [41].

2.3.3.2 Power System Dynamic Modeling

The most commonly used power system model is a set of differential algebraic equations (D.A.E.), i.e.,

$$\dot{\underline{x}}(t) = f^F(\underline{x}(t), \underline{y}(t)) \tag{2.26}$$

$$0 = g^F(\underline{x}(t), \underline{y}(t)), \tag{2.27}$$

for $0 < t \leq t_{cl}$ and

$$\dot{\underline{x}}(t) = f(\underline{x}(t), \underline{y}(t)) \tag{2.28}$$

$$0 = g(\underline{x}(t), \underline{y}(t)), \tag{2.29}$$

for $t > t_{cl}$

The function g in (2.27) and (2.29) is the set of nonlinear algebraic equations representing the machine stator and the transmission network, while the function f is the set of differential equations representing the dynamics of the synchronous machines and the related control blocks. Similar to the discussed theory of strong coupling (see equations (2.2)-(2.6)), the perturbation parameter representing the fast time constants of the the electromagnetic state variables associated with the transmission lines are very small as compared to the electromechanical dynamics, and can be approximated to zero. This results in the set of algebraic equations g.

In the literature, the modeling of equations in the form of (2.26)-(2.29) has been discussed extensively. Refer to the multimachine system modeling in [41]. Some of the examples are reduced-order models, such as a flux- decay model and classical model. The classical models may be further classified according to the type of approximation made, for instance, while obtaining the approximated model, either the network structure could be preserved as-is, or the the load buses may be eliminated, under a constant impedance assumption, to obtain an internal node model. Structure-preserving models, that have not been covered in this text, involve nonlinear algebraic equations in addition to dynamic equations, and can incorporate nonlinear load models (like frequency dependence of the load), leading to the concept of structure-preserving energy function (SPEF) $V(x, y)$. Readers are pointed to the work by Bergen and Hill in [42] for the SPEF.

For the purpose of this research work, we have considered a classical model with the loads represented as constant impedance. This results in only differential equations, as opposed to DAE equations. We first discuss this is in the multi-machine context. As it is obvious, a higher order model of the system will give a better approximation of the physical power system, but the intention here is to prove a concept related to the feasibility of Lyapunov control, rather than the accuracy. Under such consideration, the classical model may be used as the initial step, and the energy function can be later included to improve the accuracy of the models. The well known swing equations machines in an electrical network have been discussed in [41], these are reproduced here, as follows:

$$\frac{2H_i}{\omega_s}\frac{d^2\delta_i}{dt^2} + D_i\frac{d\delta_i}{dt} = P_{mi} - P_{ei}, \quad i = 1, ..., n \tag{2.30}$$

where H indicates the machine inertia, ω_s is the synchronous speed, D_i is the damping constant of the damper winding, δ is the deviation of the angle from the synchronous reference frame n is the total number of generating units in the system, and the electrical power

$$P_{ei} = E_i^2 G_{ii} + \sum_{j=1, j\neq i}^{n} (C_{ij}\sin\delta_{ij} + D_{ij}\cos\delta_{ij}) \tag{2.31}$$

where G_{ii} is a machine impedance parameter and C_{ij} and D_{ij} are the complex network admittances. Denoting $\frac{2H_i}{\omega_s} = M_i$ and $P_i = P_{mi} - E_i^2 G_{ii}$, we get

$$M_i \frac{d^2\delta_i}{dt^2} + D_i \frac{d\delta_i}{dt} = P_i - \sum_{j=1, j\neq i}^{n} (C_{ij} \sin \delta_{ij} + D_{ij} \cos \delta_{ij}) \tag{2.32}$$

which can also be written as,

$$M_i \frac{d^2\delta_i}{dt^2} + D_i \frac{d\delta_i}{dt} = P_i - P_{ei}(\delta_i, ...\delta_n), \quad i = 1, ..., n \tag{2.33}$$

Let α_i be the rotor angle with respect to a fixed reference. Then $\delta_i = \alpha_i - \omega_s t$, $\dot{\delta}_i = \frac{d\alpha_i}{dt} - \omega_s = \omega_i - \omega_s$, where ω_i is the angular velocity of the rotor and ω_s is the synchronous speed in radians per sec. Thus, both δ_i and its time derivative are expressed with respect to a synchronously rotating reference frame. Using these definitions, (2.32) can be converted to a set of first-order differential equations by introducing the state variables δ_i and ω_i:

$$\dot{\delta}_i = \omega_i - \omega_s \tag{2.34}$$

$$\dot{\omega}_i = \frac{1}{M_i}(P_i - P_{ei}(\delta_i, ...\delta_n) - D_i(\omega_i - \omega_s)), \quad i = 1, ..., n \tag{2.35}$$

Equations (2.34) and (2.35) are applicable both to the faulted state and the postfault state, with the difference that P_{ei} is different in each case, because the internal node admittance matrix is different for the faulted and postfault system. The discussed model is known as the internal-node model since the physical buses have been eliminated by network reduction. Next, we discuss some methods that have been applied for power system dynamic security assessment.

2.3.3.3 Methods for dynamic stability assessment

A transient (or dynamic) stability assessment method should be able to predict, in a post-disturbance scenario, if the system trajectory is going to be unstable. The notion of stability used here is the same as defined in section 2.3.1. Two popular methods used for power system dynamic stability assessment are: (1) Time-domain simulation, and (2) Direct Methods like the Lyapunov's second method. In the present research work, we follow the standard practice, where we use direct methods for deriving control laws, but the effectiveness of control actions is validated by executing time domain simulations. A discussion on both these method is presented below.

2.3.3.3.1 Time Domain Simulation

As discussed above, the differential equations to be solved in power system stability analysis are nonlinear ordinary differential equations with known initial values:

$$\dot{\underline{x}}(t) = f(\underline{x}, t) \tag{2.36}$$

where $\mathbf{x}$ is the state vector of n dependent variables and t is the independent variable (time). The objective is to solve $\mathbf{x}$ as a function of t, with the initial values of $\mathbf{x}$ and t equal to $\mathbf{x}_0$ and t_0, respectively. In this subsection, we provide a general description of numerical integration methods applicable to the solution of equations of the above form. In describing these methods, without loss of generality, (2.36) will be treated as a first order differential equation.

A. Euler Method

Consider the first-order differential equation,

$$\frac{dx}{dt} = f(x,t) \tag{2.37}$$

with $x = x_0$ at $t = t_0$. Fig.2.5, illustrates the principle of applying the Euler method. At $x = x_0$, $t = t_0$ we can approximate the curve representing the true solution by its tangent having a slope

$$\frac{dx}{dt}|_{x=x_0} = f(x_0,t_0)$$

Therefore,

$$\Delta x = \frac{dx}{dt}|_{x=x_0}\Delta t$$

Now we can approximate x at $t = t_1 = t_0 + \Delta t$ by

$$x_1 = x_0 + \Delta x = x_0 + \frac{dx}{dt}|_{x=x_0}.\Delta t \tag{2.38}$$

The Euler method is equivalent to the Taylor series expansion for x around the point (x_0, t_0), truncating after the first order terms:

$$x_1 = x_0 + \Delta t(\dot{(x_0)}) + \frac{\Delta t^2}{2!}(\ddot{x}_0) + ... \tag{2.39}$$

assuming very short time steps Δt so that the second order and higher terms may be neglected. Subsequently, by using a similar approximation, we can take another short time step Δt and determine x_2 corresponding to $t_2 = t_1 + \Delta t$ as follows:

$$x_2 = x_1 + \frac{dx}{dt}|_{x=x_1}\Delta t \tag{2.40}$$

The Euler technique can similarly be used to approximate all the solutions along the trajectory.

The method considers only the first derivative of x and is, therefore, referred to as a *first-order* method. To give sufficient accuracy for each step, Δt has to be small. This will increase round-off errors, and the computational effort required will be very high.

B. Modified Euler Method

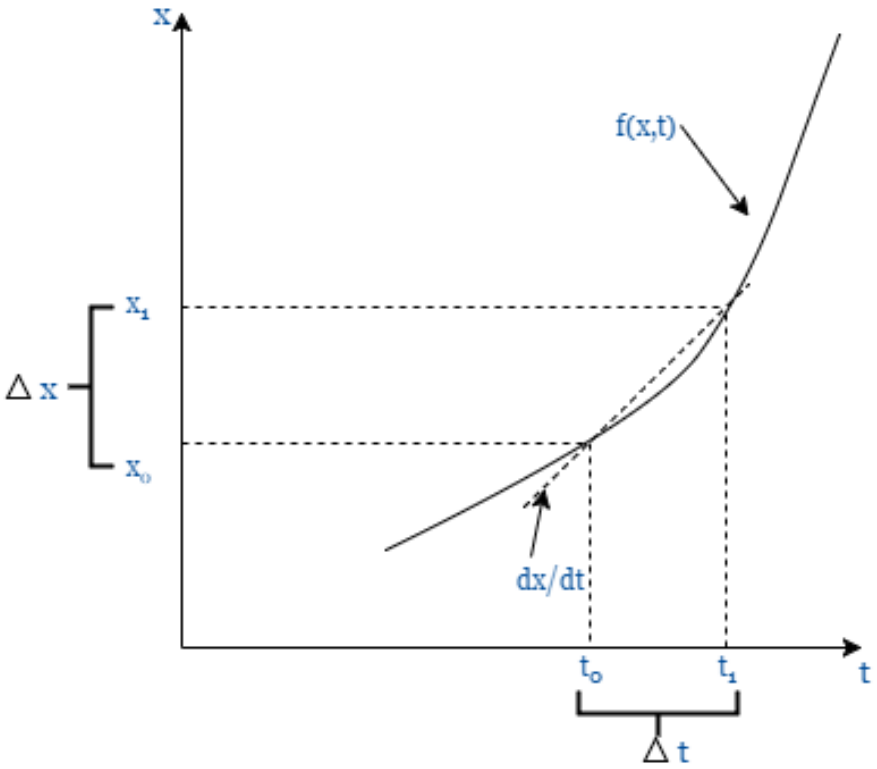

Figure 2.5: Euler Method integration

The standard Euler method results in an inaccurate estimation of x, due to the assumption that the tangent of the entire curve is same as that at the start of the interval of interest. The modified Euler method tries to overcome this problem by using the average of the derivatives at the start and the end of interval.

The modified Euler method consists of the following steps:

1. *Predictor step.* By using the derivative at the beginning of the step, the value at the end of the step is *predicted*.
$$x_1^p = x_0 + \frac{dx}{dt}|_{x=x_0}\Delta t \tag{2.41}$$

2. *Corrector step.* By using the predicted value of x_1^p, the derivative at the end of the step is computed and the average of this derivative and the derivative at the beginning of the step is used to find the *corrected value*
$$x_1^c = x_0 + \frac{1}{2}(\frac{dx}{dt}|_{x=x_0} + \frac{dx}{dt}|_{x=x_1^p})\Delta t \tag{2.42}$$

If desired, a more accurate value of the derivative at the end of the step can be calculated, again by using $x = x_1^c$. This derivative can be used to calculate a more accurate value of the

average derivative which is in turn used to apply the corrector step again. This process can be used repeatedly until successive steps converge with the desired accuracy.

C. Runge-Kutta (R-K) Methods

The R-K methods are an approximation to the Taylor series solution. However, the R-K methods have an advantage over the formal Taylor series solution, in the sense that the former do not require explicit evaluation of derivatives higher than the first. Rather, the higher order derivatives are approximated by a repeated application of the first derivative. The number of terms effectively retained in the Taylor series define the order of the R-K method.

Referring to the differential equation (2.37), a second-order R-K formula for the value of x at $t = t_0 + \Delta t$ is

$$x_1 = x_0 + \Delta x = x_0 + \frac{k_1 + k_2}{2} \tag{2.43}$$

where

$$k_1 = f(x_0, t_0)\Delta t,$$
$$k_2 = f(x_0 + k_1, t_0 + \Delta t)\Delta t$$

This method is equivalent to considering first and second derivative terms in the Taylor series; error is on the order of Δt^3.

A general formula giving the value of x for the $(n+1)^{th}$ step is

$$x_{n+1} = x_n + \frac{k_1 + k_2}{2} \tag{2.44}$$

where

$$k_1 = f(x_n, t_n)\Delta t,$$
$$k_2 = f(x_n + k_1, t_n + \Delta t)\Delta t$$

D. Issues with Numerical Integration Methods

Integration methods discussed above are also known as *explicit methods*. In these methods, the value of the dependent variable $\mathbf{x}$ at any value of t is computed as a function of the values of $\mathbf{x}$ from the previous time steps. This means that an erroneous approximation of $\mathbf{x}$ at any time-step will lead to a poor solution for $\mathbf{x}$ all the subsequent time-steps, along the trajectory. Furthermore, the numerical stability of such simulations is dependent on the modeling details of the system. A real power system may consist of various modes, with different time-constants, hence, careful consideration needs to be given during integration to the choice of step-size. Even after the fast modes die out, small time steps continue to be required to maintain numerical stability. Time-domain simulation methods might be ineffective to understand the impact of large disturbances in real-time. This is because

solution of differential equations with many thousands of state variables might take more time than the disturbance to push the system into sustained aperiodic oscillations. Hence these methods are best suited for post-analysis. The time-domain simulation methods offer a more promising real-time solution, when used in conjunction with other methods, like the direct methods of stability evaluation, to reach a faster conclusion about system stability.

Many commercial software packages like GE-PSLF® and Siemens PSS®E implement numerical integration techniques to perform time-domain simulations of the post-fault trajectory. Given below is an example of time-domain simulation of certain system on PSLF® package.

E. Time-Domain simulation example

A 9-bus, 3-machine test system was simulated in the PSLF® v 16.1 package. The test system is given in Fig.2.6. Bus-faults of different durations were simulated on the bus number 5. Different state variables, as functions of time, are stored in the channel output file produced as a result of simulation. Plots of the dynamic state variables are then created using the PSLF-Plot package. The resulting rotor angles of the three machines are plotted for two different fault durations in the figures 2.7 and 2.8. As can be observed from the figures, the larger duration of fault causes bigger amplitudes of oscillations and take more time to be damped out completely.

2.3.3.3.2 Direct methods of stability assessment

As discussed in the previous subsection, time-domain simulation methods are rather impractical for real-time transient stability assessment, hence faster methods like direct methods for stability evaluation were introduced for power systems. These methods are advantageous because the stability of the equilibrium point can be assessed without explicitly integrating the system of differential equations. This approach has received considerable attention of the research community since the seminal works of Magnusson [43] and Aylett [44], who used transient energy function (TEF) for the assessment of transient stability. The energy-based methods are a special case of the more general Lyapunov's second method or the direct method (as discussed previously); the energy function being a candidate Lyapunov function.

Energy function approach is based on the principle that the equilibrium point of a power system in normal operation has certain kinetic and potential energy. Once a large disturbance, like a short circuit occurs, energy is pushed into the system, increasing both the potential and kinetic energies of the operating point, leading to an acceleration of the synchronous machines according to (2.34)-(2.35). A common analogy for this is a ball at the bottom of a bowl, which when disturbed, will roll up to the side of the bowl. In this case, the bottom of the bowl represents the (relative) zero potential level or the equilibrium position of the operating point, the bowl represents the region of attraction of the equilibrium point, and the sides of the bowl represent the stability boundaries of the region of attraction. A stability assessment method needs to determine whether the energy introduced into the system by the disturbance is large enough to push the operating point out of its stability region of its

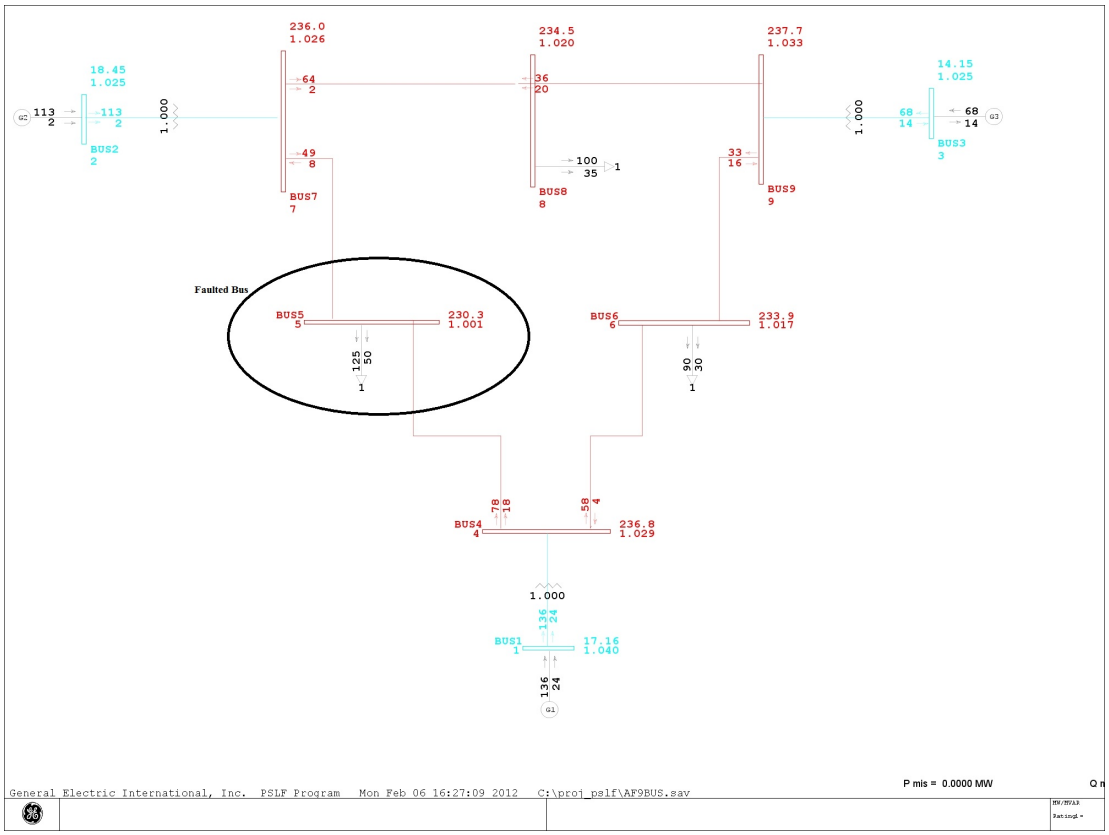

Figure 2.6: 9-bus, 3-machine test system simulated on PSLF® v 16.1

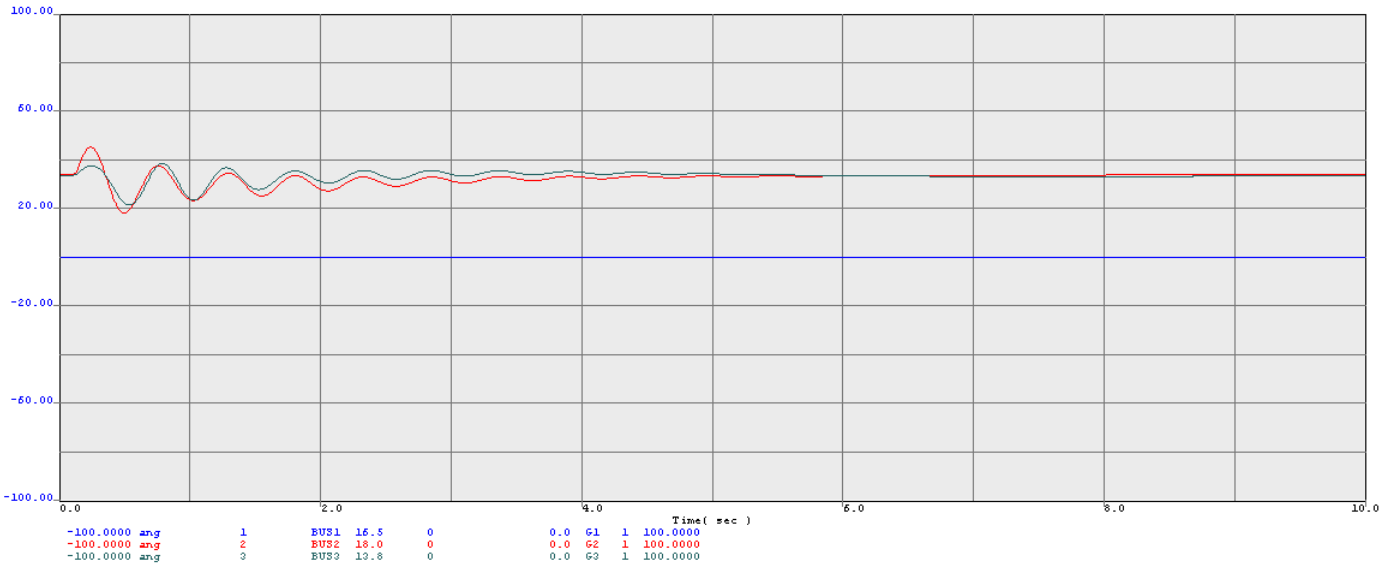

Figure 2.7: Rotor Angles of the three generators following a bus-fault of 20 ms at Bus 5.

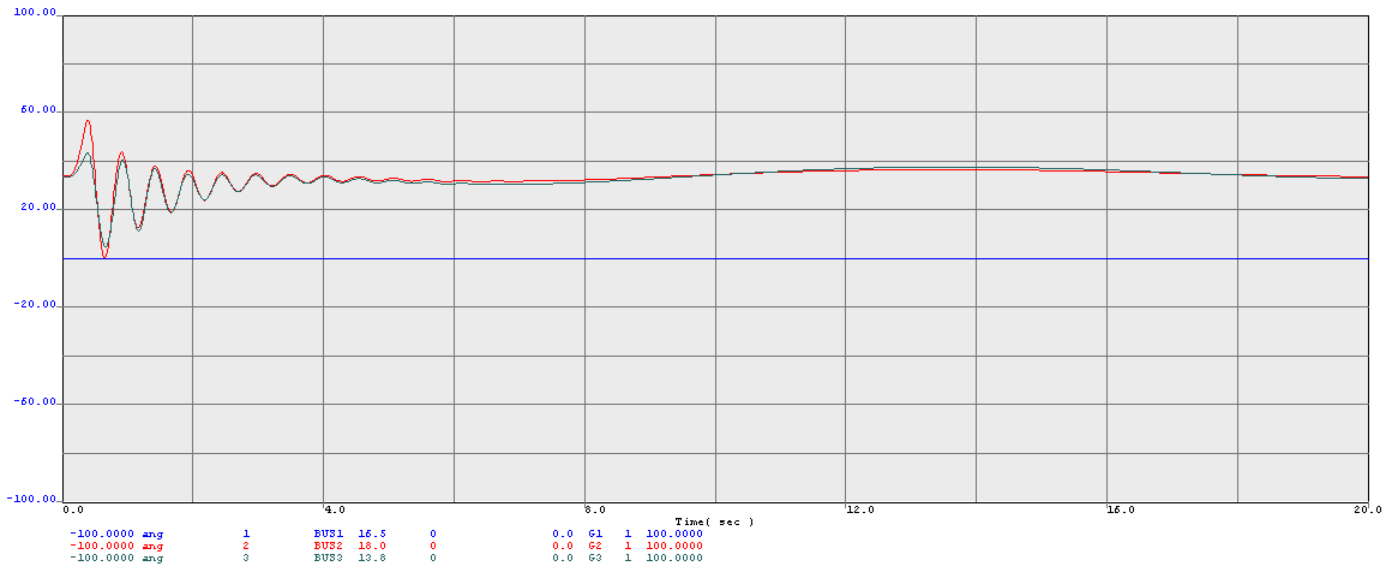

Figure 2.8: Rotor Angles of the three generators following a bus-fault of 20 ms at Bus 5.

stable equilibrium point, which is equivalent to determining if the disturbance causes the ball to be pushed out of the bowl.

A post-disturbance system will be stable if the region of attraction of the equilibrium point is large enough to absorb the amount of kinetic energy that has been introduced by the disturbance, hence bringing the operating point back to the equilibrium. For a given configuration of the system, the maximum amount of energy that can be absorbed by the system before being pushed into instability, is known as the critical energy. Even when the energy pushed in by the disturbance is not large enough to make operating point leave the region of attraction of the equilibrium point, the operating point may oscillate around the equilibrium point, if there is insufficient counterbalancing force (or damping energy) in the system. In case of practical power systems, this damping can be provided by the generator damper windings on the stator, or by the control devices (for. e.g. FACTS type), designed for damping out transient oscillations. Finding control laws for the control devices of the latter type is one of the objectives of this research. Thus, an assessment (and subsequently, enhancement) of transient stability requires:

- Determination of functions that adequately describe the transient energy responsible for separation of one or more synchronous machines from the rest of the system,
- An estimate of the *critical energy* required for the machines to lose synchronism, and
- An evaluation of the available damping in the system for developing control methods.

In the next few sections, we outline the application of transient energy function based ap-

proach for stability evaluation of power systems. Prior to that, we give a brief general background about Lyapunov functions.

A. Lyapunov's Method for Power Systems: The Transient Energy Function approach

In a previous section, we have introduced Lyapunov's second method for dynamical systems in general. Refer to section 2.2.2.1, equations (2.7)-(2.8). Here we develop the theory for finding a valid Lyapunov function for power systems.

In case of power systems, as many other physical systems, a scalar, positive definite function $V(x)$ can be defined, which represents a generalization of the concept of the energy of a system. One critical question here is whether this function also enjoys all the properties of a Lyapunov function? EL-Abiad and Nagappan [45] formally applied the general Lyapunov's second method to power systems. They provided an algorithm to compute the critical energy as discussed in the previous subsections.

For applying the Lyapunov theory in power systems, it is required to compute the region of attraction of the pre-disturbance stable equilibrium point, which also represents the initial operating condition. It is a highly complex exercise to derive the region of attraction of a nonlinear dynamical system. This is due to several reasons, like: (a) commonly, this is not a closed region, (b) the complexity becomes specially significant in a large-scale system like power systems due to its high dimensionality. The characterization of this region for power systems has been discussed in the literature [41] using simple-machine models. The stability region consists of surfaces passing through the unstable equilibrium points (u.e.p's) of the system (2.34)-(2.35). An estimate of the region of attraction is described by an inequality of the type $V(x) < V_{cr}$, where the $V(x)$, and V_{cr} represent the energy function and the critical energy (for a given configuration of power system) respectively. It should be also understood that for each disturbance causing the operating point to leave the region of attraction, the mode of instability (i.e., one or more machines going unstable) may be different, which implies that the operating point can evolve along one of the infinitely many trajectories. This last assertion adds further complexity in real-time calcualtion of V_{cr} of a high dimensional system. In case of a multi-machine classical model, with loads being treated as constant impedances, there are well-proven algorithms for the computation of V_{cr}. Next, we discuss the most commonly applied analytical formulation of the energy function for the power system in (2.34)-(2.35).

B. Energy function formulation

In this formulation, the rotor angles will be defined with respect to a reference frame, called the center of inertia (CoI), which represents the 'average motion' of the system rotor angles. Hence, the synchronous stability of every machine is assessed by monitoring the change in angles referenced only to COI instead of relative rotor angles. The COI of a multi-machine

system is defined as,

$$\delta_0 = \frac{1}{M_T}\sum_{k=1}^{n} M_k\delta_k, \quad \omega_0 = \frac{1}{M_T}\sum_{k=1}^{n} M_k\omega_k \tag{2.45}$$

where $M_T = \sum_{k=1}^{n} M_k$ is the sum of moment of inertias of the synchronous machines and n is the total number of machines. Then the rotor angle and speed variables of the individual units are transformed to $\theta_k = \delta_k - \delta_0$, $\tilde{\omega}_k = \omega_k - \omega_0$, and implicitly, $\dot{\theta}_k = \tilde{\omega}_k$. Now, referring back to the section on power system dynamic modeling, if we substitute the rotor angles referred to the CoI (2.45) in (2.32), and assume that the machine damping $D_i = 0$, we get,

$$\begin{aligned} M_i\frac{d^2\theta_i}{dt^2} &= P_i - \sum_{j=1,j\neq i}^{n}(C_{ij}\sin\theta_{ij} + D_{ij}\cos\theta_{ij}) - \frac{M_i}{M_T}P_{CoI} \\ &\triangleq f_i(\theta) \end{aligned} \tag{2.46}$$

where,

$$P_i = P_{mi} - E_i^2 G_{ii}; \quad P_{CoI} = \sum_{i=1}^{n} P_i - 2\sum_{i=1}^{n}\sum_{j=i+1}^{n} D_{ij}\cos\theta_{ij} \qquad i = 1, 2, ...n \tag{2.47}$$

It can be inferred from (2.45) that if one of the machines, say machine numbered n, has a very large inertia constant, such that $M_n \to \infty$ approximation can be made, then it is easy to see that $\frac{M_i}{M_T}P_{CoI} \approx 0, (i \neq n)$, and $\delta_0 \approx \delta_n$ and $\omega_0 \approx \omega_n$. Hence, the machine with the largest inertia constant becomes the reference, and its rotor angle δ_n can then simply be taken as zero. Equations (2.46) and (2.47) are modified accordingly and the number of equations is reduced to $n - 1$.

Next, we represent the detailed model (2.46) in the form of general dynamical system equations as presented in (2.21) and (2.22). Considering the case where all the machine inertias are finite, the system model for the faulted and post faulted state is given by,

$$\begin{aligned} M_i\frac{d\tilde{\omega}_i}{dt} &= f_i^F(\theta), \quad 0 < t \leq t_{cl} \\ \frac{d\theta_i}{dt} &= \tilde{\omega}_i, \quad i = 1, 2, ...n \end{aligned} \tag{2.48}$$

$$\begin{aligned} M_i\frac{d\tilde{\omega}_i}{dt} &= f_i(\theta), \quad t > t_{cl} \\ \frac{d\theta_i}{dt} &= \tilde{\omega}_i, \quad i = 1, 2, ...n \end{aligned} \tag{2.49}$$

The post fault-stable equlibrium point, $\theta = \theta_s$, can be determined by solving the set of non-linear algebraic equations,

$$f_i(\theta) = 0, \quad i = 1, 2, ...n \tag{2.50}$$

Having formulated the dynamic model in power systems, we discuss next a transient energy function (TEF), which is also a possible Lyapunov function for power system. From basic physics, we understand that a measure of rotational kinetic energy in the machines is given by $\int M_k \omega_k d\omega_k$, similarly $-\int f_k d\theta_k$ is a measure of the potential energy in the system. Also, from (2.49) we have,

$$dt = \frac{M_k d\tilde{\omega}_k}{f_k(\theta)} = \frac{d\theta_k}{\tilde{\omega}_k} \tag{2.51}$$

Hence a measure of total energy of machine at any point on the trajectory, say $(\theta_i, \tilde{\omega}_i)$, with respect to the equilibrium point (θ_i^s) of the dynamic system in (2.49) is given by,

$$V_i(\theta, \tilde{\omega}) = \frac{1}{2} M_i \tilde{\omega}_i^2 - \int_{\theta_i^s}^{\theta_i} f_i(\theta) d\theta_i, \quad i = 1, 2, ...n \tag{2.52}$$

Furthermore, the total energy of the system, which can be obtained by adding up the energy functions of all the machines, is given by

$$\begin{aligned} V(\theta, \tilde{\omega}) &= \frac{1}{2} \sum_{i=1}^{n} M_i \tilde{\omega}_i^2 - \sum_{i=1}^{n} \int_{\theta_i^s}^{\theta_i} f_i(\theta) d\theta_i \\ &= \frac{1}{2} \sum_{i=1}^{n} M_i \tilde{\omega}_i^2 - \sum_{i=1}^{n} P_i(\theta_i - \theta_i^s) - \sum_{i=1}^{n-1} \sum_{j=i+1}^{n} [C_{ij}(cos\theta_{ij} - cos\theta_{ij}^s) \\ &- \int_{\theta_i^s + \theta_j^s}^{\theta_i + \theta_j} D_{ij} cos\theta_{ij} d(\theta_i + \theta_j)] \end{aligned} \tag{2.53}$$

since the term related with the potential energy of the angle CoI (taken as reference) is zero by choice. It can be proven [41], that under the condition $D_{ij} = 0$, the transient energy function $V(\theta, \tilde{\omega})$ is a Lyapunov function. Hence, the approximated transient energy function for the discussed power system, assuming a lossless system with constant admittance loads, is written as,

$$\begin{aligned} V(\theta, \tilde{\omega}) = \frac{1}{2} \sum_{k=1}^{n} M_k \tilde{\omega}_k^2 - \sum_{k=1}^{n} P_k(\theta_k - \theta_k^s) - \\ \sum_{k=1}^{n} \sum_{j=k+1}^{N} C_{kj}(\cos\theta_{kj} - \cos\theta_{kj}^s) \end{aligned} \tag{2.54}$$

where P_k is the individual machine output before the disturbance, less the shunt power loss, N is the total number of generator buses in the system and C_{kj} are the entries from the admittance matrix. Once the energy function of a power system has been constructed, the critical clearing time, which is also a measure of stability margin, can be computed by: (1) first finding the critical energy V_{cr}, (2) and then solving the post-fault system equations in (2.49) to calculate the time it takes to reach the critical energy, which is the t_{cr}.

C. Control Lyapunov Functions

The theory of Lyapunov functions deals with dynamical systems without external inputs, and hence is applied to closed-loop control systems. Artstein in his seminal work [46] presented a theory to determine whether a system is *feedback stabilizable*. To caste the latter statement formally, consider an autonomous dynamical system of the type

$$\dot{\mathbf{x}} = f(\mathbf{x}, \mathbf{u}) \tag{2.55}$$

where $\mathbf{x} \in \mathbf{R}^n$ is the state vector of the dynamic system and $\mathbf{u} \in \mathbf{R}^m$ is the control vector input to the dynamic system. The objective is to control the dynamic system after a disturbance, such that the trajectory asymptotically converges to the origin, say $\mathbf{x} = \mathbf{0}$ where $\mathbf{0} \in \mathbf{R}^n$. Artstein showed that a control Lyapunov function $V \in \mathbf{R}$ is a continuously differentiable, positive definite function which satisfies,

$$\forall \mathbf{x} \neq \mathbf{0}, \exists u \quad \dot{V}(\mathbf{x}, \mathbf{u}) = \Delta V(x).f(\mathbf{x}, \mathbf{u}) < 0 \tag{2.56}$$

Ghandhari [47] and Noroozian *et.al.* [35] applied control Lyapunov function theory in power systems to determine control laws for different types of FACTS devices, which damp out transient oscillations in the dynamic rotor speed and angles after a disturbance. Specifically, Ghandhari [47] has derived the control laws for specific types of FACTS based controllable series devices (CSDs) applied to power systems. Control laws for such FACTS devices, which ensure the asymptotic stability of a power system, may be nonlinear functions of the rotor machine angles and speed. For instance, the control law for a Thyristor Controlled Series Capacitor (TCSC) is given by,

$$u_c = k \sin(\delta)\omega \tag{2.57}$$

where k is a proportionality constant, while ω and δ are machine rotor speed and angles respectively.

In this subsection we reviewed some of the transient stability monitoring and control techniques in power systems. In the next subsection we review some of the voltage stability assessment methods implemented in power systems.

2.3.4 Small-Disturbance Voltage Stability.

Voltage instability in power systems can be an after-effect of a small or a large-disturbance; here we are interested in the former type of disturbances. Small disturbances occur continuously in physical power systems in the form of slow load changes, action of discrete controls (e.g. tap changers), and generation units reaching their production capability limits. Small-disturbance voltage stability implies that the power system (with its control systems) is able to maintain voltages at normal operating limits at all the buses in the power system. A disturbance causing a progressive decrease in voltage levels at several buses may lead to 'voltage

collapse', causing a blackout, loss of load, or tripping of transmission lines in a major part of the power system, thus adversely affecting the reliability of the system.

2.3.4.1 Analysis of factors contributing to instability

The main reason of voltage collapse in a power system is the inability of the load dynamics to restore the consumption beyond the capability of combined generation and transmission system [4]. When a disturbance occurs in a power system, there might be a momentary gap in the power being supplied by the generation and that needed by the load. Subsequently, the power system tends to restore the power consumed by the load, for instance, by the action of tap changers, or naturally by the motors changing their slips due to the variation in voltage and frequency levels respectively. But this action may actually worsen the operating condition due to a resultant increase in reactive power consumption, and accompanying increase in the losses on the transmission lines. This leads to a run-down situation causing further voltage-reduction, which is usually followed by a voltage collapse.

Voltage collapse at a bus can also be explained in terms of the *bifurcation theory* of dynamical systems. The latter theory is concerned with the identification of 'branching' process in dynamical systems, wherein the qualitative or topological condition of the system is altered with a change in some of the system parameters [48]. The branching point is typically called a bifurcation point. Specifically, for power systems, treating the real and reactive load at a bus as slowly varying parameters, and observing the change in the local bus voltage and angle state variables on changing the parameters, one can construct a bifurcation curve. For instance, we can choose a parameter, λ, as a slowly varying parameter which relates to the per unit increase in loading at a bus, or,

$$P_{ik} = P_{i(k-1)}(1 + \lambda(k)) \qquad k \; \epsilon \; (1, 2, ..m) \tag{2.58}$$

$$Q_{ik} = Q_{i(k-1)}(1 + \lambda(k)) \qquad k \; \epsilon \; (1, 2, ..m) \tag{2.59}$$

where P_{ik} and Q_{ik} represents the real and reactive load at step k, and m are the total number of steps before a bifurcation occurs. This assumes that the power factor of the load is a constant.

For illustration purposes, let us consider an example of bifurcation in a standard IEEE-118 bus test-power system. The variation of load voltage magnitude V at bus number 38, with loading parameter, λ is shown in Fig.2.9. Matpower v.5.1 Continuation Power Flow (cpf) function was used for conducting this simulation. For low loading point A (such as $\lambda = 0.2$) there are two equilibrium solutions; one with high voltage (≈ 0.95 p.u.) and the other with low voltage (≈ 0.70 p.u.). The high voltage solution has low line current and the low voltage solution has high line current. As the loading slowly increases, these solutions approach each other and finally coalesce at the 'critical' loading B ($\lambda \approx 1.59$ p.u.). If the loading increases past B, there are no equilibrium solutions. The equilibrium solutions disappear in a saddle-node bifurcation at B. The point B is also commonly referred to as the nose-point and the

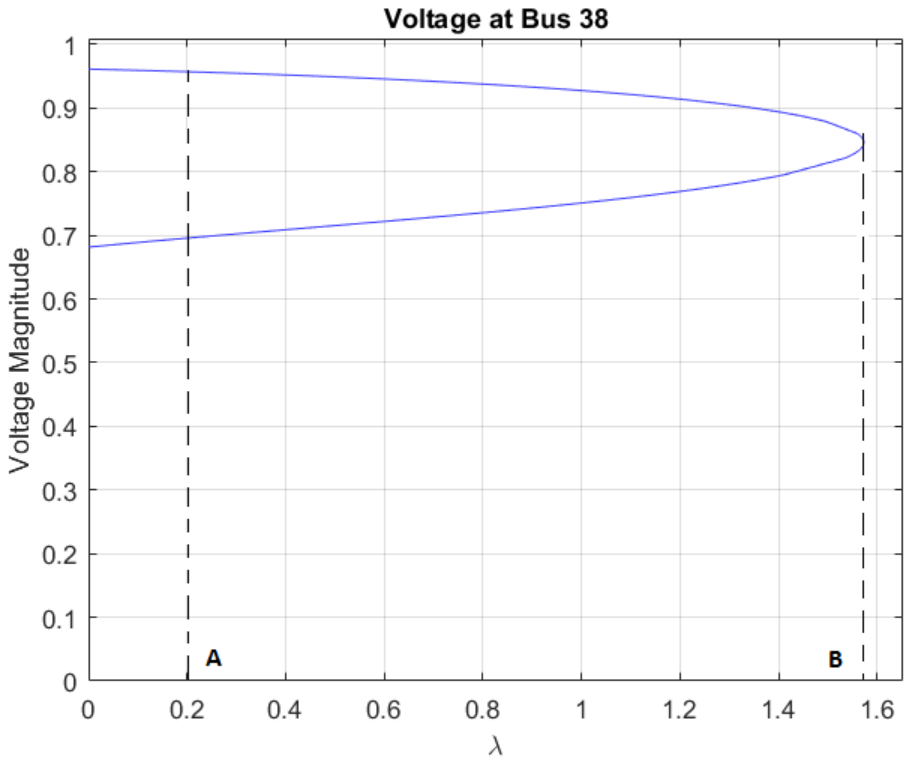

Figure 2.9: The nose curve of voltage at a bus in the IEEE standard 118 bus system.

curve in Fig.2.9 is referred to as the 'nose' curve. A detailed discussion on the mathematical analysis of this bifurcation curve is beyond the scope of this work.

2.3.4.2 Detection methods

A. General Methods

Some of the initially proposed instability detection schemes focus on taking power system equivalents at a given bus and then finding the maximum loadability of the system for which a instability may occur [49]-[50]. Many online voltage security assessment techniques have also been discussed using the artificial intelligence techniques, which aim to classify a post-disturbance system state as stable or unstable, for example, see [51]. One of the obvious causes of voltage instability in large transmission systems, during stressed conditions, is the large amount of voltage drop in the conductor impedances while transmitting the real and reactive power, thus severely limiting the overall available transfer capacity (ATC) and the voltage support. The condition is aggravated if there are generating units which have reached their capability limits of reactive power production. Van Cutsem [25] formally showed that the a system's proximity to voltage collapse can be estimated in terms of the available reac-

tive power. Schlueter *et.al.* [52] also discussed a method of instability detection in terms of loss of voltage controllability in a voltage control area, which is caused due to the depletion of reactive power basin (reserves) in that area.

B. Reactive Reserve Monitoring based

The techniques to monitor reactive reserves in the system, for an assessment of voltage stability are increasingly becoming popular. Bao et al. [24] propose a technique in which an approximation is done for the Voltage Stability Margin (VSM) of a system by monitoring its reactive reserves. A linear regression model is developed that relates the reactive reserves to VSM using offline data, with the intent to apply it in real time for instability detection. A multi-linear regression quadratic model was proposed by Leonardi and Ajjarapu [26], for improving the accuracy of the VSM estimation, especially in the non-linear regions of the P-V curve. Here we briefly outline the method to model the relationship between voltage stability margins and reactive power reserves based on regression techniques.

A simulation model of the power system under study is required for this offline exercise. Next, N-1 credible contingencies are simulated for the system, and under each contingency the loads at different buses are changed similar to (2.58)-(2.59). Assume that the net base load at i_{th} bus is denoted by $P_{i0} + jQ_{i0}$. If the net load is varied in m different steps before a local collapse occurs, loading at k_{th} step can be increased according to,

$$P_{ik} = P_{i0}(1 + \lambda_{ik}) \qquad k \; \epsilon \; (1, 2, ..m) \tag{2.60}$$

$$Q_{ik} = Q_{i0}(1 + \lambda_{ik}) \qquad k \; \epsilon \; (1, 2, ..m) \tag{2.61}$$

where $i \; \epsilon \; [1, n]$, n denotes the number of buses in the system under study. We assume a constant power factor load and λ_{ik} denotes the value of the loading parameter. The load increase direction (LID) at the k_{th} step is given by

$$\underline{\Lambda}_k = [\lambda_{1k}, \lambda_{2k}, ...\lambda_{nk}] \tag{2.62}$$

If the LID at the point of voltage collapse is denoted by $\underline{\Lambda}^* = \underline{\Lambda}_m$, then the stability margin at the k_{th} step is given by

$$VSM_k = \left\| \underline{\Lambda}^* - \underline{\Lambda}_k \right\| \tag{2.63}$$

and the reactive power reserve of the j_{th} control device at the k_{th} step is given by

$$RPR_{j_k} = Q_{j^*} - Q_{jgen_k} \tag{2.64}$$

where $j \; \epsilon \; [1, p]$, p is total number of reactive power generators (or continuous control devices) in the system under study. Q_{j^*} denotes the limit of reactive power production for j_{th} control device and Q_{jgen_k} is the amount of reactive power produced at the k_{th} step. Loading parameter $\underline{\Lambda}$ is changed and the values of VSMs and RPRs are recorded. Assume that each

observation on the voltage stability margin (y) is related with the vector of reactive reserves as

$$y = \beta_0 + x\beta_1 + x^2\beta_2 + e \tag{2.65}$$

yeilding the matrix form given by

$$\underline{y} = \underline{X}\underline{\beta} + \underline{e} \tag{2.66}$$

where $\underline{y}$ is the vector of VSM data, $\underline{X}$ is the matrix of RPRs, $\underline{\beta}$ is the parameter vector, and $\underline{e}$ is the error vector. Note that the individual elements of $\underline{\beta} = [\beta_1, \beta_2, ..\beta_p]$ represent the contribution of local reactive power generators to the stability margin. Now, under the assumption of Gaussianity, say, the errors follow $\underline{e} \sim N(\underline{0}, \sigma^2)$. It is known that if L2 norm is used, i.e.,

$$\underline{\hat{\beta}} = \arg\min_{\underline{\beta}} \left\| \underline{y} - \underline{X}\underline{\beta} \right\|_{\underline{W}}^2 \tag{2.67}$$

the optimal β is given by,

$$\underline{\hat{\beta}} = (\underline{X}^T \underline{W} \underline{X})^{-1} (\underline{X}^T \underline{W} \underline{y})^T, \tag{2.68}$$

and hence,

$$\underline{\hat{y}} = \underline{X}\underline{\hat{\beta}} \tag{2.69}$$

This method for online estimation has been studied in the present research work.

2.4 Conclusion

In this chapter we reviewed existing literature for methods of controlling dynamical system in general. Concepts of strong and weak coupling in interconnected systems were also reviewed. Necessary and sufficient conditions for stabilizing interconnected systems were shown. A brief discussion on stability assessment methods in power systems is done. Transient Energy function, which is a Lyapunov function for power systems, was studied. We also outlined a regression analysis approach to estimate voltage stability margins by measuring the available reactive power in a system.

Chapter 3

Statistical Techniques for Uncertainty Estimation: Background and Examples

Modern control techniques applied to power systems rely on decisions depending on a mixture of *measured* and *forecasted* data related to system state variables. There is uncertainty in the errors from both these sources of data. The sensor measurement errors are uncertain due to the environmental noise, while the forecasting error may have uncertainty because of reasons like inaccuracy in system models. This problem is worsened due to the increased penetration of renewable generation resources, whose forecast is dependent on weather models, which do not provide a sufficient level of accuracy. Hence, there is a necessity to estimate the uncertainty in control decisions.

It should be noted that many of the software algorithms utilized for operations, security assessment, and hence, control of power systems actually require data fusion of some type. One such class of problems discussed in power system literature is the stochastic powerflow analysis [53]-[54], which requires the sum of probability distributions of power injections at various nodes. If we were to approximate levels of uncertainty in control decisions at various hierarchical levels, then two things would be required : (a) some initial approximation/quantification of the uncertainty in errors at the primary level (like sensor reliabilities), (b) tools for approximating uncertainty in fused information at other hierarchical levels.

In this chapter, we briefly outline two methods for determining accurately the distributions of random variables. First, we discuss random coefficient regression methods, which is useful in modeling uncertainties when the independent variables are sampled from a large population. These models called 'random' (or 'mixed') effects model, accurately capture the covariances amongst the regression coefficients, which is otherwise ignored in 'fixed' effect modeling, which relies on capturing all the uncertainties in a single error term. Then, we briefly discuss the saddlepoint approximation method which is used to accurately estimate distributions of

thick-tailed (or thin-tailed) random variables. This technique will be used in the future to approximate the uncertainties in the global control decision variables, given the distributions of local control decision variables.

3.1 Why is uncertainty estimation required for power system decentralized control?

As discussed previously, the advent of new technologies in power systems, a new type of software, communication, sensing and control infrastructure is being introduced. There is an increased risk of erroneous decisions due to the software based or software supported human agents. Few examples of the causes of erroneous decisions can be:

- inaccurate measurements by the sensor systems,
- addition of noise over the metered data in the communication channel, or
- misinterpretation of the data by software or human agents

Hence, it is imperative to implement methods to determine errors in agent decisions, and to minimize them. As will be shown later, the exact computation of errors in multi-agent decision type of problems is infeasible, and hence it is easier to approximate these error probabilities. Techniques like normal approximation methods are already widely used for estimation of uncertainties. But, there a few specific reasons why power system control decision errors cannot be accurately approximated by normal approximation techniques, namely:

1. there is a multitude of sensors in power system, having different levels of reliability, measuring different state variables in the same environment,
2. the measurements might be non-identically distributed,
3. the communication channel might be noisy, causing a noise to be added to the measurements, and this noise might be non-Gaussian

3.2 Example statistical techniques for uncertainty estimation

In this section we discuss only two example classes of statistical techniques which are relevant to our research work in terms of modeling the uncertainties in the estimation of stability

margins. The first class discusses approximation of the distribution of the dependent variable in regression modeling. The second example discussed is saddlepoint approximation, which is a general class of techniques that can be also used to accurately approximate distribution of sums of (iid or non-iid) random variables.

3.2.1 Regression models with random effects

A simple regression model, is also known as a fixed effects model, because there is no uncertainty in the indpendent variable (X), and the regression coefficients (β) are assumed to have zero variance. All randomness in the model is assumed to be captured by the error terms (ϵ). Thus, a simple linear regression model is depicted as,

$$Y_i = \beta_0 + \beta_1 X_i + \epsilon_i, \quad i = 1, 2, ...n \tag{3.1}$$

In this model, an assumption of independence of error terms ϵ implies the independence of the observations Y_i and vice-versa. If the $\mathbf{Var}(\boldsymbol{\epsilon}) = \mathbf{I}\sigma^2$, then $\mathbf{Var(Y)} = \mathbf{I}\sigma^2$. Such models are also called **fixed effect models**. Many situations call for models which have random slopes (β_1) and/or random intercepts (β_0) along with the random error (ϵ) term. As discussed by Green and Tukey [101], in such models, usually the independent variables are a random sample from a population of a large set of variables. The individual variables themselves are not of any particular importance, because they may change every time a new random sample is taken, but the information provided by such random variables on the variance components in the slopes or intercepts is significant. Models in which all the regressors or 'effects' are assumed to be random are called **random effects models**. The models which have both random and fixed effects are called **mixed effect models**.

The consequence of having random terms other than the error term in a regression model is that $\mathbf{Var(Y)} \neq \mathbf{I}\sigma^2$ even when $\mathbf{Var}(\boldsymbol{\epsilon}) = \mathbf{I}\sigma^2$. It is well understood, (for instance see [96, chap.12]), that in this case the ordinary least square estimators of the type mentioned in the second chapter (2.68)-(2.69) may be inefficient. Furthermore, the standard errors computed using $\mathbf{Var}(\hat{\boldsymbol{\beta}}) = (\mathbf{X}_i^{'}\mathbf{X}_i)^{-1}\sigma^2$ are inappropriate. In the mixed effect models $\mathbf{Var}(\mathbf{Y})$ is modeled as a function of some unknown variance and covariance parameters. In such cases, estimates of the variance-covariance parameters are used to obtain the estimated generalized least squares estimates of the fixed effects. Next, first we discuss a classical statistical test based on analysis of variance to analyze random effects in such mixed effect regression models. Then, we briefly discuss a maximum likelihood approach for estimation of variance components in random regressors.

One Way Anova Model

Suppose our target is to analyze the variability in a particular random variable X with a known mean μ. Also assume that the random variable can be directly measured, and its

measurements, Y, are divided into n different groups having a measurements each. We want to analyze if the mean of each of the n groups is close to the mean of the entire population (μ), or if there is significant variability between the means of individual groups ($\mu + \alpha_i$). An appropriate model that can be used for testing in this case is the one-way Analysis of Variance (ANOVA) model:

$$\begin{aligned} Y_{ij} = \mu + \alpha_i + \epsilon_{ij}, \quad & i = 1, 2, ...a \\ & j = 1, 2, ...n \end{aligned} \tag{3.2}$$

where the α_i are assumed to be independent $N(0, \sigma_\alpha^2)$, the ϵ_{ij} are assumed to be independent $N(0, \sigma^2)$, and α_i and ϵ_{ij} are independent. A motivation for the model in (3.2) is given next.

Consider the model,

$$Y_{kj} = B_k + \epsilon_{kj}, \tag{3.3}$$

where B_k is the mean of the k^{th} group. The variability around its mean B_k for the k^{th} group of the population is measured by its variance. Assume that the population is large. Let the population mean be denoted by μ and the variance in the mean be denoted by σ_α^2. Then, from (3.3),

$$Y_{kj} = \mu + A_k + \epsilon_{kj}, \tag{3.4}$$

where $A_k = B_k - \mu$ has mean zero and variance σ_α^2. The α_is in (3.2) can thus be visualized as random samples from the population of the random variable A_k. That is, the α_i can also be assumed as random variables with mean zero and variance σ_α^2.

The model (3.2) contains two random components α_i and ϵ_{ij}. Hence, in this case,

$$Var(Y_{ij}) = \sigma_\alpha^2 + \sigma^2 \tag{3.5}$$

and, σ_α^2, σ^2 are called the **components of variance**. Thus, $\mathbf{Var(Y)} \neq \mathbf{I}\sigma^2$. Our primary goal is to first test the hypothesis, if $\sigma_\alpha^2 = 0$, and then to estimate the two components of variances σ_α^2 and σ^2 in this type of model.

One of the widely used approaches to estimate the variance components in a random effects model, based on the minimization of the sum of squares of errors, is called the analysis of variance approach. In this case, the sum of squares are calculated as though all the 'effects', other than the unique error assigned to each observation, were fixed effects. These sums of squares and their expectations under the *random* model can then be used to estimate the said variance components.

For conducting an analysis of variance for the model mentioned in (3.2), we need to estimate two quantities, the first one being the variance of means of the sample groups, given by,

$$E[GroupVar] = n \sum_{i=1}^{a} (\bar{Y}_i - \mu)^2/(a-1) \tag{3.6}$$

and the estimation of variance within each group, given by,

$$\begin{aligned} E[IntraGroupVar] &= \sum_{i=1}^{a}\sum_{j=1}^{n}(\bar{Y}_{ij} - \bar{Y}_i)^2/(a(n-1)) \\ &= \frac{1}{a}\sum_{i=1}^{a} E[\sum_{j=1}^{n}(\bar{\epsilon}_{ij} - \bar{\epsilon}_i)^2/(n-1)] = \sigma^2 \end{aligned} \tag{3.7}$$

A test for the null hypothesis $H_0 : \sigma_\alpha^2 = 0$ can now be conducted using the test statistic,

$$F = \frac{E[GroupVar]}{E[IntraGroupVar]} \tag{3.8}$$

which has the numerator with degrees of freedom $a-1$ and denominator with degress of freedom $a(n-1)$ if H_0 is true. Thus, an α-level test criterion for testing no random effect in (3.2) is that $\sigma_\alpha^2 = 0$. The test rejects the null hypothesis if $F > F_{\alpha;(a-1),a(n-1)}$. Now, if a significant variance exists, there are several methods like the maximum likelihood estimation, that can be adopted for accurately estimating the variance σ_α^2. It is discussed next, using the example of random coefficient regression model.

Random coefficient regression model

In several fields like agriculture, medicine, finance and biology, studies are performed on certain independent variables, where several measurements are taken on the same random variable over time, or under different experimental conditions, with the objective of fitting a response curve to the observed data. Such data can be analyzed using **Random coefficient regression models**. For an instance, consider a study where n different individuals are selected from a population. Each individual is administered with a medication for muscle pain, and response time is recorded. Let X_{ij} and Y_{ij} denote the dosage and the response times of the i^{th} individual on the j^{th} day. An appropriate model for such data is,

$$\begin{aligned} Y_{ij} = \alpha_i + \beta_i X_{ij} + \epsilon_{ij},\ i = 1, ..., n : individuals, \\ j = 1, ..., r : days, \end{aligned} \tag{3.9}$$

where α_i and β_i are the intercept and slope for the regression model related to the i^{th} individual. Since individuals are assumed to be a random sample from a population, it is common to assume that,

$$\begin{bmatrix}\alpha_i \\ \beta_i\end{bmatrix} \sim NID(\begin{bmatrix}\bar{\alpha} \\ \bar{\beta}\end{bmatrix}, \mathbf{\Sigma} = \begin{bmatrix}\sigma_\alpha^2 & \sigma_{\alpha\beta} \\ \sigma_{\alpha\beta} & \sigma_\beta^2\end{bmatrix}), \tag{3.10}$$

and,

$$\epsilon_{ij} \sim NID(0, \sigma^2), \tag{3.11}$$

and $[\alpha_i,\beta_i]'$ and ϵ_{ij} are independent. The equations (3.9) can further be put in a matrix form as,

$$\mathbf{Y}_i = \mathbf{X}_i\beta_i + \epsilon_i, \quad i = 1, ..., n, \tag{3.12}$$

where $\mathbf{Y}_i = (Y_{i1}...Y_{ij})'$ is a $j \times 1$ vector of responses for the i^{th} individual, $\mathbf{X}_i$ is a $j \times k$ matrix of observations on k explanatory variables, β_i is $k \times 1$ vector of coefficients belonging to the i^{th} experimental unit, and ϵ_i is a $j \times 1$ vector of errors. Furthermore, the distributions of the coefficients are denoted by $\boldsymbol{\beta}_i \sim NID(\boldsymbol{\beta}, \boldsymbol{\Sigma})$, $\boldsymbol{\epsilon}_i \sim NID(\mathbf{0}, \mathbf{I}\sigma^2)$, and $\boldsymbol{\beta}_i$ and $\boldsymbol{\epsilon}_i$ are independent. Here our focus is on estimating $\boldsymbol{\beta}$ and $\boldsymbol{\Sigma}$. Now, assuming that each of $\mathbf{X}_i'\mathbf{X}_i$ is nonsingular, we can obtain least squares estimates $\hat{\boldsymbol{\beta}}_i$ of $\boldsymbol{\beta}_i$ for each individual. That is,

$$\hat{\boldsymbol{\beta}}_i = (\mathbf{X}_i'\mathbf{X}_i)^{-1}\mathbf{X}_i'\mathbf{Y}_i \tag{3.13}$$

In this case,

$$\mathbf{Var}(\mathbf{Y}_i) = \mathbf{X}_i\boldsymbol{\Sigma}\mathbf{X}_i' + \mathbf{I}\sigma^2 \tag{3.14}$$

Furthermore, the estimator of the population mean can be simply estimated using [98],

$$\hat{\boldsymbol{\beta}} = \frac{1}{n}\sum_{i=1}^{n}\hat{\boldsymbol{\beta}}_i \tag{3.15}$$

and the unbiased estimator of the covariance matrix by,

$$\hat{\boldsymbol{\Sigma}} = (n-1)^{-1}\sum_{i=1}^{n}(\hat{\boldsymbol{\beta}}_i - \hat{\boldsymbol{\beta}})(\hat{\boldsymbol{\beta}}_i - \hat{\boldsymbol{\beta}})' - \hat{\sigma}^2 n^{-1}\sum_{i=1}^{n}(\mathbf{X}_i'\mathbf{X}_i)^{-1} \tag{3.16}$$

and the unbiased estimator of the variance by,

$$\hat{\sigma}^2 = [n(t-k)]^{-1}\sum_{i=1}^{n}[\mathbf{Y}_i'\mathbf{Y}_i - \hat{\boldsymbol{\beta}}_i'\mathbf{X}_i'\mathbf{Y}_i] \tag{3.17}$$

These simple approaches are suitable for balanced data. When the data are not balanced or have missing values, such approaches may be infeasible and lead to inefficient estimators. Maximum likelihood or Maximum Apriori Estimation based techniques are better estimators in such cases. Using this technique, we can approximate the distribution of $\mathbf{Y}$ accurately. In the next subsection, we discuss a general technique for accurately approximating distributions of certain class of random variables.

3.2.2 Saddlepoint approximation technique

The saddlepoint approximation is a valuable tool for doing asymptotic analysis. Various techniques for accurate approximation relying on saddlepoint approximations have been developed since the seminal paper by Daniels [55]. Reid [56] gives a comprehensive review

of the applications and a broad coverage of the relevant literature. Next, we present results from Daniels' seminal paper *'Saddlepoint approximations in statistics'* [55], wherein he uses this technique to approximate the distribution of the mean of n independent identically distributed random variables.

Let x be a continuously distributed random variable with distribution function $F(x)$. Assume that a density function $f(x) = F^{'}(x)$ exists and suppose the moment-generating function

$$M(T) = e^{K(T)} = \int_{-\infty}^{\infty} e^{Tx} f(x) dx \tag{3.18}$$

converges for real T in some interval containing origin. Consider the mean $\overline{x}$ of n i.i.d. random variables whose realizations can be denoted by x_i. A saddlepoint approximation to the pdf of the mean $f_n(\overline{x}) = F_n^{'}(\overline{x})$ is given by

$$\boxed{g_n(\overline{x}) = \Big[\frac{n}{2\pi K^{''}(T_0)}\Big]^{1/2} e^{n[K(T_0) - T_0\overline{x}]}}$$

and $g_n(\overline{x})$ is called the saddlepoint approximation to $f_n(\overline{x})$.

Saddlepoint approximations to the sum of known distributions

The saddlepoint approximation is applied to two examples.

Example 1. Normal distribution

$$f(x) = \frac{1}{\sigma\sqrt{2\pi}} e^{-(x-m)^2/2\sigma^2}, \qquad -\infty \leq x \leq \infty.$$

$$K(T) = mT + \frac{1}{2}\sigma^2 T^2, \qquad K^{'}(T) = m + \sigma^2 T_0 = \overline{x},$$

$$T_0 = (\overline{x} - m)/\sigma^2, \qquad K^{''}(T_0) = \sigma^2,$$

$$g_n(\overline{x}) = \frac{\sqrt{n}}{\sigma\sqrt{2\pi}} e^{-n(x-m)^2/2\sigma^2}$$

Hence, we find that the saddlepoint approximation of the sum of i.i.d. gaussian random variables is exactly equal to the real sum for all values of $\overline{x}$.

Example 2. Gamma Distribution

$$f(x) = (c^{\alpha}/\Gamma(\alpha)) x^{\alpha-1} e^{-cx}, \qquad -0 \leq x \leq \infty.$$

$$K(T) = -\alpha\, log(1 - T/c), \quad K^{'}(T_0) = \alpha/(C - T_0) = \overline{x},$$

$$K^{''}(T_0) = \overline{x}^2/\alpha,$$

and hence,

$$g_n(\overline{x}) = (n\alpha/2\pi)^{1/2} e^{n\alpha} (c/\alpha)^{n\alpha}\, \overline{x}^{n\alpha-1} e^{-nc\overline{x}}$$

The exact result is

$$f_n(\overline{x}) = [(nc)^{n\alpha}/\Gamma(n\alpha)]\overline{x}^{n\alpha-1} e^{-nc\overline{x}}$$

which differs from $g_n\overline{x}$ only in that $\Gamma(n\alpha)$ is replaced by Stirling's approximation in the normalizing factor.

Comparison of saddlepoint and normal approximations

A study was conducted to compare the performance of the saddlepoint and normal approximation. First, the saddlepoint and normal approximations were derived analytically, like in the examples above, and then simulations were carried to graph the errors in approximation. As an example, a normal approximation for the sum of i.i.d. random variables following a gamma distribution can be determined by noticing,

$$\mu_n(x) = nE(X) = n\frac{\alpha}{c}, \quad Var_n[X] = n\frac{\alpha}{c^2}$$

hence sum of i.i.d. gamma random variables follows a normal distribution $\sim N(\frac{n\alpha}{c}, \frac{n\alpha}{c^2})$. In fig. 3.1, a comparison of normal approximation with saddlepoint approximation is given for the sum of i.i.d. Gamma random variables. It can be observed that the normal distributions poorly approximate the sum, specially at the tails.

Similar approximation was determined for the sum of Laplacian Random Variables. In Fig.3.2, a comparison is given for the saddlepoint and normal approximations for Laplacian random variable. Notice that for slightly thick tailed Laplace distribution, the normal distribution performs poorly at the tails.

There are some obvious disadvantages associated with the normal approximations, which saddlepoint approximations do not suffer:

1. the Central Limit Theorem is valid only for a very large number of random variables, with low to moderate sized systems, it might not give a good approximation
2. the approximation might be unsuitable for estimating the tail probabilities, when the tail probabilities themselves are very small.
3. the normal approximation has an error proportional to $O(n^{-1/2})$ while there exist better approximations like the saddlepoint with errors proportional to $O(n^{-1})$

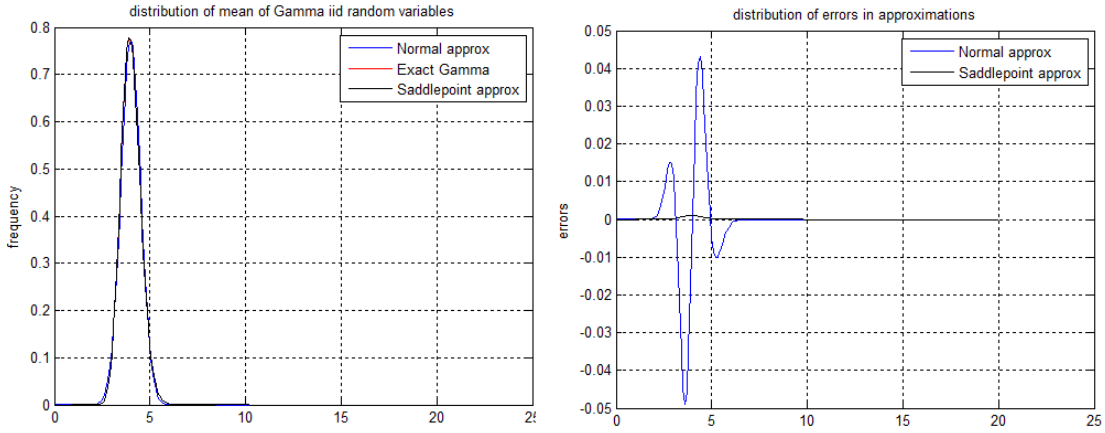

Figure 3.1: Approximations to the sum of n Gamma i.i.d random variables. Left: Approximated distributions compared with the original distribution. Right: Errors in approximation. Blue curves represent normal approximation and black curves represent saddlepoint approximation

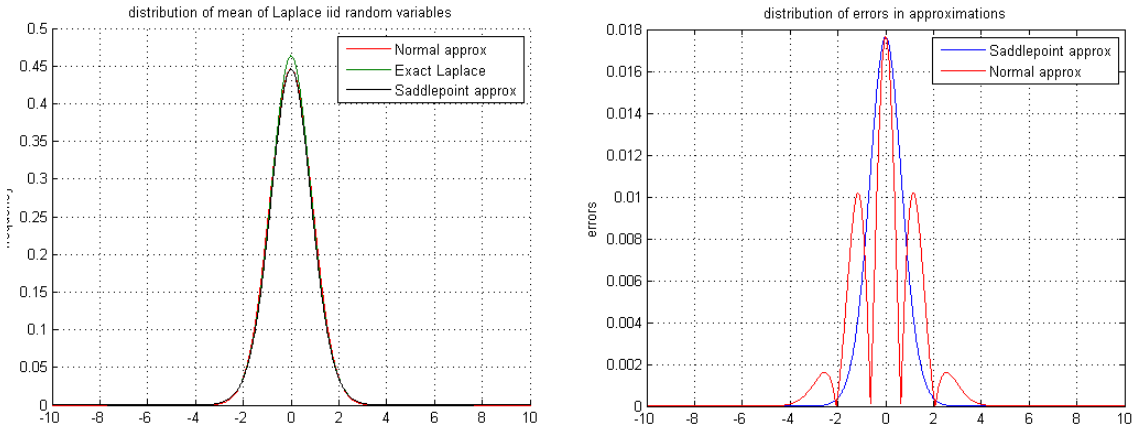

Figure 3.2: Approximations to the sum of n Laplacian i.i.d random variables. Left: Approximated distributions compared with the original distribution. Right: (Absolute) Errors in approximation. Red curves represent normal approximation and blue represent saddlepoint.

Chapter 4

Hierarchical Decentralized Control for Enhanced Rotor Angle and Voltage Stability of Large-Scale Power Systems

4.1 Introduction

A[1] reliable delivery of electrical power to the end customer necessitates stable operation of the power grid at all times. Power utilities ensure stable operation of the grid by implementing frequency, voltage and rotor angle instability detection and control mechanisms. Furthermore, the deployment of synchropahsor measurement units (PMUs) and FACTS devices in power transmission systems by many electric power utilities, worldwide, have opened the door to wide-area dynamic monitoring and control, as evidenced by the growing literature on that topic. For instance, Kamwa *et al.* [57],[58] provided an overview of the research undertaken in that area at Hydro-Quebec. Sun *et al.* [59] developed an online dynamic security assessment method using a decision tree technique. Mehrjerdi *et. al.* [31],[32] initiated a graph-theoretic method together with a wide-area fuzzy-logic control scheme. Ghandhari [47] and Noroozian *et al.* [35] derived control laws on FACTS devices to damp transient oscillations in power systems using an energy function approach. Leonardi and Ajjarapu [26] proposed a method to estimate the reactive power availability in a power system from wide-area measurements. It turns out that the aforementioned techniques neither exploit the presence of coherent areas in large-scale power systems nor do they make use of decentralized control techniques to damp system instabilities, for example as proposed by Sandell *et al.* [5] and Bailey [10]). Moreover, no control mechanisms were proposed to damp in a unified

[1] Based on our work in [92]

way both transient rotor angle and voltage instabilities. The only exception is the work of Guo *et al.* [34], who proposed global control using energy functions to damp transient angle and voltage instabilities at an individual synchronous machine level, not at the system level.

In this chapter, we propose hierarchical decentralized control schemes for both rotor angle and voltage instabilities based on PMU measurements collected from each coherent area of a large-scale power system, without any exchange of information between areas. To this end, we make use of a method proposed by Lie *et al.* [60] based on voltage controllability to identify the coherent areas of an interconnected power system. We provide a theoretical foundation of that method using the singular perturbation method of Chow [36]. We introduce a multi-agent system framework for decentralized damping of rotor-angle oscillations (post large disturbances) and hierarchical decentralized voltage control (post small disturbances). Following Bailey [10], we derive a local control law using Lyapunov's second method for interconnected systems to damp rotor angle instabilities in one area, which are induced by neighboring areas. For this control law, we prove sufficient conditions of asymptotic stability of the power system. Furthermore, we develop coherent area-wise regression models between available reactive power and voltage stability margins, as opposed to a centralized model developed by Leonardi and Ajjarapu [36]. The proposed regression estimator can handle heterosckedasticity in the independent variable data. We develop a three-level hierarchical control scheme for voltage stability. In this scheme, each secondary control agent monitors its own coherent ('control') area and initiates local proactive control actions based on estimated stability margins; a tertiary control agent provides steady-state reference settings for each coherent area and takes slower reactive control actions in case the local agents fail to prevent instabilities, or worse, destabilize the system. As opposed to traditional hierarchical control schemes, our scheme does not need to exchange information between control areas or to send signals to a central controller, which leads to smaller communication requirements than those of completely centralized wide-area controllers. Furthermore, it exhibits better situational awareness than those of completely localized control schemes.

Development of such coordinated decentralized control schemes is even more important today due to continual integration of distributed generation resources in the power grids, which can be intermittent in nature. The intermittent nature of the power produced from the renewable resources, may sometimes lead to a low voltage situation at certain nodes, while at other times, excessive power production might cause local over-voltages and congestion in lines. Line congestion may further lead to other type of instability phenomena in the system. In Fig.4.1, three loosely coupled areas are shown for an example power system. Each of these areas has its local generation, load and local controllers. The generation and load in the figure represents a host of generation and energy consumers (respectively) aggregated together. These areas are interconnected with high reactance tie lines, forming the boundaries between areas, depicted by dotted blue lines in the figure. In this chapter, we discuss: (a) methods to determine such decoupled areas, (b) methods to observe state variables in each area, (c) methods to detect instabilities in each area, (d) implementation of a hierarchical voltage control mechanism and (e) distributed control mechanism for transient

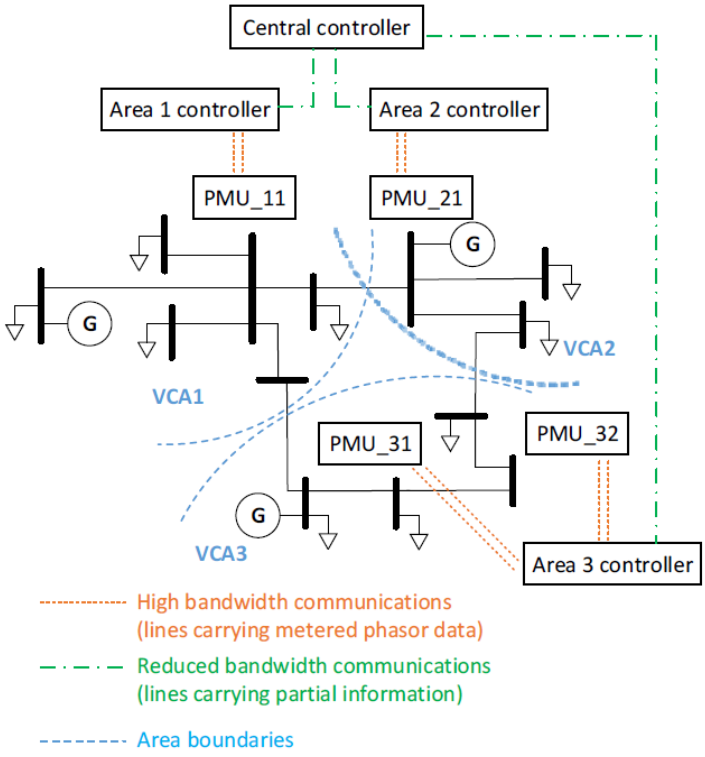

Figure 4.1: Decentralized voltage control in a loosely coupled power system. Three control areas are depicted in this figure

instability.

The rest of this paper is organized as follows. Section 4.2 gives an overview of the proposed framework for hierarchical, coordinated control. Sections 4.3 and 4.4 outline power system implementation of the proposed framework. Chapter 7 discusses simulation results of the proposed scheme on the IEEE 118-bus system.

4.2 Hierarchical, decentralized control framework

In this section, we describe the architecture and operation of the proposed hierarchical, coordinated, decentralized voltage instability detection and control scheme using a framework compliant with the Foundation of Physical Agents (FIPA) standards [7],[8].

4.2.1 Assumptions

Let us state the assumptions underlying the proposed MAS framework for power system hierarchical control:

- The power system is a weakly coupled system, that is, it consists of a collection of subsystems loosely connected through long lines with high reactances;
- Each subsystem is controllable when disconnected from the rest of the power system;
- Each subsystem is completely observed by fast synchrophasor measurement devices;
- Control devices such as capacitor banks and FACTS devices have been installed at strategic locations within each coherent area;
- Some of the aforementioned devices are fast responding controllers to transient oscillations;
- System dynamics such as Hopf bifurcation, limit cycles, and chaos are absent;
- High-speed communication networks are available so that time-lags of control signals may be neglected.
- The demand has a certain degree of elasticity.

4.2.2 Multi-agent framework for hierarchical control

At this point we assume the presence of sub-control areas (or simply, control areas) within the power system under study. In a later subsection we will outline one of the methods to determine different control areas in a loosely interconnected power system. A Multi-Agent System architecture for Decentralized Control of a large-scale, interconnected power system is illustrated in Fig.4.2. Each regional control area may consist of load buses representing several aggregated distribution substations at close electrical distances or an industrial substation supplying a larger load. Each of these control areas is supervised by a secondary or 'local control agent.' A tertiary or 'global control agent', supervises a number of local control agents. Usually small to medium size utilities will be supervised tertiary level controller, while very large interconnected grids might be supervised by multiple tertiary controllers.

As illustrated in Fig.4.2, each local control agent has three types of inputs: 1) metered data from local measurement devices (PMUs), 2) Voltage reference settings from the tertiary controller for steady state of operation, and 3) Each local control agent executes a state estimator to estimate its respective area state [30]. The state estimates can be used to compute local stability margins, which can be regarded as a metric of the overall stability of the corresponding area. For instance, the difference between the critical clearing angle and

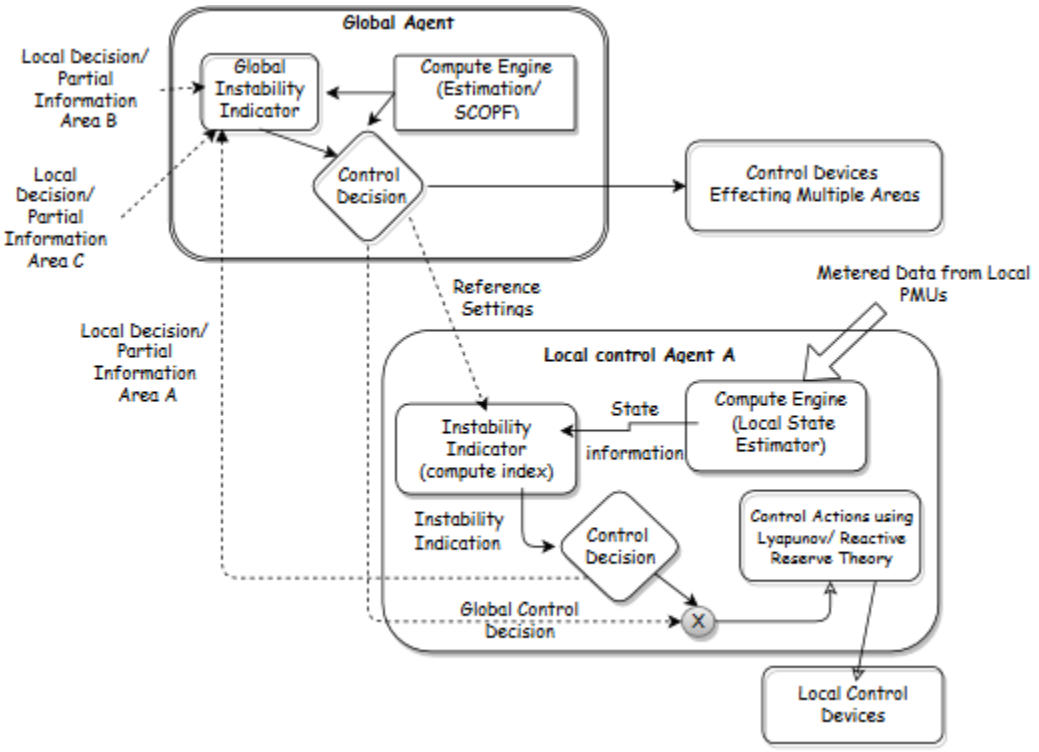

Figure 4.2: Multi-Agent System Architecture for Hierarchical Voltage Control.

estimated rotor angle is a measure of the angular stability margin. Similarly, the difference between the estimated of reactive power available in the area currently and that during a voltage collapse condition is a measure of the voltage stability margin for the area. Using these stability margins, a local control device (controller) may initiate control actions based on two different control laws depending upon whether the system experiences a large or a small disturbance. It should be noted that control agents may execute control actions based on different control laws, during the large and small disturbances in the system. These can be discrete control actions like turning off and on of a capacitor bank or moving load tap changers, or continuous control actions like modulating the power output from a STATCOM. (The reader is referred to Sections 4.3, 4.4 for details about the control laws underlying these actions.) The control actions can be inhibited by the decision of the global controller from the previous decision cycle, for example in case of a cascading failure situation.

As for the global (system) control agent, it receives and processes the state estimates of all the areas along with the SCADA measurements of the tie-lines, if any, and calculates the state estimates of the overall system [61]. The global agent may run an hourly Security Constrained Optimal Powerflow (SCOPF) based on these state estimates to determine the voltage/power references for each of the local control agents. One of the critical tasks of the global control agent is to achieve the oversight of the complete system, hence ensuring global situational awareness, which none of the local control agents have independently. To

this end, when it detects an emergency situation (e.g., a cascading failure in the system) it may do the following: (i) Inhibit some of the local agents from taking any actions in the next decision cycle and control some devices that impact the stability of multiple areas; (ii) Support the local agents with additional control signals; (iii) Do nothing when the local agents take actions. As an example, the tertiary controller can block the action of OLTCs (which may be otherwise controlled locally) during system emergencies.

It should be noted that it is of paramount importance that the actions of secondary and tertiary controllers should not conflict with each other, or lead to any unnecessary instability in the system. Hence, actions of type (b) are not recommended. By design, the scheme should ensure a time-scale decomposition where the local control agents should proactively take actions by predicting incipient instabilities in the sub-systems. Once the local control agents have taken their actions, then the global control agent should react (if required) in the next decision cycle, for example by taking action (a) or (c). These decision cycles shall continue recursively. Furthermore, different secondary controllers are allowed to function simultaneously within different subsystems. As discussed later, sufficient conditions can be determined so that there is no conflict between different secondary controller actions. Next, we present a method based on singular perturbation to identify the coherent areas of a power system.

4.2.3 Methods for identifying weakly coupled coherent areas

Many power systems are weakly coupled [60],[36]. They are composed of areas whose state variables are responding 'coherently' (i.e., in synchronism) [36] to specific types of disturbances. For instance, 18 control areas for secondary voltage control have been identified [28] at the 400/230 kV levels of the Italian power system while 9 coherent areas have been identified at the 315/735 kV levels of the 783-bus Hydro-Québec system [58] for dynamic security assessment.

A weakly-interconnected system of N coherent areas whose system matrix has been re-ordered such that the state variables of each area are listed together is given by

$$\begin{bmatrix} \dot{\underline{x}}_1 \\ \dot{\underline{x}}_2 \\ \vdots \\ \dot{\underline{x}}_N \end{bmatrix} = \begin{bmatrix} \mathbf{A}_{11} & \epsilon\mathbf{A}_{12} & ...\epsilon\mathbf{A}_{1N} \\ \epsilon\mathbf{A}_{21} & \mathbf{A}_{22} & ...\epsilon\mathbf{A}_{2N} \\ \vdots & & \\ \epsilon\mathbf{A}_{N1} & \epsilon\mathbf{A}_{N2} & ...\mathbf{A}_{NN} \end{bmatrix} \begin{bmatrix} \underline{x}_1 \\ \underline{x}_2 \\ \vdots \\ \underline{x}_N \end{bmatrix} + \begin{bmatrix} \mathbf{B}_{11} & \mathbf{B}_{12} & ...\mathbf{B}_{1N} \\ \mathbf{B}_{21} & \mathbf{B}_{22} & ...\mathbf{B}_{2N} \\ \vdots & & \\ \mathbf{B}_{N1} & \mathbf{B}_{N2} & ...\mathbf{B}_{NN} \end{bmatrix} \begin{bmatrix} \mathbf{u}_1 \\ \mathbf{u}_2 \\ \vdots \\ \mathbf{u}_N \end{bmatrix}. \tag{4.1}$$

Here ϵ is a small positive parameter that is indicative of a weak coupling amongst subsystems. Obviously, the control areas will evolve into independent subsystems if $\epsilon \to 0$ and $\mathbf{B}_{ij} = 0$

for $i \neq j$. In general, an interconnected power system linearized around an operating point in the quasi steady-state can be represented by a dynamical model expressed as

$$\begin{bmatrix} \Delta\underline{\ddot{\delta}} \\ \mathbf{0} \end{bmatrix} = \begin{bmatrix} \underline{\mathbf{A}} & \underline{\mathbf{B}} \\ \underline{\mathbf{C}} & \underline{\mathbf{D}} \end{bmatrix}_{\delta_0, V_0} \begin{bmatrix} \Delta\underline{\delta} \\ \Delta\underline{V} \end{bmatrix} + \begin{bmatrix} \underline{\mathbf{E}} \\ \mathbf{0} \end{bmatrix}, \tag{4.2}$$

where the upper part of the relationship describes the dynamical equations of the classical models of the synchronous machines and the lower part represents the load-flow algebraic equations. In (4.2), δ denotes the rotor angle of a machine, E denotes its internal e.m.f. and V denotes a nodal voltage phasor of the transmission system. It has been shown in [36],[60] that the network admittance matrix $\underline{\mathbf{D}}$ in (4.2) can be used to identify the weakly coupled areas of a power system, yielding a dynamical model given by (1).

Specifically, Chow [36, Chapter 3] showed that the network admittance matrix $\underline{\mathbf{D}}$ can be decomposed into two matrices representing internal and external connections denoted by the subscripts I and E, respectively, yielding

$$\underline{\mathbf{D}} = \underline{\mathbf{D}}^I + \epsilon_D \underline{\mathbf{D}}^E. \tag{4.3}$$

The weak coupling parameter, ϵ_D, which is also a perturbation parameter, classifies the dynamical state variables associated with $\underline{\mathbf{D}}^I$ into strongly coherent groups that form coherent areas and that are weakly (or slowly) coherent with each other in the sense that their nodal voltage magnitude and rotor angle differences remain nearly constant when the system is subject to large disturbances, for example induced by short-circuits. The weak coupling parameter in (4.3) is defined as

$$\epsilon_D = \frac{B^E_{ij} \gamma^E_{max}}{B^I_{pq} \gamma^I_{min}}, \tag{4.4}$$

where B^E_{ij} and B^I_{pq} denote the maximum admittances and γ^E_{max} and γ^I_{min} denote the maximum number of connections of the external and internal subsystems, respectively, which are all calculated from $\underline{\mathbf{D}}$. The reader is referred to [36] for a detailed discussion on the coupling parameter. We will refer to this method as the Weak Coupling Parameter (WCP) method.

Another approach was developed by Schlueter [52], termed the Weak Branch (WBE) method. This method determines the coherent areas of a system as the ones encompassing buses that have similar voltage collapse patterns when the system undergoes slow increases in demand. It consists of the following steps. First, the parameter B^I_{pq} is used to normalize all the admittances in $\underline{\mathbf{D}}$. Then, a threshold α is chosen for every row of that matrix, and a subset of the matrix elements whose sum is less than α are eliminated. We argue that both the WBE and the WCP methods will lead to the identification of nearly the same coherent areas of a power system. The reason is that they implement similar procedures. To see that, let us analyze the expression given by (4.4) for the WBE method. Since the factor γ^E_{max} is the total number of external branches, the numerator of that ratio normalized by the maximum admittance forms an upper-bound for the threshold α. In our work, we use first the WBE method to identify the coherent area boundaries and then we apply the WCP

method based on equivalent machine inertias to find the equivalent machine representations for every coherent area. Once the coherent areas are determined, it is important to check the observability of the power system, which has to be equipped with a redundant collection of synchrophasor measurements that provide a time-stamped snapshot of the system state.

4.2.4 PMU placement and dynamic state estimation

Although not directly applicable for our simulation based study, yet it is important to briefly discuss observability of the system. Synchronized phasor measurement devices like PMUs provide a time-stamped snapshot of the system state, which is key for the proposed online stability analysis and control of power system [62]. Mili *et. al.* [63] pointed out that only pilot point measurements may not be sufficient for complete observability, and proposed a simulated annealing based method for optimally placing the synchrophasor units. As detailed in the next subsection, our method depends on monitoring the reactive reserves of the system, and hence an estimation of the state of the control area is required. We propose the use of simulated annealing method to optimally place the PMU units in every voltage control area such that each of the state variables is observed at every node. This does lead to a sub-optimal solution inasmuch as the number of installed PMU devices is concerned, but, no inter-area communication will be required and the local controllers will take control actions based on locally observed state leading to a lesser overall infrastructure cost. In the next section, we derive local control laws based on Lyapunov's second method that ensures global rotor angle stability following large disturbances.

4.3 Decentralized control for rotor angle stability improvement

4.3.1 An energy function perspective for system stability

There exists a large literature that deals with Lyapunov's direct method for analyzing power system stability (see for example [47],[41]). As discussed in chapter 2, this method states that if (i) there exists a positive definite function $V(\underline{x})$ of the system states $(\underline{x})$ that is positive definite and (ii) if the derivative of this function, $\dot{V}(\underline{x})$, with respect to time is negative semidefinite, along the trajectory of the states post a disturbance, then the system is stable in the sense of Lyapunov. It has been shown that the energy function, which is the sum of the kinetic and potential energy of the system for post-fault condition [41], is a candidate Lyapunov function for a power system. It can be deduced from the energy function theory that during power system operation, there is a region of attraction of an equilibrium point, which is often referred to as the 'stability region'. Two important characteristics of this region, both of which serve as instability indices, can now be outlined:

- The **size** of this stability region around any equilibrium point, which is dependent upon the system loading. During a small disturbance such as a slow load increase, the system moves from one stable equilibrium point (s.e.p.) to another, along the stability boundary, due to which the surface of the stability region shrinks.
- The **distance** of the current stable equilibrium point to the closest unstable equilibrium point (u.e.p.) along the boundary of stable region, which characterizes the critical energy (V_{cr}) that can be pushed into the system before the system looses its stability.

Traditionally, the steady state voltage stability is studied by only effecting the system load slowly, while causing no external disturbances on any other state variable. This causes the system trajectory to slowly evolve along the stable manifold such that it continually approaches an u.e.p. where a saddle-node bifurcation occurs and no s.e.p exists on further loading. As pointed earlier, this type of instability can be studied by understanding the shape of the stability region at each system loading, but as pointed by Overbye [64] such methods are unsuitable for an online implementation due to the computational complexity. We propose a voltage instability detection and control method suitable for online implementation, which is discussed in the section 4.4. This method doesn't rely on inferring the shape or size of the stability region. In a subsequent section, we discuss the system stability under large disturbances, which is studied using the classical energy function approach, with one modification. The global asymptotic stability conditions are derived using Lypunov's second method for interconnected systems, which suits the proposed decentralized control approach.

4.3.2 Local control agent action post large disturbances.

By contrast to prior work that models a power system as a strongly interconnected one, we assume that the system is weakly interconnected as defined by (4.1). We also assume that each subsystem is equipped with control devices such as FACTS based SVCs and TCSCs. Using the sufficient conditions proposed by Bailey in [10] for stability of such system following a large disturbance, we derive the control laws for each of the local control devices. Note that here the approximation $\epsilon \rightarrow 0$ is invalid. Furthermore, we assume that each subsystem of a weakly interconnected system is independently stabilizable and that it has a Lyapunov function. Denoting the latter by V_i and its time-derivative by $\dot{V}_i$ of the i_{th} subsystem, for $i \; \epsilon \; [1, N]$, the global asymptotic stability of the system when subject to a disturbance is ensured if we can find an M-matrix $\underline{\mathbf{H}}$ such that

$$\dot{\mathbf{V}} \leq \underline{\mathbf{H}} \, \mathbf{V}, \tag{4.5}$$

where $\mathbf{V}$ and $\dot{\mathbf{V}}$ are the column vectors consisting of the Lyapunov functions of all the subsystems and their time derivatives, respectively [10]. Next, we first derive the individual energy functions, $V_i(\underline{\mathbf{x}}_i)$, for each of the power system control areas and then we determine the control laws for every control devices using (4.5) to ensure global system stability.

Let δ_{0_i} and ω_{0_i} respectively denote the center of inertia and the center of speed of the i_{th} coherent area, which are given by

$$\delta_{0_i} = \frac{1}{M_{T_i}} \sum_{k_i=1}^{n_i} M_{k_i} \delta_{k_i}, \quad \omega_{0_i} = \frac{1}{M_{T_i}} \sum_{k_i=1}^{n_i} M_{k_i} \omega_{k_i}. \tag{4.6}$$

Here n_i denotes the total number of generator units and $M_{T_i} = \sum_{k_i=1}^{n_i} M_{k_i}$ is the sum of the moments of inertia of the units in the area. The rotor angle and speed variables of the individual units are transformed to $\theta_{k_i} = \delta_{k_i} - \delta_{0_i}$ and $\tilde{\omega}_{k_i} = \omega_{k_i} - \omega_{0_i}$, yielding $\dot{\theta}_{k_i} = \tilde{\omega}_{k_i}$. The approximated transient energy function [41] for this control area, assuming a lossless system with constant admittance loads, is written as

$$\begin{aligned} V_i(\theta, \tilde{\omega}) = \frac{1}{2} \sum_{k_i=1}^{n_i} M_{k_i} \tilde{\omega}_{k_i}^2 - \sum_{k_i=1}^{n_i} P_{k_i}(\theta_{k_i} - \theta_{k_i}^s) - \\ \sum_{k_i=1}^{n_i} \sum_{j=k_i+1}^{N_g} C_{k_i j}(\cos\theta_{k_i j} - \cos\theta_{k_i j}^s), \end{aligned} \tag{4.7}$$

where P_{k_i} denotes the individual machine output before the disturbance is applied, less the shunt power loss, N_g denotes the total number of generator buses in the system (internal & external), and $C_{k_i j}$ are the elements of the admittance matrix. Similarly, the time derivative of the energy function for the i_{th} area derived in [47] is expressed as

$$\dot{V}_i = -\sum_{k_i=1}^{n_i} D_{k_i} \tilde{\omega}_{k_i}^2 + f_i(\theta, \tilde{\omega}), \tag{4.8}$$

where D_{k_i} denotes the damping constant of the k_{th} machine and $f_i(\theta, \tilde{\omega})$ denotes the control law for the FACTS device in the i_{th} area. The energy function given by (4.7) has to be modified, depending upon the specific type of control device implemented. Similarly in (4.8), the control law is implemented for the device(s) included in (4.7). The reader is referred to [35] for a detailed derivation of the energy function and control law of a power system provided with two TCSCs and one SVC.

Next, we make some approximations to simplify the derivation of the local control laws. Based on the results given by Chow [36] and assuming that the machines in each of the coherent areas are strongly coherent, we further simplify the energy function given by (4.7). According to the definition of strong coherency, each of the machines belonging to a coherent area will have coherent swings that are represented as $(\delta_{k_i} - \delta_{0_i}) \approx c_{k_i l_i}(\delta_{l_i} - \delta_{0_i})$ and $(\omega_{k_i} - \omega_{0_i}) \approx c_{k_i l_i}(\omega_{l_i} - \omega_{0_i})$, where k_i and l_i are indexes of two machines in the i_{th} coherent area and $c_{k_i l_i}$ is a positive constant close to one. This assumption leads to the following simplifications:

$$\frac{1}{2} \sum_{k_i=1}^{n_i} M_{k_i} \tilde{\omega}_{k_i}^2 \approx \frac{1}{2} \tilde{\omega}_i^2 \sum M_{k_i} c_{k_i l_i} \approx \frac{1}{2} \tilde{\omega}_i^2 M_i, \tag{4.9}$$

where $M_i = \sum M_{k_i} c_{k_i l_i}$ is an approximation of the area inertia and $\tilde{\omega}_i^2$ is the equivalent rotor speed, which takes close values for all the coherent machines. Similarly, we have

$$\begin{aligned} \sum_{k_i=1}^{n_i} P_{k_i}(\theta_{k_i} - \theta_{k_i}^s) &\approx (\theta_{k_i} - \theta_{k_i}^s) \sum P_{k_i} c_{k_i l_i} \\ &\approx (\theta_i - \theta_i^s) P_i. \end{aligned} \tag{4.10}$$

For the synchronous machines located in the same coherent area, we can assume that $\cos\theta_{k_i j} \approx 1$, yielding $(\cos\theta_{k_i j} - \cos\theta_{k_i j}^s) \approx 0$. The last summation term in (4.7) reduces to

$$\sum_{j=1}^{N_g} C_{ij}(\cos\theta_{ij} - \cos\theta_{ij}^s), \tag{4.11}$$

where j is the index of the summation over the external tie-lines of the i_{th} coherent area. Using (4.9)-(4.11), the relationships (4.7) and (4.8) are written as

$$\begin{aligned} V_i(\theta, \tilde{\omega}) = \frac{1}{2} M_i \tilde{\omega}_i^2 - P_i(\theta_i - \theta_i^s) - \\ \sum_{j=1}^{N_g} C_{ij}(\cos\theta_{ij} - \cos\theta_{ij}^s), \end{aligned} \tag{4.12}$$

and

$$\dot{V}_i(\theta, \tilde{\omega}) = -D_i \tilde{\omega}_i^2 + f_i(\theta, \tilde{\omega}), \tag{4.13}$$

where D_i denotes the equivalent damping of the coherent area. Now, the derivation of the local control law requires finding $f_i(\theta, \tilde{\omega})$ and the entries h_{ij} of the matrix $\underline{\mathbf{H}}$ such that

$$-D_i \tilde{\omega}_i^2 + f_i(\theta, \tilde{\omega}) \leq -h_{ii} V_i(\theta, \tilde{\omega}) + \sum_{j=1, j\neq i}^{N} h_{ij} V_j(\theta, \tilde{\omega}). \tag{4.14}$$

Here the conditions for $\underline{\mathbf{H}}$ being an M-matrix dictates that h_{ij} are positive constants under the condition

$$h_{ii} \geq \sum_{j=1, j\neq i}^{N} h_{ij}. \tag{4.15}$$

It can be seen that these conditions are satisfied if the entries are chosen such that

$$h_{ii} = \frac{2D_i}{M_i}, \tag{4.16}$$

$$h_{ij} = \begin{cases} \frac{h_{ii}}{m_i} & \text{if } C_{ij} \neq 0, \\ 0 & \text{if } C_{ij} = 0, \end{cases} \tag{4.17}$$

where m_i is the total number of non-zero entries in the i_{th} row of the C matrix. From (4.14), we have

$$-D_i\tilde{\omega}_i^2 + f_i(\theta,\tilde{\omega}) \leq -\frac{2D_i}{M_i}V_i(\theta,\tilde{\omega}) + \frac{2D_i}{m_i M_i}\sum_{j=1,j\neq i}^{N} V_j(\theta,\tilde{\omega}). \tag{4.18}$$

Substituting (4.12) in (4.18) yields

$$\begin{aligned} f_i(\theta,\tilde{\omega}) \leq -\frac{2D_i}{M_i}[P_i(\theta_i-\theta_i^s) - \sum_{j=1,j\neq i}^{m_i}\frac{1}{m_i}P_j(\theta_j-\theta_j^s) \\ - \sum_{j=1,j\neq i}^{m_i} C_{ij}(1-\frac{1}{m_i})\cos\theta_{ij} + \sum_{j=1,j\neq i}^{m}\frac{1}{2}\tilde{\omega}_j^2 M_j]. \end{aligned} \tag{4.19}$$

Since the last term in the r.h.s. of the inequality is always positive, we can now define the local control law as

$$\begin{aligned} f_i(\theta,\tilde{\omega}) = -\frac{2D_i}{M_i}[P_i(\theta_i-\theta_i^s) - \sum_{j=1,j\neq i}^{m_i}\{\frac{1}{m_i}P_j(\theta_j^{cr}-\theta_j^s) \\ -C_{ij}(1-\frac{1}{m_i})\cos\theta_{ij}^{cr}\}], \end{aligned} \tag{4.20}$$

where θ_j^{cr} is the critical clearing angle of the j_{th} area and $\theta_{ij}^{cr} = \theta_i - \theta_j^{cr}$. It is noteworthy that in a decentralized control scenario, each control device has three types of information: (i) some constant parameter values such as those of M_i, D_i, C_{ij}, and m; (ii) locally estimated state variables like θ_i, P_i; from the secondary control agent, and (iii) information received from the global control agent after the execution of the optimization routine, like generator power injections P_j. However, the information of measured signals from other areas like θ_j is not available; hence for designing the control law in (4.20) we use the critical clearing angle θ_j^{cr} for the interconnected areas, which can be calculated a priori and sent to each area by the tertiary control agents. Furthermore, if the disturbance is such that the system does not become unstable after the first swing, that is, if $\theta_j \leq \theta_j^{cr}$ along the trajectory, then it is easy to see that $-(\theta_j^{cr}-\theta_j^s) \leq -(\theta_j-\theta_j^s)$ and $-\cos\theta_{ij}^{cr} \leq -\cos\theta_{ij}$. It is obvious that the control law derived in (4.20) has a linear dependence on the angle θ. This local control law can be implemented on a FACTS based controller belonging within a specific region, working on locally measured control signals. As an example, it can be shown by arguments similar to the ones presented in [35] that the series reactance of such a TCSC should be varied according to $X_i^{TCSC} = kf_i^2(\theta,\tilde{\omega})\frac{d}{dt}V_{TCSC}^2$, where k is a positive constant and V_{TCSC} is the locally measured voltage. By using this control technique, we ensure that there is no inter-area communication required, and that the global asymptotic stability is achieved.

4.4 Hierarchical control for voltage stability improvement

In this section, we present the secondary and tertiary control actions for voltage stability improvement.

4.4.1 Actions of the local control agents

Now, we discuss the action of local control agents under small disturbances, in the quasi steady-state of operation. Assuming that only slow load changes take place while other state variables are not disturbed externally, a direct relationship can be found between the proximity to a voltage collapse and the availability of local reactive power. The proximity to voltage collapse, also known as the *Voltage Stability Margin* (VSM), can be represented in terms of the difference between the existing system load and the system load at the point of collapse [25]. Previous researchers have suggested using regression models to represent the relationship between voltage stability margins and reactive power reserves [4], [26]. Leonardi and Ajjarapu [26] propose a multi-regression model that can also capture the non-linearities when system is heavily loaded. Here, we develop multi-linear regression models for capturing the relationship between the available reactive power reserves (RPRs) and stability margins in *each control area*. The approximation $\epsilon \rightarrow 0$ in (4.1) is valid here, since there is minimal exchange of reactive power due to the high reactance of the interconnecting branches.

In the proposed technique, N-1 credible contingencies are simulated for the system, and under each contingency the loads specific to each of the control areas are increased in succession. Assume that the net base load at the i_{th} bus is denoted by $P_{i0}+jQ_{i0}$. If the net load is varied in m different steps before a local collapse occurs, loading at the k_{th} step can be increased according to $P_{ik} = P_{i0}(1+\lambda_{ik})$ and $Q_{ik} = Q_{i0}(1+\lambda_{ik})$, where $k \, \epsilon \;\; (1, 2, ..m)$, $i \, \epsilon \, [1, n]$, and n denotes the number of buses in the coherent area under study. We assume a constant power factor load and λ_{ik} denotes the value of the loading parameter. The Load Increase Direction (LID) at the k_{th} step is given by $\underline{\Lambda}_k = [\lambda_{1k}, \lambda_{2k}, ...\lambda_{nk}]^T$. If the LID at the point of voltage collapse is denoted by $\underline{\Lambda}^* = \underline{\Lambda}_m$, then the stability margin at the k_{th} step is expressed as

$$VSM_k = \left\| \underline{\Lambda}^* - \underline{\Lambda}_k \right\|, \tag{4.21}$$

and the reactive power reserve of the j_{th} control device at the k_{th} step is given by

$$RPR_{j_k} = Q_{j^*} - Q_{jgen_k}, \tag{4.22}$$

where $j \, \epsilon \, [1, p]$, p denotes the total number of reactive power generators (or continuous control devices) in the control area under study. Here Q_{j^*} denotes the limit of reactive power production for the j_{th} control device and Q_{jgen_k} is the amount of reactive power produced at the k_{th} step. Loading parameters in $\underline{\Lambda}$ are changed and the values of VSMs and

RPRs are recorded according to (4.21) and (4.22). These data sets are used to determine robust regression models between these two types of variables, for each control area. Each of the subsystem regression models can be expressed as

$$y = \beta_0 + \sum_{j=1}^{p} x_j \beta_j + \sum_{j=1}^{p} \sum_{i=1}^{p} x_j x_i \beta_{ij} + e, \tag{4.23}$$

yielding the matrix form given by $\underline{y} = \underline{X}\underline{\beta} + \underline{e}$, where $\underline{y}$ is the vector of VSM data, $\underline{X}$ is the matrix of RPRs, $\underline{\beta}$ is the parameter vector and $\underline{e}$ is the error vector. Note that the $\beta_i's$ represent the contribution of local reactive power generators to the stability margin. In [26], it is noted that the variances of the errors vary with the independent variables, a characteristic denominated 'heterosckedasticity'. We carried out simulations and observed that the variances of the residuals of the VSMs actually increase as the loading in the system is increased or the RPRs are decreased. One possible explanation is that as the generators reach their reactive power generation limit, the reactive power flows in the system will change drastically even on slightest perturbation around that operating point. For simplicity, we assume here that the variances of the errors are linearly proportional to the change in independent variables. Now, let us assume that the errors follow a Gaussian distribution, $\underline{e} \sim N(\underline{0}, \sigma^2 \underline{D})$, where $\underline{D}$ is a non-unitary diagonal matrix; if the residuals are weighted inversely proportional to their associated variances, heteroskedasticity is reduced. Hence, using $\underline{W} = \sigma^2 \underline{D}^{-1}$, we get

$$\underline{\hat{\beta}} = \arg\min_{\underline{\beta}} \left\| \underline{y} - \underline{X}\underline{\beta} \right\|_{\underline{W}}^2, \tag{4.24}$$

yielding $\underline{\hat{\beta}} = (\underline{X}^T \underline{W} \underline{X})^{-1} \underline{X}^T \underline{W} \underline{y}$ and $\underline{\hat{y}} = \underline{X}\underline{\hat{\beta}}$. Since the above weighted least square method is not robust to outliers, a statistical test should be performed on the standardized residuals to detect and reject the outliers. Furthermore, tests like White's Test [65] can be performed for testing the improvement in heteroskedasticity.

As far as the online control is concerned, the incoming PMU metered values are used first to estimate the available reactive power locally; then the voltage stability margin are estimated using the developed regression models at each time unit. Assume that for a voltage control area a, $a \,\epsilon\, [1, N]$, the optimal stability margin set by the tertiary agent is VSM_{set_a}. Also, if post disturbance condition starts say at time t, the estimated stability margin by the local control agent is VSM_{t_a}, then the secondary control agent can use a sensitivity based analysis to decide the required control action. Now, the (secondary) local control agent a can change the reactive power production of control device k as $\Delta RPR_k = \Delta VSM_k / \beta_k$ such that

$$\sum \Delta VSM_k = \sum \Delta RPR_k \times \beta_k \geq |VSM_{set_a} - VSM_{t_a}|. \tag{4.25}$$

If there is no cost attached to the reactive power production from any device, then the control agent changes the setting of the device with the maximum sensitivity β_k followed by the next most sensitive device, until the VSM reaches back to the threshold according to (4.25). If there are costs attached with the reactive power production, then the control agent may

run an optimization algorithm to find the optimal settings. If all the devices exhaust there reactive reserves before the VSM_{set_a} point is reached, then the local agent may first try to mitigate the instability, for instance by turning on a discrete control device or altering the position of tap changers, and if the instability remains, then will send a 'unstable' decision to the global agent. The latter will resolve this instability issue in the next decision cycle as outlined next.

4.4.2 Actions of the global control agent

When the secondary control agents have taken local control actions, the system will usually reach a stable equilibrium point. There may be enough stability margin, and the oscillations caused due to transients might be sufficiently damped. It is noteworthy that the if there are any major violations in the system like severe undervoltages, or large undamped oscillations, the system integrity and protection schemes (relays) will get initiated and remove problematic conducting equipment (lines/generators) from the system, irrespective of the control agent actions. The local control agent transmits the information of the local state to the global (tertiary) control agent. In case the actions of a local controller are incapable of stabilizing respective control area, the tertiary control agent will take additional measures to stabilize that subsystem, and hence the overall system. It should be emphasized here that time-constants for transient instabilities are in the sub-seconds to a couple of seconds range, hence practically it is infeasible to initiate a tertiary control action before the protection schemes operate. Therefore, under large disturbances either the secondary control use the local signals to damp out the oscillations, or the protection schemes get initiated. The tertiary control actions are reserved exclusively for steady state instabilities, which can be resolved in sub-minute time frames.

Next we discuss the procedure of transmitting information to the tertiary controller. It should be pointed that this information is complementary to (but not redundant with) the SCADA measurements since its sampling rate is much higher than that of the latter. It is noteworthy that there are some disadvantages in transmitting all the measurement data from the sensors installed in each control area directly to the tertiary controller.Namely, it will require a very high bandwidth for communication and will lead to a slower processing of information and slower control actions, similar to a centralized control. To address this issue, partial information, pre-processed by each local control agent is sent to the tertiary agent. To this end, we adopt the decentralized inference technique [15] for transmitting the system state information to the latter. As shown in Fig. 4.3, Following a disturbance, the power system (or the 'environment' which the sensors are observing) is either stable or experiencing an instability, that is, it cannot be stabilized by local control actions. The system condition is tested by each of the secondary agents, using the partially observed state information metered from the PMUs. This results in a binary choice, between the null hypothesis, denoted by H_0, representing a stable system and the alternate denoted by H_1. The local control agents perform a stability analysis on the metered values (as discussed

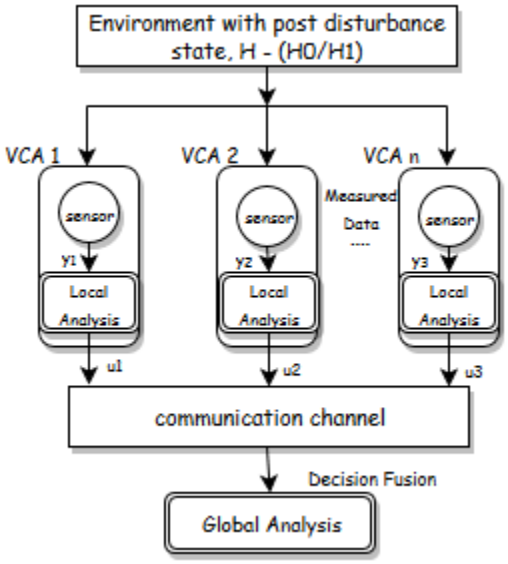

Figure 4.3: Distributed Decision Fusion

previously) and give a local inference (decision) of the system state referred to as u_i, where $u_i \epsilon \{H_0, H_1\}$. These local decisions, requiring lesser communication bandwidth than the metered data, are transmitted to the global control agent, where a decision regarding the stability of the system is made, that is, $u_g = f(u_1, u_2, ...u_N) = H_i, i = 0, 1$. Conditions for the optimality of this decision rule are discussed in [15]. To be precise, if the a priori probabilities of errors in decision of each local control agent are same (they are equally reliable), then the optimal decision fusion rule is given by

$$\Sigma\, u_i \underset{H_0}{\overset{H_1}{\gtrless}} [\tfrac{N}{2}], \tag{4.26}$$

where the square brackets denote the greatest integer function. The decision rule given by (4.26) can simply be interpreted as the global decision in choosing H_0 (alternatively H_1) if the majority of the local agents are flagging stability (alternatively instability). A list of global control actions may be applied according to the utility practice. For instance, if the global control decision is H_0, the global decision may be to do nothing if none of the areas are unstable or, if a local instabilities are detected in an area, to use reactive power resources or to shed a fraction of the elastic loads while blocking OTLCs. On the other hand, if the global decision is H_1 or the above actions are unable to mitigate local instabilities, the global agent may initiate the shedding of some fraction of the inelastic load or may block the TCSCs control signals to prevent the triggering of highly non-linear oscillations; it may also take heroic actions such as initiating subsystem islanding to decrease the risk of a large-scale blackout. As seen, the global agent plays a crucial role during an emergency or extremis state of a power system. The simulation results of implementation of the proposed decentralized control techniques on IEEE test-beds is given in Chapter 7.

4.5 Conclusions and scope of future work

In this paper, unified hierarchical decentralized control schemes for rotor angle and voltage stability improvement have been developed. Control laws applied to FACTS devices have been derived using Lyapunov's second method for rotor angle stability and a multiple regression method for voltage stability. It has been shown that they require lesser communication bandwidth than traditional wide-area control techniques. Their good performance has been assessed and illustrated on standard test-beds. As a future work, the proposed decision rules will be extended through the saddle point approximation to better evaluate the risks of first and second kind.

Chapter 5

Multi-Agent Systems for Power Engineering Applications

For over two decades now, researchers have discussed the pertinence of Multi-Agent Systems (MAS) based solutions for addressing several challenging problems in Power Engineering [66]-[73]. As an example, MAS based solutions have been proposed for power systems condition monitoring [67], market control [69], automation [72], and restoration [68]. Furthermore, the IEEE Power Engineering Society's (PES) Intelligent System Subcommittee formed a Working Group [74] with the aim of providing "technical leadership in terms of recommendation and guidance on the appropriate use of standards, design methodologies, and implementation approaches" for the application of MAS in power engineering. An analysis of the concepts, practices and tools developed for MAS in Power Engineering applications is summarized by the working group in two IEEE transaction papers [7]-[8].

In this chapter, a brief overview of MAS technology and recommended standard is presented. In the last part of this chapter, we also discuss a case study where the agent based communication interfaces with the OSI network model for a power engineering application. In the next chapter, a detailed discussion is given on the proposed Hierarchical Instability Detection and Control scheme using Multi-Agent Systems.

5.1 Multi-Agent Systems (MAS): an overview.

It is important to discuss and define here few basic building blocks of Multi-Agent Systems. It should be noted that the research community has discussed concepts like *agency* and *agents* for many different types of applications, hence there are no standard definitions of these terms. Most definitions outlined here are due to Wooldridge [75]. An **agent** is a computer system, situated in an *environment*, wherein it can take *autonomous* actions on behalf of its owner or user. Everything external to the agent is known as its *environment*. An

agent is able to *observe* its environment, at least in part. In case of the power systems, the environment is physical, usually observable via sensors, while in case of computing systems, the environment is observable via system calls and messaging. An agent may be able to alter its environment by taking certain actions, like altering switch positions to reconfigure the topology of its physical environment.

An **intelligent agent** is an extension of the concept of agent in the sense that an intelligent agent necessarily exhibits the following characteristics: **reactivity**, **pro-activeness** and **social ability**. Whereas *reactivity* or an ability to react to changes in its environment is a desired characteristic for every agent, *intelligent* agents also exhibit *pro-activenes*. The latter is the ability of an agent to dynamically change its behavior in order to achieve its pre-set goals. The characteristic of intelligent agents that forms the basis of *Multi-Agent Systems* is their *social ability*. The latter is the ability of an agent to interact with other social agents. Over and above the ability to pass data messages, social ability implies the capability to *negotiate*, interact and make decisions *cooperatively*. A **Multi-Agent System** is, thus, a system comprising of two or more intelligent agents which can interact and coordinate to reach a directed goal. Next, we highlight the distinctive characteristics of MAS useful for power engineering problems in general, and for the hierarchical control problem in specific.

5.2 Characteristics of Multi-Agent Systems (MAS) advantageous for power engineering applications

Following are some characteristics that the MAS exhibit, and their potential usefulness:

- **interaction, coordination and cooperation:** the social ability of agents, expressed by their capability to interact by exchanging information, and reaching decisions by coordination, is best applicable for implementation in coordinated control systems. Hence, MAS architectures can be implemented when there is a need for interaction amongst distinct conceptual entities; and traditional methods are unsuitable. As an example, in a deregulated market environment, where energy could be sold by traditional dispatchable or intermittent renewable resources, and can be bought by traditional consumers or storage elements, multi-agent systems can reach a global nash equilibrium by method of coordination.

- **open architecture:** supported by international open standards like FIPA, multi-agent systems are an imperative solution for interoperability. This basically means that for a large, interconnected power grid (consisting of a single or multiple utilities) agent-based control for different subsystems can be developed by different parties as long as all comply to the same open standard. It is needless to mention that in the past, power systems have been riddled by the widespread use of software that was proprietary and not interoperable. This caused major problems regarding data exchange and hence, the

standards like IEC-61850 [76] and IEC-CIM [77] had to be evolved for the mitigation of this issue.

- **fault tolerance :** Intelligent Agents can be built with fault-tolerance, a property which is a pre-requisite for self-healing and resilient power-grid of the future. Fault tolerant design can be build very simplistically by creating redundancy, that is, by assigning same set of tasks to multiple agents in the system. In such a system if a part of the system fails, still the overall objectives of the system can be achieved because the responsibilities of the agents in the failed part would be taken up by the remaining agents. A more complex implementation of fault-tolerance is when the remaining set of agents are able to bring the failed part of the system back online.

- **autonomy:** This signifies that the agents can schedule their own tasks for achieving the directed goal. One advantage of autonomy, when compared to the traditional modular programming approach, is that the agents are not bound to execute requests from other agents. If an agent requests another agent to perform a specific task, the latter can deny the request or give it a low priority depending upon its own scheduled list of tasks. This property is useful when a very large number of entities are overwhelming an agent with different task requests and the agent is unable to process them simultaneously. This property is highly beneficial in system emergencies. As an example, when an interconnected power system needs to go into graceful degradation, like controlled islanding, different subsystems can be islanded, controlled independently, and reconnected using multi-agent control systems.

- **extensibility:** A MAS platform can be extended by easily replicating a set of agents and their respective behavior when a new subsystem is added into the original system. Extensibility also includes easily adding a new set of functionalities or upgrading the older ones. The ease of addition implies increasing functions for an without having to re-implement the complete agent behavior. As an example, assume that a SCADA system is upgraded with a new set of sensors; the agents which process this data can be easily upgraded with a new data analysis algorithm compatible with the new sensors.

- **flexibility:** This implies that an agent is able to reschedule and re-prioritize its actions dynamically depending on the situation of its environment. Flexibility essentially denotes that the agent is able to select the most appropriate action while its environment is dynamically changing. This property is another building block for power system resilience and is specially useful during emergency/restorative conditions.

As mentioned previously, these characteristics of Multi-Agent Systems have been exploited in developing power engineering applications like Monitoring and Diagnostics, System Integrity Protection Schemes (SIPS), Power System Restoration, Modeling and Simulation and Microgrid Control.

5.2.1 Intelligent agent characteristics imperative for decentralized instability detection and control

As far as application to Hierarchical Voltage Control Scheme is concerned, secondary control agents may need to *interact* and *cooperate* with each other for ensuring the local stability. Furthermore, each secondary agent has to *cooperate* and *interact* with the tertiary agent for achieving global (the entire interconnected system) stability. The property of *autonomy* gives a secondary (local) control agent an authority to respond to any instability situation locally, while the property of *flexibility* is necessary to take adaptive actions when the system is evolving towards instability, post a disturbance. If a new type of PMU is added to monitor pilot point voltages in a control area which was not observed previously, the *extensibility* and *replicability* of multi-agent architecture is capable of handling these additions without increasing the complexity of control.

A coordinated hierarchical control scheme needs interaction of multiple different types of control entities which take complex decisions, based on inferences about the observed system state. As discussed, this is an enhancement over the traditional voltage control schemes which either (a) estimate a local instability index and take independent control actions, or (b) take control actions based on wide area measurements, but the decision about control actions for different control devices is made at a central control location (usually by human operators). Both (a) and (b) do not require any coordinated control, while the hierarchical control schemes (of the type discussed in this text) require features like coordination between agents, fault-tolerance, flexibility, and even a certain degree of autonomy which makes the choice of Multi-Agent System based control schemes obvious.

The FIPA specifications for implementation of Multi-Agent Systems, which have been recommended by the IEEE Working Group are discussed next.

5.3 Recommended standard for implementing Multi-Agent Systems: FIPA

The PES Intelligent System Subcommittee recommends the use of Foundation of Intelligent Physical Agents' (FIPA) standards for the development of MAS framework [78]. FIPA sets standards for the inter-agent communication procedure and for the basic architecture of a multi-agent system. In this section, first, a background about FIPA is outlined in brief, then, we review the FIPA recommendations for Agent Management Systems (AMS) and inter-agent communication language, ACL.

5.3.1 FIPA standards, a background

FIPA [link] "is an IEEE Computer Society standards organization that promotes agent-based technology and the interoperability of its standards with other technologies." FIPA specifications "represent a collection of standards which are intended to promote the inter-operation of heterogeneous agents and the services that they can represent." Besides FIPA, the Knowledge Query Meta Language (KQML) and the Object Management Group's Mobile Agent System Interoperability Facility (OMG MASIF) are other widely used standards that describe the interoperability, mobility and inter-agent communication protocols. While the KQML also specifies agent communication standards based on speech acts like FIPA, and OMG MASIF defines specific methodologies for agent platform mobility, none of these standards are generic enough to cover all the aspects related to both mobile and static agents like FIPA. Hence, in the past decade, FIPA standards have become the de-facto standards used and implemented by the MAS community.

FIPA provides normative specifications defining various aspects of multi-agent system design, including the existence and operation of agents. These standards specify a 'logical reference model' for creation, location, and retirement of agents. FIPA specifications primarily concerned with two entities necessary for developing a MAS, namely:

- Agent Management Specification: Refers to Agent Management Services (AMS), Agent Management Ontology and Agent Platform Message Transport. (FIPA SC00023K)
- Agent Communication Language Specification: Refers to FIPA ACL message parameters.(FIPA SC00061G)

5.3.2 FIPA - Agent Management Specification (AMS)

The FIPA agent management reference model, taken from the Agent Management Specification (FIPA SC00023K), is shown in Fig. 5.1. It is interesting to note that the various entities in this reference model represent logical capability sets and do not entail any specific physical configuration. The actual implementation details of each of these blocks are left to the discretion of the MAS designer. *The specific implementation of each of the components for the purpose of Hierarchical Voltage control will be given in the next chapter.* Here, we given a brief overview of the FIPA guidelines. The discussed reference model is comprised of the following entities:

- **Agent Platfrom (AP)** is the physical infrastructure in which an agent can be deployed. It comprises of the machine (hardware), an operating system and other agent management components. Interestingly, all the components of an Agent Platform do not need to be co-located on one host computer. FIPA also envisages an entirely distributed implementation of APs, which comes in handy for applications in power

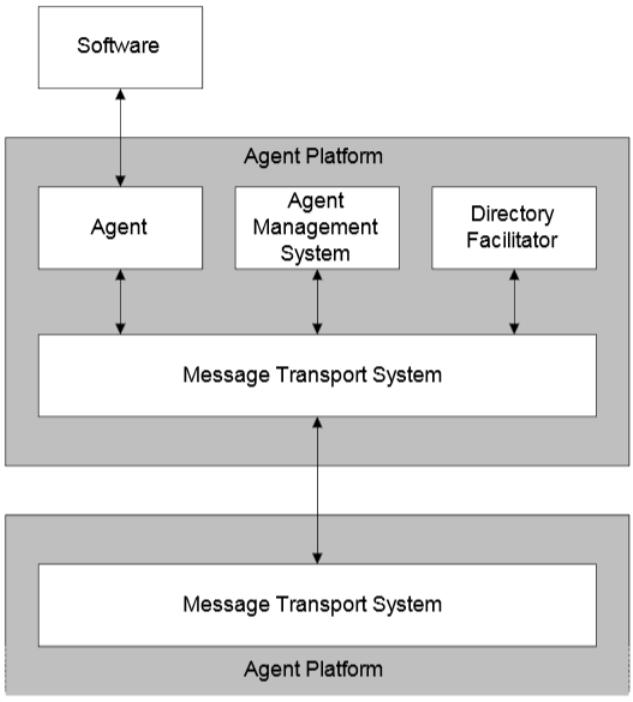

Figure 5.1: Agent Management Reference Model. (Refer FIPA SC0023K)

engineering applications. As an example, an agent platform for a control application in power systems can have member agents which are not co-located geographically.

- An **Agent** is a 'fundamental actor' within a platform which can provide one or multiple services. Each service is generally a sequence of tasks, and its the responsibility of an agent to execute the tasks for different services based on a logical pattern. Each agent should be distinguishable by a unique Agent Identifier (AID) and it must have at least one owner.

- A **Directory Facilitator (DF)** is not a mandatory part of an AP, but wherever it is implemented, it serves as a directory of Agents registered in the platform. This component was not implemented as a part of current research work.

- A **Message Transport Service (MTS)** is a service provided by the AP for transmitting information between two different agents located on the same AP or two different APs. As specified by FIPA (SC00067F) The structure of the messages carrying the information consists of (1) a message envelope indicating the transport information (eg. AIDs of sender, receiver) and (2) a message payload comprising of the actual information in the Agent Communication Language (ACL) format. Typical messages used for inter-agent communication are described in the next section.

- An **Agent Management System (AMS)** is an essential building block of an AP.

Table 5.1: FIPA ACL message parameters. Reproduced from FIPA SC00061G.

Parameter	Category of Parameters
performative	Type of communicative acts
sender	Participant in communication
receiver	Participant in communication
reply-to	Participant in communication
content	Content of message
language	Description of Content
encoding	Description of Content
ontology	Description of Content
protocol	Control of conversation
conversation-id	Control of conversation
reply-with	Control of conversation
in-reply-to	Control of conversation
reply-by	Control of conversation

An unique AMS will exist in every AP. An AMS actually functions as the managing authority of the entire AP, responsible for activities such as the creation, deletion and migration of agents. If, in a distributed environment, an AP spans over multiple machines, then the AMS will be the responsible managing authority across all those machines. The AMS maintains an index of all the agents on its AP, using their unique AIDs. Whenever an agent is created or migrated to an AP, the AMS will *register* the agent on the AP. Similarly, if the agent is migrated away or gets retired, it will *deregister* it from the AP. Furthermore the AMS has the authority to *modify* the description of any particular agent. Any agent can be *searched* via AMS if it is registered on the AP. In addition to the aforementioned functions, the AMS can 'instruct' the AP to *create, suspend, terminate, pause the execution of* any agent.

This completes the discussion on the Agent Management Reference Model. Before we proceed to the specifics of AMS implementation in the Hierarchical Voltage Control scheme, we discuss briefly the role of Agent Communication Langugage.

5.3.3 FIPA - Agent Communication Language Specification (ACLS)

As pointed before, *social ability* is one of the key characteristics of an intelligent agent. A communication language for agents is necessary to create a 'society' where different agents can not only exchange data, but also coordinate and reach cooperative decisions. FIPA specifies the FIPA-ACL (FIPA- Agent Communication Language) message structure with

an objective of ensuring interoperability between different agent platforms.

A typical FIPA ACL message will define a set of parameters. A list of FIPA ACL message parameters is provided in Table 5.1, which is reproduced from the FIPA specification SC00061G. A parameter, simply put, is a component in a message frame. Which parameters will be used for a specific design is upto the designer. Furthermore, a designer can define additional fields in a FIPA message and enhance its structure. The only mandatory parameter that needs to be defined in all the FIPA ACL message is the *performative*. As indicated before, ACL messages are based on acts of speech like *query, response, request, inform*. A *performative* denotes a type of communicative act. FIPA defines 22 different communicative acts (FIPA00037). Next, we discuss the flow diagrams of some of the agent 'speech acts' or performatives specified by FIPA. We also discuss some potential power engineering applications of these performatives. In Fig.5.2 (a), a flow diagram of a 'Query-Ref' communicative act is given. Assume that in case of Automated Metering Infrastructure, there is an Agent (of the type B) attached to a meter at every house and an Agent A sits at a central location and tries to query energy data from the meter. This energy data might be used by A for power quality analytics, or simply, for billing. In such a case, Agent A will send a query asking for the new metering data. The parameters for the message will be set as follows,

(`query-ref`
`:sender` AgentA
`:receiver` AgentB
`:content` 'send new metering data'
)

The meter Agent B may (a) agree to respond to the agent A, (b) deny the response, if it detects that the query is not coming from an authorized user, but from a hacker. If the Agent B agrees to respond to A, then B sends back an inform message having the location of the file containing all the metered data, as follows,

(`inform`
`:sender` AgentB
`:receiver` AgentA
`:content` 'encryptedPath'
)

Or if an error occured, the Agent B can send a failure message. Similarly, in the Fig.5.2.(b), a 'call for proposal' type of FIPA speech act is illustrated. This is a performative used to begin any kind of negotiation between two agents. For example the 'initiator' agent is a distribution management system requesting a distributed generation resource to submit a bid to buy some amount of active power. The Participant agent is a distributed generation resource which can either (a) refuse to submit a bid, indicating unavailability of power or (b) propose a bid saying that it can sell 'x' MW of power at 'y' dollars per unit, or (c) it

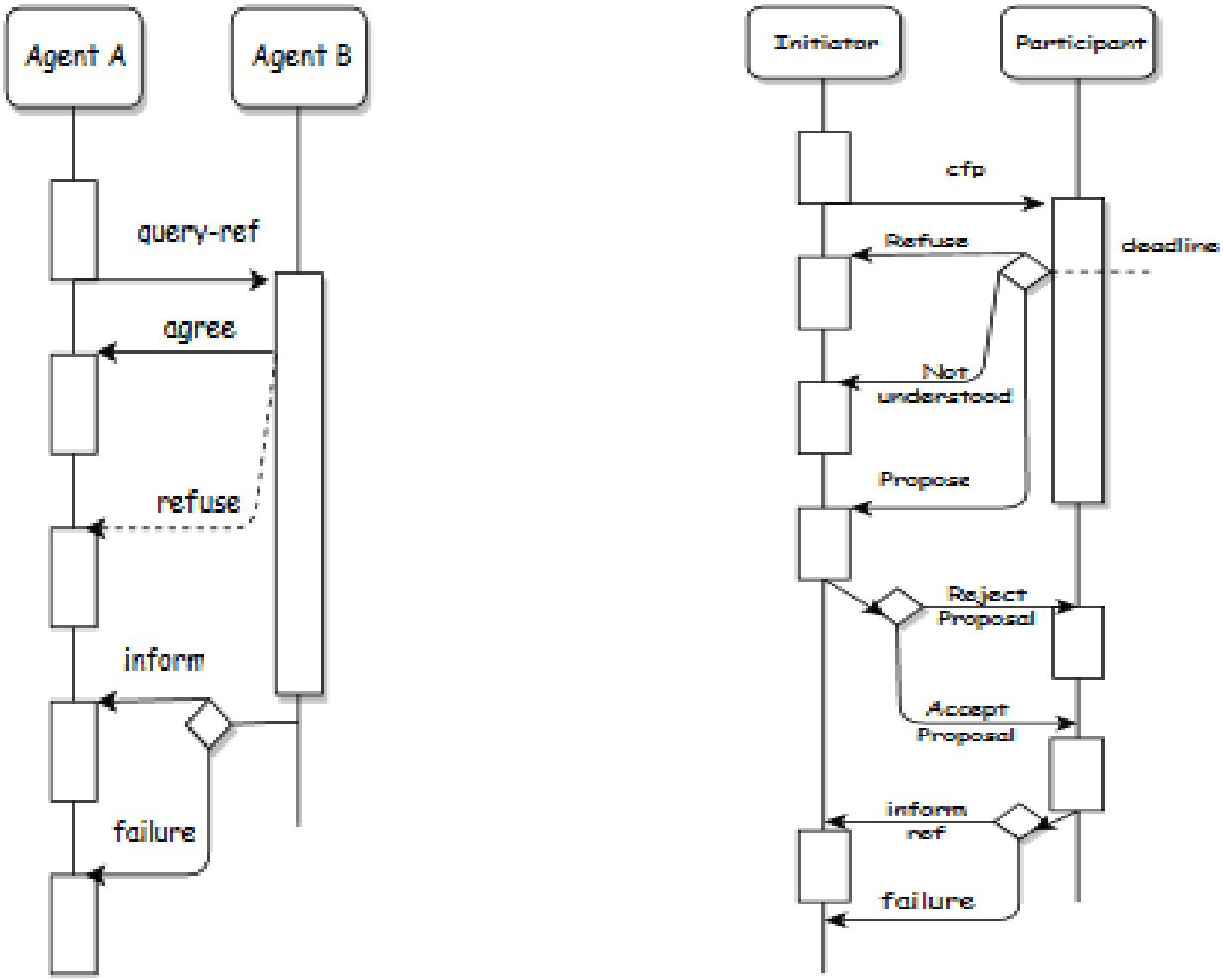

(a) Query-Ref performative

(b) Call-for-proposal performative

Figure 5.2: Agent Interaction diagram showing the flow of messages using FIPA performatives

can say that the type of cfp is not understood. The initiator agent can then either accept the 'x' MW at 'y' per unit or reject it, and re-initate a negotiation cycle. In the subsequent chapter, we will discuss the ACL messages exchanged between agents for the Hierarchical Voltage Control Application.

5.3.4 A reference model for multi-agent communication

In the previous subsection, Fig. 5.2. (a), an ACL message structure for Automatic Metering Infrastructure (AMI) is presented, where using the 'query-ref' performative, the energy data is collected from a meter. Here, we describe the FIPA ACL interface with the Open Systems

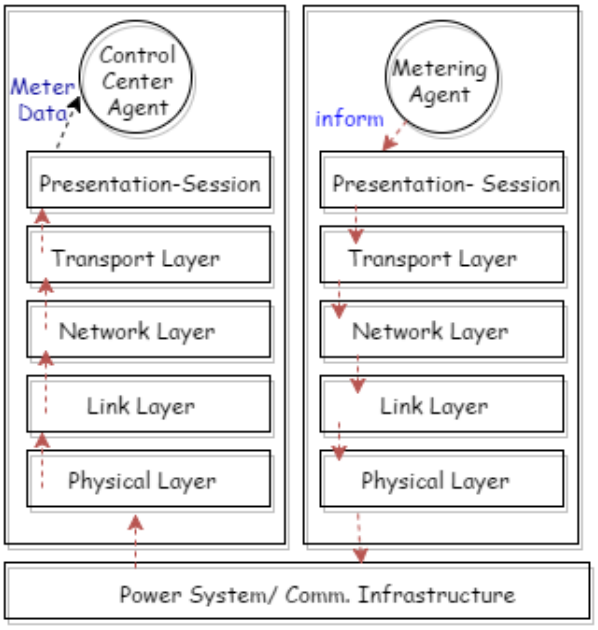

Figure 5.3: A Reference Model for Multi-Agent Communication. ACL acts as an application layer protocol.

Interconnection (OSI) 7-layer model for transmission of data between the microgrid/metering agents and a control center at sub-transmission or transmission system in the grid.

A multi-agent communication reference model, showing the interface of FIPA-ACL with the 7-layered Open System Interconnection (OSI) communication model, is depicted in Fig 5.3. As shown, a mutli-agent system is entirely implemented in the application layer of the OSI model. An ACL 'inform' message is passed from the Metering Agent in the application layer, running one host Agent Platform, to the Control Center agent in another application layer, probably running on another host Agent Platform. The body of the 'inform' message is broken down in Fig 5.4. This ACL message has the metering data included in the 'content' parameter, and the application layer address of the control center agent in the 'receiver' parameter. The message content, besides the metering data, also has the lower layer addresses (namely: transport, network and data link) of the control center agent.

5.4 Communication network design for multi-agent based AMI & microgrid systems: A case study

Using[1] the reference model described above, we can implement a communication infrastructure for the MAS based power engineering application. Hence, in the following subsections,

[1]based on our work in [93]

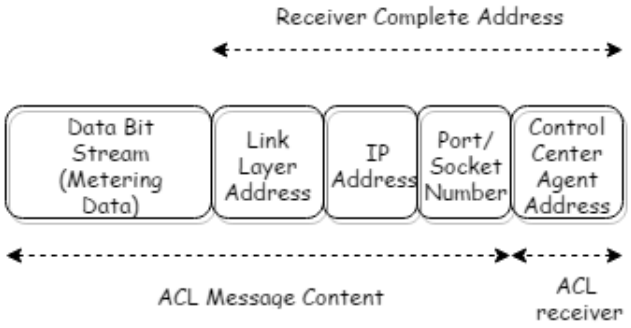

Figure 5.4: FIPA ACL inform message parameters. The 'content' part includes the metering data and the addresses of the lower layers in the stack.

a case study on implementation of a communication network for a group of microgrids is presented. These microgrids are located in the distribution grid, at residential levels, where an Automatic Metering Infrastructure (AMI) is also in place. During system emergency conditions, a multi-agent based microgrid management system might need to respond by providing power to the grid. The focus in this study is on analyzing the Data Link layer protocols which can be used for channel access by the metering and microgrid agents during the normal and emergency conditions in the power grid. An illustration of the discussed architecture is given in Fig 5.5. It is noteworthy that the existing communication infrastructure doesn't deal with Multi-Agent System based applications.

To this end, first, a review of the previously proposed and existing communication infrastructure in power engineering is provided. Then, some important issues regarding the construction of a communication network for MAS based power engineering applications have been highlighted. Subsequently, data link layer protocols used for communication channel access have been studied for both the meshed and one point to multipoint (wireless) architectures. Finally, an implementation of queue handling mechanisms for suitably tranmitting both metering agent and microgrid agent messages to their respective control centers (over the same backhaul) has been discussed. Our investigation reveals that the communications infrastructure must use differentiated service mechanisms for handling the variety of traffic patterns generated by the microgrids' control actions. If such mechanisms are not used, the performance of the controllers degrades. In addition, a few reasonable remedial actions for improving the current network design have been proposed and a set of best practices targeting the network architects have been suggested in this study. Here, the emphasis is on bringing out the issues rather than solving all the problems.

5.4.1 Existing power system communication infrastructure

As outlined in the report authored by the Pacific National Northwest Laboratory [82], the existing communication architecture of an electric power system is mainly based on wireless

technologies and complies with IEEE 802.11 a/b while the backhaul is majorly based on the Ethernet and complies with IEEE 802.3. Gungor and Lambert [81] provide a comprehensive survey on the various types of existing communication networks for the automation of an electric power system. This includes power line communications, satellite communications, internet based Virtual Private Networks (VPN), wireless sensor networks, wireless mesh networks, and WiMAX, among others. While Power Line Carrier Communication (PLCC) is also receiving a great deal of attention [83], other well-established technologies are currently being deployed. These are optical-fiber and hard-wired communication networks for urban distribution power system and wireless networks for suburban and rural distribution systems. These networks are characterized by a nearly constant data rate with a smooth traffic and no stringent requirement of Quality of Service (QoS) under best-effort service requirements. Current and future applications include: Home Area Network (HAN), Automatic Metering Infrastructure (AMI), Substation Automation (SA) and Distribution Automation (DA) etc. In the near future, such communication infrastructures must expand to accommodate microgrids.

5.4.2 Purpose of the study

The overall performance of any agent based control application for Power Systems is directly dependent on the underlying communication infrastructure. This is because all the information including the sensor measurements, the control signals, and the inter-agent coordination messages, are continuously transmitted over the communication network. It is needles to mention that a reliable and fast communication network is of paramount importance for an instability to be detected and control actions to be taken in a timely manner. Furthermore, since the capacity of communication infrastructure is usually limited, it becomes necessary to evaluate the performance of the network when multiple applications are sharing the infrastructure and the access of communication channels by one application might conflict with the other. In this study few important issues are outlined, which need attention if a network design of the type shown in Fig.5.5, is implemented. The performance of the implemented network needs to be evaluated in terms of various metrics. These include the data throughput achieved by the communication data-link layer; the upper bounds of latency in sending and receiving the data packets; the fraction of traffic dropped (if any) in communicating the information; and the amount and cost of communication media involved. This type of study gives the application layer designer a good estimate of the (a) communication delays, (b) reliability of message delivery due to the data-link layer channel access mechanisms.

It is needless to mention that the time-outs for the transmission of application layer communication messages (based on FIPA-ACL) are decided on the basis of these performance metrics of the lower-layers (physical, data-link layer). Moreover, this type of study is necessary if an application like a multi-agent based control of power system needs to be implemented, and the designer has an apriori knowledge of different parameters including sensor data sampling rate, control device time constants. Using the results of this study he/she can fine-tune the

communication network design to achieve the overall desired performance.

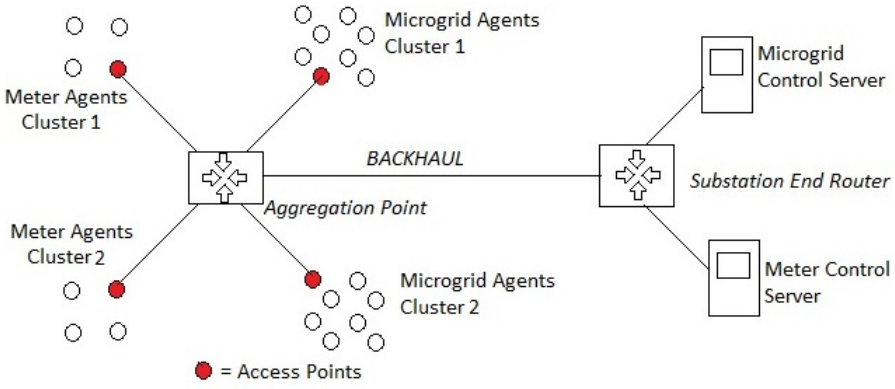

Figure 5.5: Proposed architecture for a system of microgrids and AMI applications

In the following sections, we investigate the performance of the communication network for power distribution systems (equipped with AMI) to accommodate a large penetration of microgrids. To this end, we carry out the investigation on the OPNET^{TM} simulation tool in two specific case studies, namely (i) a local network of intelligent agents that supervise the control of a collection of microgrids and (ii) a common link to transmit different types of traffic (metering and microgrid) generated in the distribution system during emergency conditions.

5.4.3 Proposed communication infrastructure for distribution systems having microgrids and AMI

Microgrids can be viewed as a subsystem of the power system consisting of distributed generation sources and the associated loads. These units will be located at the distribution end and will potentially function as components of smartgrids. At the same distribution end, Automatic Metering Infrastructure (AMI) would be deployed, which will execute applications like Automated Meter Reading (AMR). Under normal operating conditions, the microgrids will function in a grid connected mode, but under emergency conditions, they might need to disassociate, function independent of the grid and meet the demand of local loads. Each microgrid is controlled by a multi-agent based microgrid management system. Furthermore, we assume that the microgrids of the distribution feeders which are connected to the same HV-MV substation constitute a common cluster, controlled by a agent based Distribution Management System (DMS).

Evidently, a high penetration of distributed generation units and microgrids will require the deployment of a variety of sensors along the distribution feeders for monitoring and control

purpose. These sensors may provide metered values on voltage magnitudes and phase angles, real and reactive power flows and injections, and frequency, for example by means of FNETs [84]. The caveat here is that the data sent by the sensors may not be smooth or periodic. To see that, let us consider the case where these data are being used to estimate some precursor to transient instability of the power system. Upon the occurrence of a disturbance in the transmission network, the data rate suddenly increases while maintaining a high QoS, making the traffic bursty in nature.

From the previous discussions, it is evident that the current communications infrastructure, which is characterized by a low bandwidth and a low data rate, does not meet the needs of a large penetration of microgrids. The upgrade of that infrastructure is required. At this point, we may make the following remarks:

- The cost of setting up a wireless network with signal repeaters is lower than the one of any other wired media, especially those based on optic-fiber cable;
- The addition of new nodes is easier in a wireless network than in a wired one;
- A wireless infrastructure has been already installed at the distribution level by many utilities to serve substation and distribution automation functions.

Therefore, in this work, we assume that the AMI and the microgrid agents communicate via a wireless network. This network can have point-to-multipoint or multipoint-to-multipoint connection. Moreover, as shown in Fig.5.5, the agents of the same cluster can transmit their data to a supervising control center over a common backhaul network. Considering that microgrid agents generate a bursty traffic while AMI agents generate a rather smooth traffic and that they both communicate via Wireless Local Area Networks (WLANs), the following questions arise: which channel access mechanism and which shared backhaul ensure minimum delays, least channel loads, least packet loss, and minimum retransmission attempts during emergency operating conditions? These questions are addressed next.

5.4.4 Channel access mechanisms for microgrid and metering agents

Before transmitting the data to the control center, the microgrid agents share information among themselves with the access point. As for the meter agent nodes, they may exchange information among themselves before sending it to the access point for forward transmission.

In a wireless medium, the data sent by each node is transmitted through the same channel. This is ensured via some standard protocols. In general, when multiple hosts attempt to transmit packets on the shared communication channels, collisions of data packets may occur. To mitigate these risks, a channel access protocol is used to control the access to the shared channel. There are two types of channel access mechanisms, namely (i) the collision-based

channel access, i.e. the Point Coordination Function (PCF) protocol and (ii) the collision-free channel access, i.e. the Distributed Coordination Function (DCF) protocol [88]. Note that each type fulfills a specific QoS requirement. Extensive simulation results comparing the two protocols are covered in the second section of chapter 7.

Chapter 6

Estimation of Uncertainties in Hierarchical Decentralized Stability Analysis Process

6.1 Background

In chapters II-IV we developed the concept of voltage and rotor angle instability detection in power systems and the hierarchical, decentralized control mechanisms for mitigating such instabilities. It should be noted that since such instability detection mechanisms in power systems rely upon an *estimation* of the current state of the system based on noisy measurements and an approximate system model, it is impractical to predict the nature of stability with absolute certainty. If such uncertainties are large in a control system design, it may lead to inaccurate decisions, for instance, failing to initiate a control action, when the system is moving towards instability. Thus, a power system control engineer must make an effort to (a) identify the sources of uncertainty in the design of a control scheme, (b) approximate the probability of errors of the first and second type in the control decision process, and (c) use the quantification of error probabilities to optimize the control scheme.

For instance, as discussed in the second chapter, voltage stability margins of a power system can be correlated with locally available reactive power [24]-[26]. This philosophy has been applied in [24], [26] for online assessment of voltage stability of a power system by developing linear regression models between reactive power reserves and voltage stability margins. Recently, Shukla and Mili [91],[92] propose the use of regression modeling based schemes in hierarchical, decentralized voltage stability enhancement. Interestingly, the aforementioned prior literature does not discuss estimation of error probabilities in the instability assessment process. In this chapter we extend the works in [24], [26] to address that issue. We illustrate the process of estimating and quantifying uncertainties in a hierarchical decentralized control

process, taking the example of voltage instability detection and control. To that end, we quantify the probabilities of errors in detection of voltage instability at each local, and at the global control agent levels. We borrow certain tools proposed in the statistical and signal processing literature to analyze the uncertainty in control decisions. Although we develop the theory using a specific example of voltage instability detection using regression based models, yet the applicability of the techniques discussed in this chapter is rather general and is equally germane to multi-agent based coordinated control schemes proposed in [94]-[97]. It is also obvious that the process of estimation of error probabilities at the global control agent level is akin to that of a centralized control process, with the only difference that in the latter process, the information to be fused is direct sensor measurements rather than partial information provided by the local agents.

The major contributions of this work are as follows. We illustrate that the multi-linear regression models between the Voltage Stability Margins (VSMs) and Reactive Power Reserves (RPRs) as proposed in [26] do not capture the randomness in the regressors β, which leads to increased inaccuracies in the model. We use standard statistical tests like analysis of variance and maximum likelihood [98, chap.18] to prove that there are random effects in the model. Subsequently, for accurately estimating the random βs, we use the least-informative priors and maximum-aposteriori (MAP) estimation approach [99] for covariance matrix ($\mathbf{Cov}(\beta)$) estimation. This leads to an accurate estimation of the probability distribution functions (pdfs) of local voltage stability margins. We can thus accurately approximate the probability of errors at local agents using the accurate pdfs of local VSMs. Subsequently, we use the saddlepoint approximation approach [55],[56],[17] to accurately approximate the distribution of fused information (decisions/sensor data) at the global control agent level, which helps us determine the global probabilities of errors of the first and the second kind.

6.2 Multilinear regression models for Voltage Stability Margins (VSMs) with random regressors.

6.2.1 Fixed and random effects in VSM modeling

As discussed previously, the voltage stability margins in a large scale power system can be related to the locally available reactive power by a multi-linear regression model, as,

$$y_k = \beta_{0k} + \sum_{j=1}^{p} x_{jk}\beta_{jk} + e_k, \tag{6.1}$$

where y_k, $k = 1, 2, ...n$ is the k^{th} measurement of the local voltage stability margin, x_{jk}, $j = 1, 2, ..p$, denote the reactive power available with the j^{th} reactive power producing device (e.g. synchronous generator) in the region during the k^{th} measurement. (6.1) can be written in

matrix form as,

$$\underline{y} = \mathbf{X}\underline{\beta} + \underline{e} \tag{6.2}$$

This choice of regression models essentially indicates that the sensitivities or the 'effects' represented by the coefficients βs are fixed, while the error term (e) captures any random effect or uncertainty in the model. Furthermore, this also leads to the assumption that if the errors e_k are independent, then y_k are also independent. We claim that such modeling of the relationship between Voltage Stability Margins and the Reactive Power Reserves, discussed in the prior literature, fails to capture some important random effects explicitly. It should be noted that in (6.1) and (6.2) error term captures the combined effects of all the variability, but it fails to capture the 'random' effects caused by the fact that each 'design variable' x_j is also random in nature. As pointed by Green and Tukey in [101], if the design variables x_j exhaust the entire design space, then it is appropriate to model the related coefficient βs as fixed, while if the design variables are only a representative sample of the entire design space, the related βs should be modeled as random coefficients to indicate the uncertainty caused by that subspace of the domain which has not been accounted for by the measurements. This is specially true in the case under discussion, where our design variable, the reactive power produced by different generators (x_j), is only a realization of a continuous random variable. The randomness in the latter being caused by the random demand of reactive power in a given region of the power system. In the next subsection, we start with providing simulation based evidence and then discuss statistical tests for random effects in VSM regression modeling.

6.2.2 Tests for random effects in the regression model

Here we illustrate random effects in regression models of voltage stability margin with reactive power reserves by using both: simulation based experiments and statistical methods like ANOVA and Maximum Likelihood [98]. A voltage control area in the IEEE standard 118 bus system was considered for the purpose of simulation based study. A detailed discussion on determination of such coherent areas is given in chapter 4, and simulation results specific to the IEEE 118 bus system is given in Table 7.1 in the chapter 7. Following the procedure discussed by Leonardi and Ajjarapu [26], data was collected for developing a regression model for the area A_3 in IEEE 118 system (see table 7.1). The loads were varied on buses 39 - 42, and for each load change, the reactive power being produced by local generators ($1-x_{jk},\ \ j = 1, 2$ for two generators on buses 39 and 42) along with the local voltage stability margins (y_k) were recorded. Here we intend to estimate the regression coefficients (βs) of the following regression model:

$$y_k = x_{1k}\beta_1 + x_{2k}\beta_2 + x_{1k}^2\beta_{11} + x_{2k}^2\beta_{22} + x_{1k}x_{2k}\beta_{12} + e_k, \quad k = 1, 2, 3...K \tag{6.3}$$

A specific procedure is followed to record the data while changing the loads on various buses, which helps us observe the effect of random effects. As pointed before, in the discussed

models, the collected samples of reactive power reserves and associated estimations of voltage stability margins do not exhaust the entire population of the independent variables. To illustrate this in a simple manner, assume that the loads on three buses: 39, 40, and 42 in the area A_3 can be changed randomly. As shown in Fig.6.1, the vector $l_{39}\mathbf{x} + l_{40}\mathbf{y} + l_{42}\mathbf{z}$ represents the change of load (Load Increase Direction or (LID)) on the three buses. A load increase might happen only on one of the three buses (e.g. $l_{40} \neq 0, l_{39} = 0, l_{42} = 0$), or on all the three buses together ($l_{40}, l_{39}, l_{42} \neq 0$). As is obvious, that there are infinitely many load increase directions, and the recorded samples do not exhaust the entire sample space. We simulated similar scenarios while recording samples for the regression analysis. Load increase was simulated in different load increase directions, and samples were grouped according the specific direction of the LID vector.

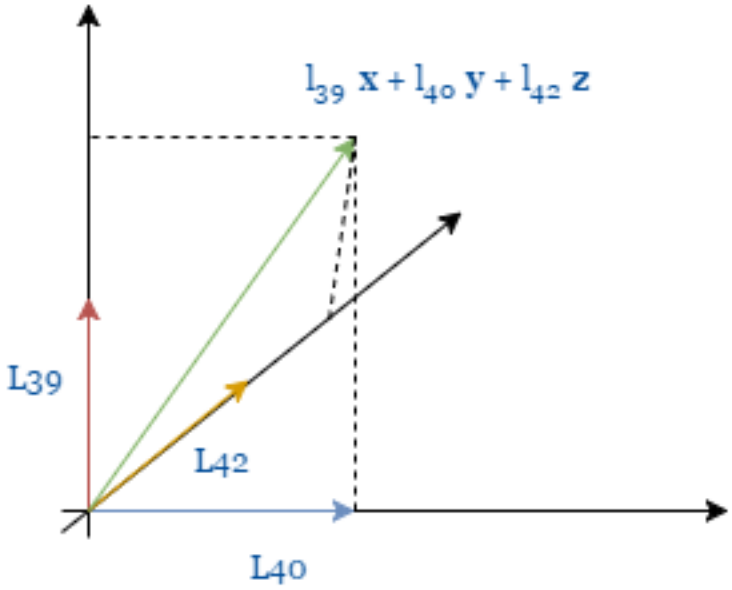

Figure 6.1: Different Load Increase Directions for loads on 3 buses in A_3 of 118 bus system.

Then, the K samples (as in (6.3)) can be grouped into n different groups according to the different load increase directions as,

$$y_{ki} = x_{1ki}\beta_{1i} + x_{2ki}\beta_{2i} + x_{1ki}^2\beta_{11i} + x_{2ki}^2\beta_{22i} + x_{1ki}x_{2kn}\beta_{12i} + e_{ki} \tag{6.4}$$

for $i = 1, 2, 3..., n$, and $k = 1, 2, ..., M$, and $M = \frac{K}{n}$. The quadratic terms can be denoted with new variables, by representing x_1^2 as x_3, x_2^2 as x_4, and x_1x_2 as x_5. Also, for sake of clarity, rename β_{11} as β_3, β_{22} as β_4, and β_{12} as β_5. Each of the n sets of equations in (6.4) can be written as matrix form as,

$$[\mathbf{Y}_i]_{M\times 1} = [\mathbf{X}_i]_{M\times 5}[\boldsymbol{\beta}_i]_{5\times 1} + [\mathbf{e}_i]_{M\times 1} \tag{6.5}$$

$\boldsymbol{\beta}_i$ can be thus estimated for each of the n groups, according to

$$\hat{\boldsymbol{\beta}}_i = (\mathbf{X}_i'\mathbf{X}_i)^{-1}\mathbf{X}_i'\mathbf{Y}_i, \quad i = 1, 2, ...n \tag{6.6}$$

For the discussed case, data was collected for $n = 32$ different load increase directions, and $\boldsymbol{\beta}_i$ was estimated for each of the groups. Histograms were plotted for each of the $\hat{\beta}_j$ $(j = 1, 2, ...5)$. For an instance, the histogram of $\hat{\beta}_2$ in the discussed case is shown in Fig.6.2.

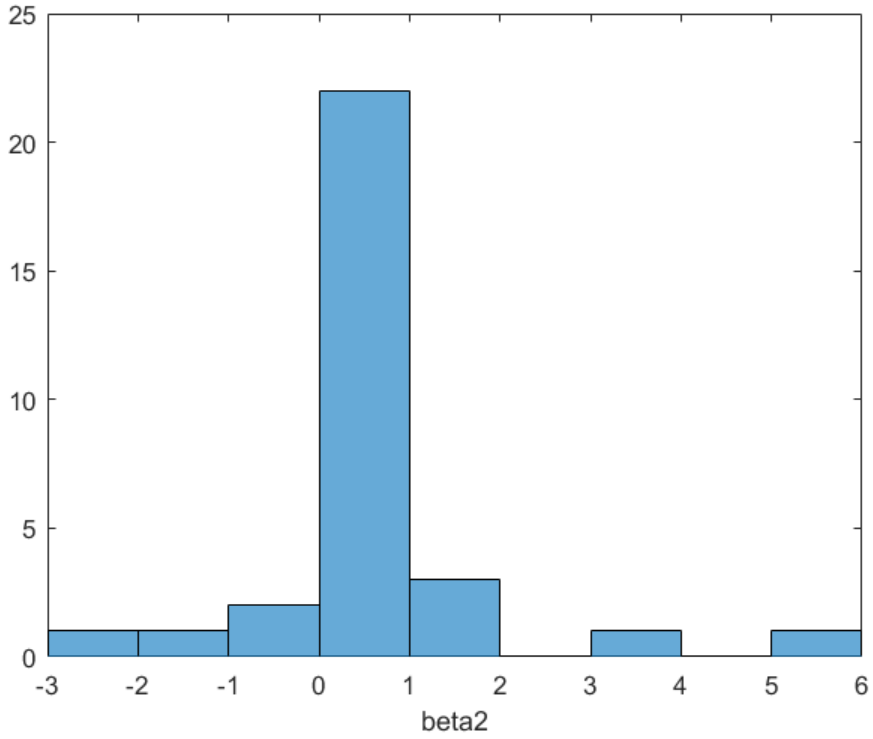

Figure 6.2: Histogram of coefficient $\hat{\beta}_2$ related with the reactive power reserve of generator at bus 40 in IEEE standard 118 bus system.

Now, we want test if the variance in each $\hat{\beta}$ is statistically significant. To that end we, perform statistical tests on the collected data samples, of the type,

$$\begin{aligned} H_0 &: \sigma^2_{\hat{\beta}} = 0 \\ H_1 &: \sigma^2_{\hat{\beta}} \neq 0 \end{aligned} \tag{6.7}$$

which test the significance of random effects in the regression models [98].

Chapter 7

Simulation Results and Discussion

In this chapter we discuss simulation results related with techniques proposed in chapters 4-6.

7.1 Simulations related to decentralized stability enhancement

7.1.1 Decentralized damping of transient oscillations

The control law (4.20) was tested on Kundur's two-area system [40, Chap.12], which was implemented on the PST simulation tool [100]. A three-phase short-circuit was applied for a duration of 150 ms to Line 8-9 of Kundur's two area system for three scenarios: (i) no TCSC; (ii) a single TCSC between Buses 7-8; and (iii) two TCSCs, one between Buses 5 and 6 and one between Buses 10 and 11. Figs. 7.1 (a) and 7.2 (b) illustrate the damping of the oscillations in speed deviation and voltage angle of Generator 1 of Area 1 with respect to Area 2, respectively, while Figs. 2c and 2d illustrate the damping of the oscillations of the power flows on Lines 5-6 and 7-8, respectively. It can be observed that implementing the control law (4.20) on local TCSCs, good damping is achieved of these signals. Furthermore, a better damping is obtained if the TCSCs are located closer to the boundaries of two areas.

7.1.2 Hierarchical decentralized voltage control

For testing the proposed hierarchical decentralized control scheme, the weakly coupled areas of the IEEE 118-bus test system are first determined. System data is used to construct the $\underline{\mathbf{D}}$ matrix given by (3). A suitable α is selected and used for identifying the 'weak' tie-lines that connect the voltage control areas, which are found to be eight areas. The buses belonging to

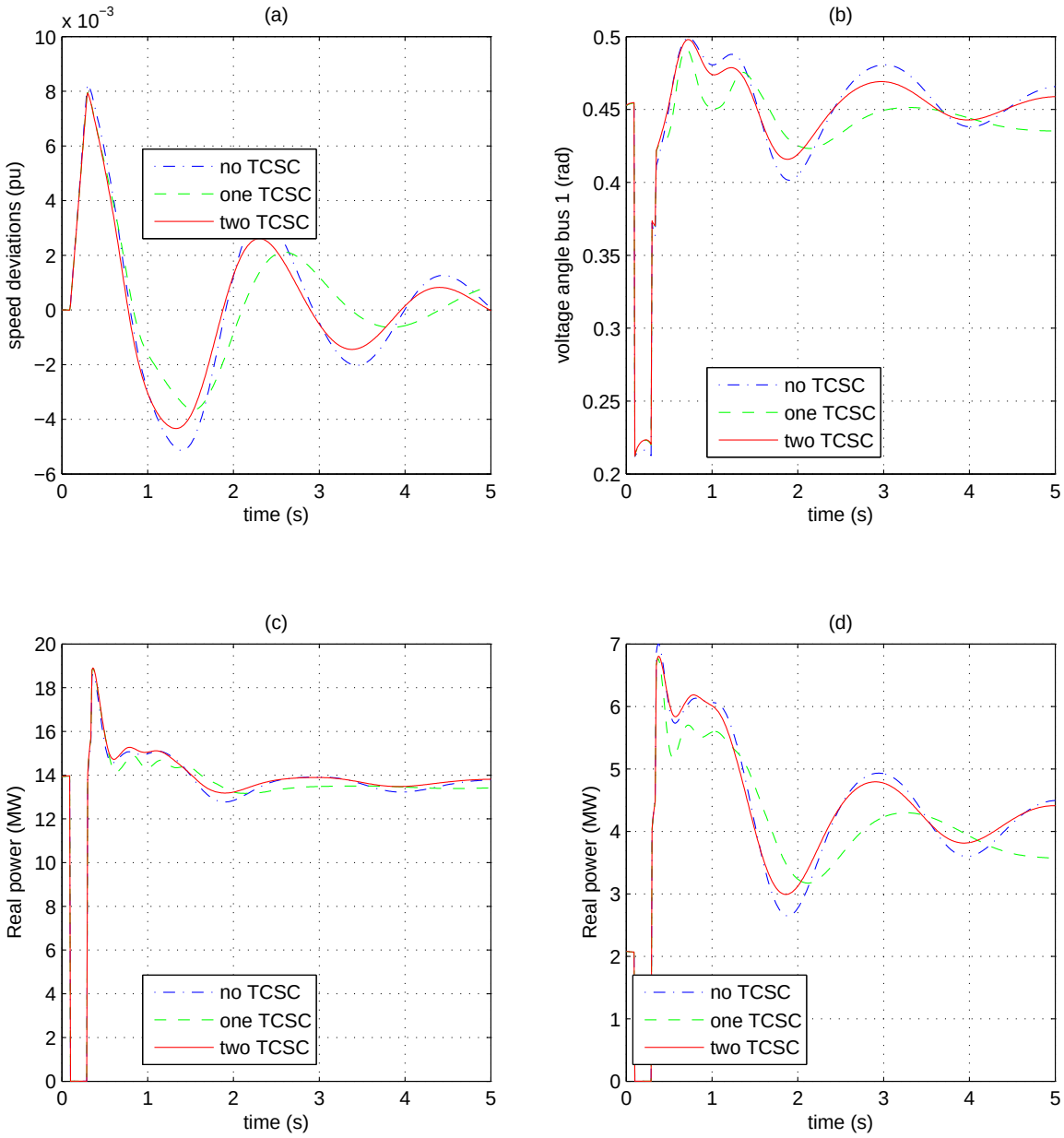

Figure 7.1: Graphs of (a) the speed deviation and (b) the terminal voltage angle of Generator located at Bus 1, and of the power flow on (c) Line 5-6 and (d) Line 7-8 of Kundur's 2-area system with no TCSC (blue dotted line); one TCSC (green dashed line); two TCSCs (red solid line) following a three-phase short-circuit (150 ms) on Line 8-9.

each of these areas (A_1 to A_8) are listed in Table I. The results are consistent with the ones given in [101]. Each control area is observed by means of local PMUs as shown in Table I. This leads to a larger number of PMUs than the one given by the minimum placement, but it eliminates the need of inter-area communication. This results in a bandwidth saving given by $(1 - n_{ba}N_a)/(n_{bp}n_p)$, where n_{ba} and n_{bp} respectively denote the rates of data transmitted by secondary agents and PMUs and N_a and n_p respectively denote the number of voltage control areas and the number of PMUs.

Table 7.1: Coherent Buses and PMU placement for the 118-bus system

Area	**Buses**	**PMU Placement**
A_1	1-14,16,117	1,5,9,12,13
A_2	15,17-22,30,33-38,43,113	17,21,34,37
A_3	39-42,49	40,42
A_4	52-59,49	52,54
A_5	44-51,59-67	45,49,59,62,64
A_6	23-29,31-32,114-115	23,25,29,114
A_7	68-103,116,118	68,71,75,77,79,80,85,87,90,92,103
A_8	104-112	105,110

Next, a simulation model of the IEEE 118-bus system was developed in PSS/E® Ver. 32. The MAS framework is implemented in a software program written in Python 2.5, which can instantiate the PSS/E using its Python compatible API. Local (secondary) control agents are implemented in each of the control areas as displayed in Table I while one tertiary control agent is implemented for the whole system. TCSCs are installed in each coherent area such that they can damp area oscillations according to (4.20) using only local area measurements. Furthermore, switched capacitors are installed on the critical buses of each area. Simulations are carried out while slowly increasing the load, which results in the decrease of system voltage stability margins. A daily load profile is simulated by varying the p.u. loading in Area 5, as shown by the red curve in Fig. 7.2. The secondary agent is set to maintain enough stability margin in the area such that the voltage at Bus 45 remains between 0.85 p.u. to 1.15 p.u. As shown during the peak load of the first day, the secondary control agent turns on the capacitor bank of an area as soon as it estimates a low stability margin based on the local metered reactive reserves. On the second day, we observe that the instabilities cannot be controlled by the secondary agent acting alone; hence the tertiary agent sheds 15% of inelastic load to stabilize the system. As shown by the dashed blue lines in Fig. 7.2, without any secondary or tertiary control actions, all the node voltages of Area 5 fall below 0.85 p.u. during peak loads. This occurs even after the peaking units are connected to the system because of high congestion of the transmission lines that may wheel

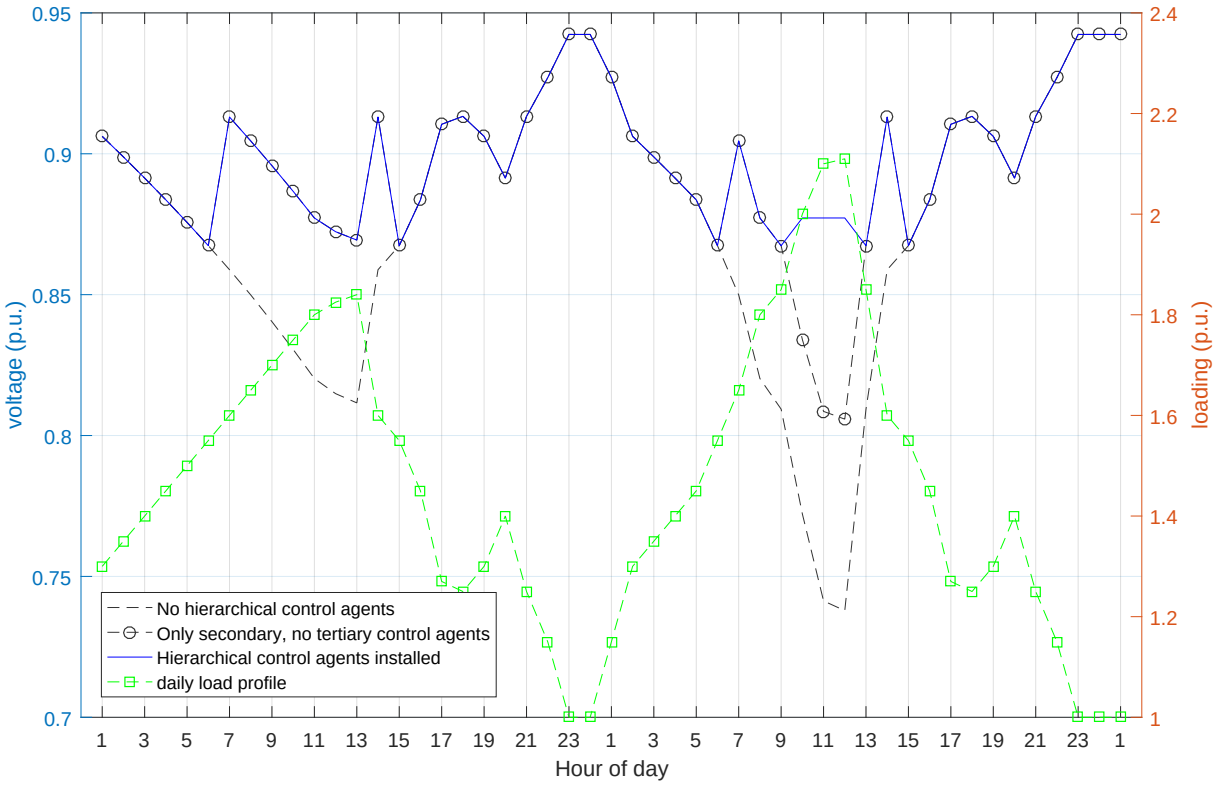

Figure 7.2: Voltage magnitude at Bus 45 of the IEEE 118-bus system: no hierarchical controllers (dashed black line), only secondary controllers (dash-dot black line), hierarchical controllers (blue solid line), load profile (green).

reactive power to critical buses.

7.2 Simulation results related to communication network design of microgrids

7.2.1 Specification configuration

Network architecture for a system consisting of both microgrid and AMI applications has been simulated. As depicted in Fig.5.5, it consists of two clusters of meter nodes running metering applications. Each cluster has four meters, one of which is acting as an access point to connect to the backhaul network. There are two clusters of microgrid sensor nodes that continuously monitor the state of the power system to detect impending power system instability. Each cluster has one access point with seven nodes in all. All of these clusters are connected to the aggregation which, in turn, is connected to the substation router. This

router is in turn connected to two servers, one of which is the microgrids control center and the other one is the AMI application control center.

All the simulations were carried out on the OPNET Modeler 17.1. Multiple scenarios were simulated for the previously described network architecture, namely (a) all nodes following the DCF protocol; (b) all nodes following DCF with fragmentation of packets when they reach a threshold, which is set to 256 bytes; (c) half of the nodes following a point coordination with a single access point protocol (PCF) and half following the DCF without any fragmentation; and (d) half of the nodes following PCF protocol and half following the DCF with fragmentation. All of these scenarios were simulated for 4 different types of inter-node distances. This was done to evaluate the suitability of different channel access mechanisms for the WLANs of the metering and the microgrid agents.

For simulation purposes, the internode distances are varied in steps from very small to very large as displayed in Table 7.2. This table shows the distance between the destination and source node in the cluster. It is observed that, multiple factors such as the number of agents, the channel access protocol and distances between source and destination nodes affect the network performance. Note that while in reality the nodes are located in a 3-dimensional space, we will assume them to be spread in a plane for simplicity.

Table 7.2: Distances between source and destination node pair 1 and 5 for simulations

Simulation Case Number	**Distance(meters)**
Case 1	23.5
Case 2	76.16
Case 3	104.4
Case 4	131.25

7.2.2 Simulation results

Fig.7.3 shows the simulation results in four cases. It is observed that a network where all the nodes are accessing channel via the PCF protocol has a lower time-averaged load than the network in which all the nodes follow a DCF protocol for channel access. But, if only half of the nodes are PCF enabled, the time-averaged load is approximately equal (and even higher in some cases) to the fully DCF-enabled network. Here, the load of a channel represents the total load (in bits/sec) that the physical layer receives from the higher layers, e.g. the application layer. As observed in Fig.7.3, the time averaged load is only slightly lower in networks (b) and (c), which is at medium distances between the nodes. In Fig.7.3 (a) and (d), the time averaged load for the partially PCF enabled network is slightly higher.

Table 7.3 provides a list of applications and mechanisms. Using PCF, the access point polls all the nodes one-by-one for data packets. Due to this point coordination, all the nodes are able to transmit their data efficiently with lesser packet losses and lesser retransmission attempts as compared with DCF. When the nodes make use of the DCF protocol, the channel may not be efficiently utilized due to the occurrence of a high number of packet collisions; this may occur even when a backoff mechanism is included in the protocol for decreasing the frequency of collisions. The reason is that, with the DCF being implemented, the channel may be heavily loaded due to the occurrence of too many nodes transmitting simultaneously at one instant of time while, at another instant of time, the channel is vacant for a longer period without any node transmitting due to backoffs after packet collisions.

If the network packets are dropped during the data transmission, the sender will try to retransmit the packets. Fig.7.4 shows the number of retransmission attempts for different nodes in the wireless meshed network. We see that for the DCF, the retransmission attempts are much higher than those of the PCF due to lack of coordination and high number of collisions. This increases the amount of traffic to be sent because many packets are dropped and, therefore, have to be resent. When the nodes are very distant from each other, the DCF performs almost similarly to the PCF in load carrying because the probability of packet collisions, packets drops, and retransmission attempts decreases. As seen from Fig.7.5, the larger the number of PCF nodes in the network, the higher the delay. This is due to the fact that the PCF algorithm takes longer time because of the Short and the Priority Inter Frame Spacing during the polling mechanism. The higher is the number of nodes used by PCF, the longer is the delay being introduced.

As for the metering applications, they have low data rate requirements whereas the traffic is smooth in nature. Since the metering traffic can bear some latencies, we infer that the PCF protocol is the best suited for metering applications since it will decrease the overall load on the channel. To the contrary, the microgrid agent traffic requires minimal delays for best performance. In an emergency state, this traffic is bursty and non-periodic in nature, which precludes the utilization of data polling. The problem of high channel loading can be solved by keeping sufficiently large distances between the microgrid nodes. The recommended solution for microgrids is therefore the use of a DCF protocol with large internode distances since it entails lesser latency and optimizes channel loading.

7.2.3 AQM scheme for AMI and microgrid agents

As discussed in the previous subsection, all the different types of traffic generated by the microgrid and the AMI applications must be transmitted over the same backhaul. To provide each packet a specific treatment, the network infrastructure must have the ability to distinguish between packets by means of property-based classification. This classification enables it to separately queue the packets and to schedule the packet queues, with the aim to implement a differential treatment to them and to provide means for measuring, moni-

Table 7.3: Proposed Channel Access Mechanisms for Different Applications

Application	**Traffic Type**	**Network Architecture**	**Access Protocol Recommendation**
AMI	Smooth Traffic, Periodic, Fixed data rate.	Wireless, point to multipoint architecture	PCF
HAN	Smooth Traffic, Fixed data rate.	Wireless, point to point architecture	DCF or PCF
DA, SA	Smooth Traffic, Fixed data rate.	Wireless: WDS	DCF
Microgrids	Bursty Traffic, Non-periodic.	Wireless, both point to point and point to multi-point	DCF with large internode distances

toring, and conditioning packet streams with specific QoS levels. These can all be realized through the implementation of scheduling mechanisms in the packet forwarding path.

Commonly used packet scheduling mechanisms in existing communication systems the: First-In-First-Out (FIFO), Priority Queuing (PQ) and Weighted Fair Queuing (WFQ). For the present study, a model of such mechanisms has been developed for the communication network carrying the traffics of AMI and microgrids and implemented on OPNET. As depicted in Fig.7.6, it consists of three servers displayed on the left of the figure, which include (1) one server implementing the File Transfer Protocol (FTP) and generating a smooth AMI traffic; (2) one server generating the bursty traffic of microgrids, which for example instantiate a VoIP application; and (3) one server generating the bursty traffic of microgrids agents, which, for instance, utilizes a video conferencing application.

7.2.4 Specification configuration

The aggregation point and the substation-end aggregator are two standard Ethernet routers. Both routers are connected using a bidirectional DSL link using Point-to-Point Protocol (PPP). The access points and the servers are connected with the routers using 10 Mbps links. These links have been implemented for simulation purposes to provide a better bandwidth. In the field, these links may be either wireless links or connected via xDSL links or 'T1/E1' links. The FTP is a metering traffic considered to be High Load with constant inter-request times, which are set up to 10 seconds in this application.

With the deployment of smart meters, the files carrying the metering data may be very large as compared to the existing metering data files. This is because, apart from the normal energy metering, there are a number of additional features provided by the smart meters.

For the purpose of such simulation, all the applications are configured in such a way to generate a certain traffic pattern and to provide differentiated services. These configurations are listed in Table 7.4. For simulating a certain emergency event, the microgrid applications start to generate a bursty traffic 100 seconds after the beginning of the simulation. Note that the three types of queuing management mechanisms discussed above are configured on the links of the routers.

In the next subsection we will discuss some simulation results including the IP packets dropped, delay variation and actual delays, when the agents communicate with their respective control centers under an emergency condition.

7.2.5 Simulation results and discussions

We simulate three different scenarios of the queue management schemes, which are run for 2.5 simulation minutes. Various network performance metrics like the traffic dropped, the transmission delays and the jitter in the delays are compared. As shown in Fig.7.7, it is observed that at the end of two and half minutes of simulation, the amount of traffic dropped is 40 packets/sec for the FIFO, 25 packets/sec for PQ and 16 packets/sec for WFQ. Also the PQ starts rejecting the traffic almost 25 seconds earlier than the WFQ scheme. This happens at the simulation time of 100 seconds, when the bursty traffic kicks in. Hence, by prioritizing the microgrid traffic or giving it higher weights while transmitting it to the neighboring substations, lesser amount of traffic is dropped and better performance is achieved. This results from the inherent implementation of the FIFO mechanism, which does not provide service differentiation in terms of bandwidth and delay. In FIFO mechanism, it is obvious that the flow with a higher bandwidth will use a large portion of the transmission bandwidth. Consequently, for the microgrid agents, which are characterized by a bursty traffic, FIFO mechanism will lead to an increase of the average packet delays per flow and a higher rate of packet drop. As observed in Fig.7.8, the overall delay is high and jittery when the bursty traffic of microgrid agents starts filling the queue in presence of smooth traffic. This is due to the fact that the FIFO mechanism does not differentiate between the traffics originating from different sources. Consequently, the traffic does not receive any priority handling, resulting in a quick fill up of the queues. By contrast, there is almost no variation in delays when using either PQ or WFQ. Hence, due to increased jitter and latencies, the time critical task of improving the stability margin of the power system may not be achieved. AQM mechanisms are highly recommended for transmitting this critical traffic over the backhaul to achieve minimal delays.

7.2.6 Conclusions

From the constructed experiments and simulations results, we obtained some significant experiences that may help microgrid practitioners or researchers guiding their future designs.

Table 7.4: Traffic and Service Configuration for Studied Applications

Application	**Type of Traffic**	**Type of Service**
AMI	FTP(file type)	Best Effort
Microgrid Agent Cluster 1	Low Resolution Video	Streaming Multimedia
Microgrid Agent Cluster 2	PCM quality speech/voice	Interactive Voice

The faster channel access mechanisms like DCF are suitable for microgrid clusters. If the microgrid agents make use of PCF, their traffic will suffer from large latency, which may preclude them from stabilizing the power system subject to a major disturbance. Also, implementing active queue management mechanisms in the shared links is necessary for better network performance in emergency states of a power system. Otherwise, a loss of a significant amount of data in the communication process may result.

7.3 Simulation results related to uncertainty estimation in VSM vs. RPR regression model

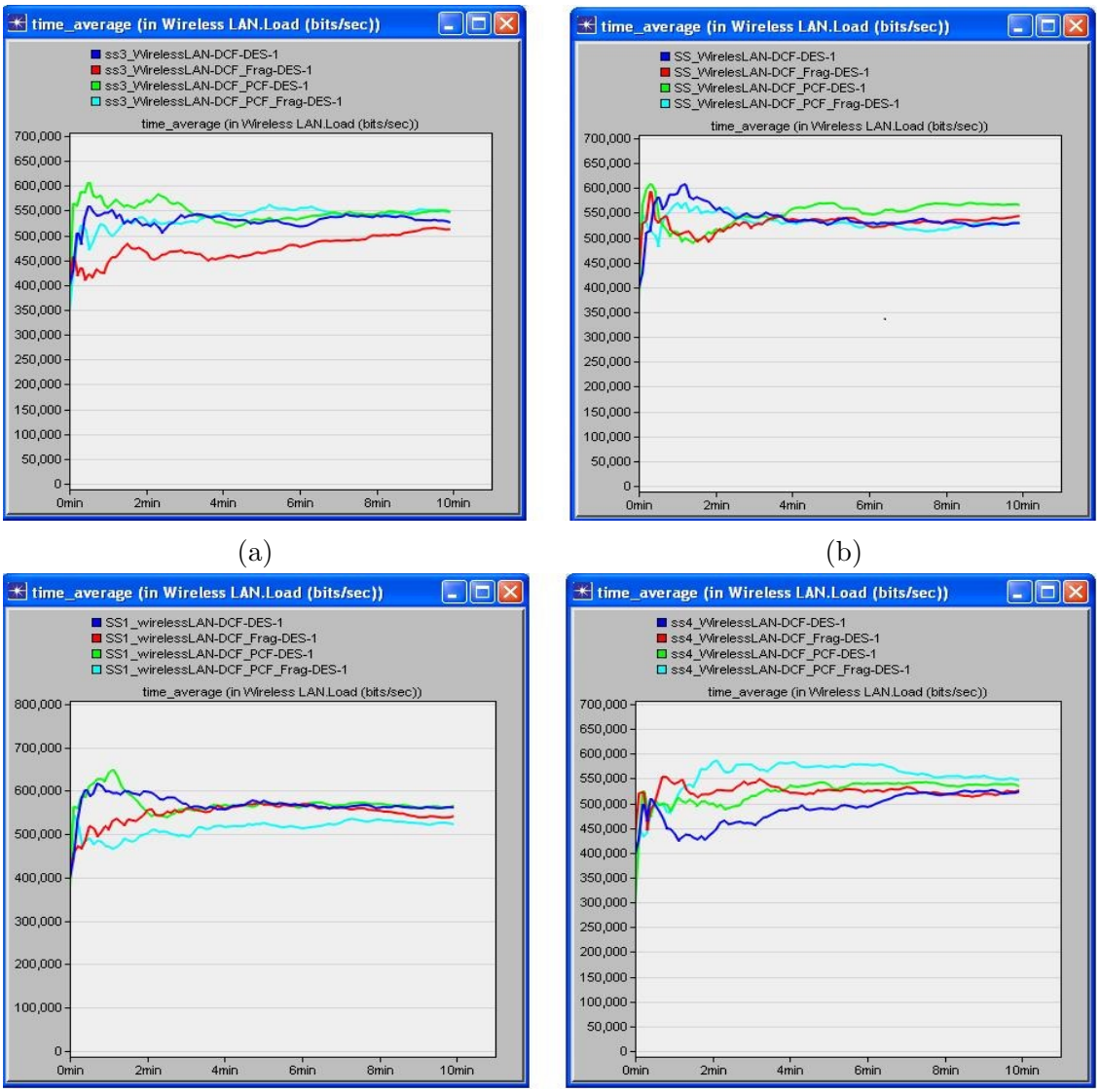

Figure 7.3: Load in (bits/sec) for the four different networks. Dark Blue: All DCF nodes; Red: All DCF nodes with fragmentation; Green: Half DCF and Half PCF nodes; Light Blue: Half DCF and Half PCF nodes with fragmentation. Internode distance increases from (a) to (d)

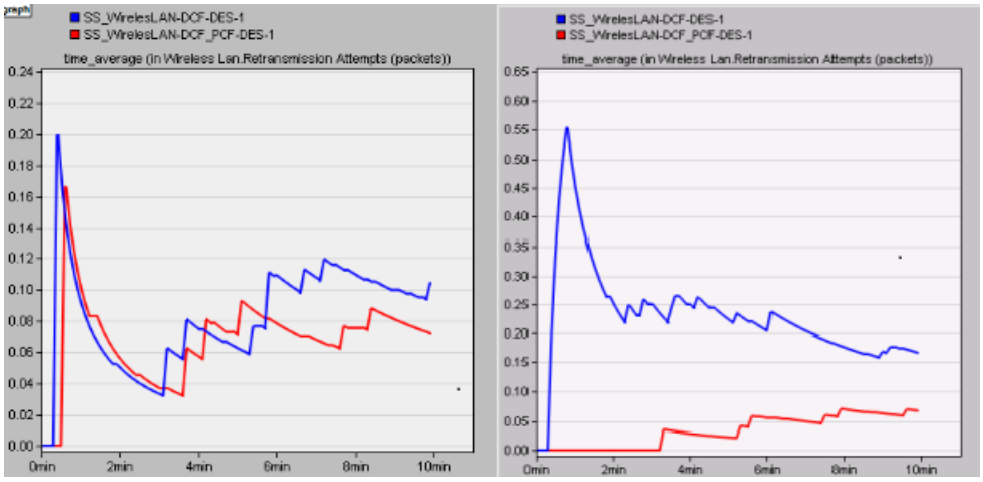

Figure 7.4: retransmission attempts at one DCF enabled (left) and at one PCF enabled (right) node in terms of packets. (Time average) Dark Blue: All others are DCF nodes; Red: Half DCF and Half PCF nodes

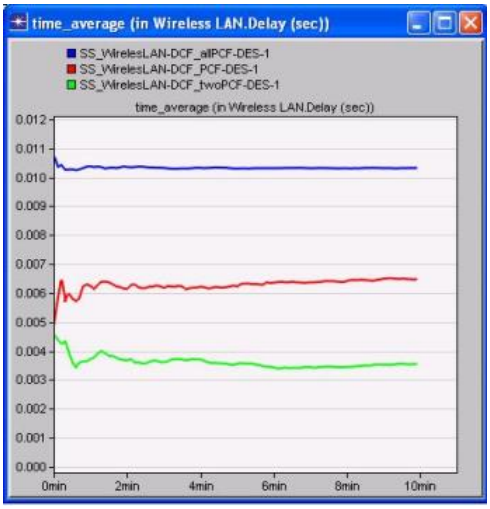

Figure 7.5: Average Delay (sec) of the network for different number of PCF nodes

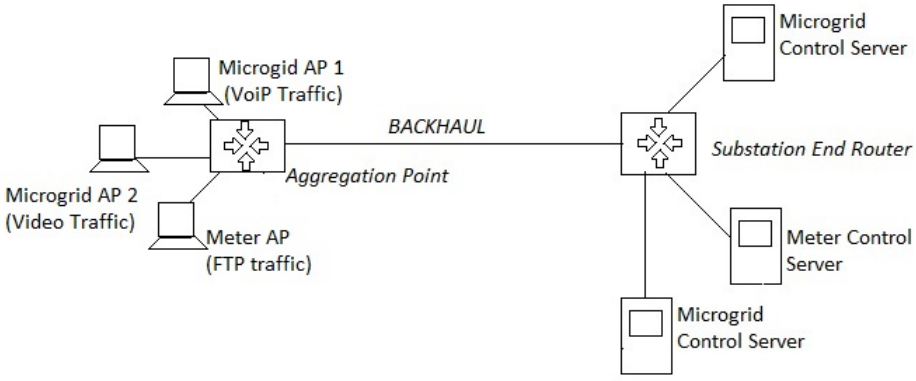

Figure 7.6: Traffic from variety of agents sharing a common backhaul beyond the aggregation point

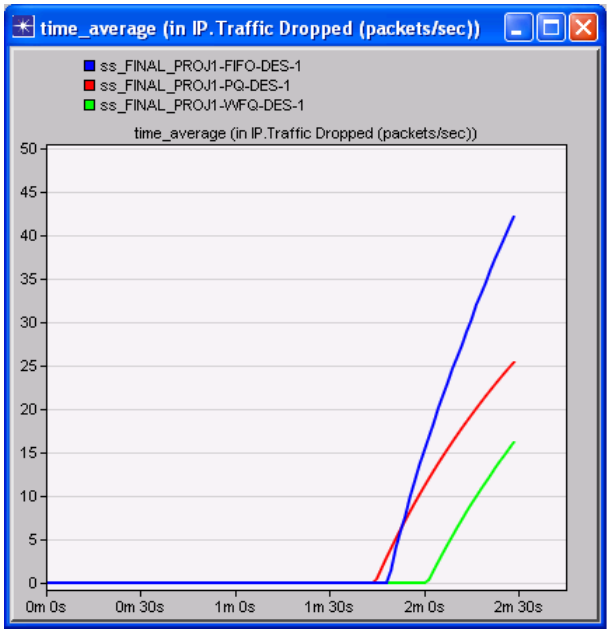

Figure 7.7: IP Traffic dropped (packets/sec) for three AQM schemes

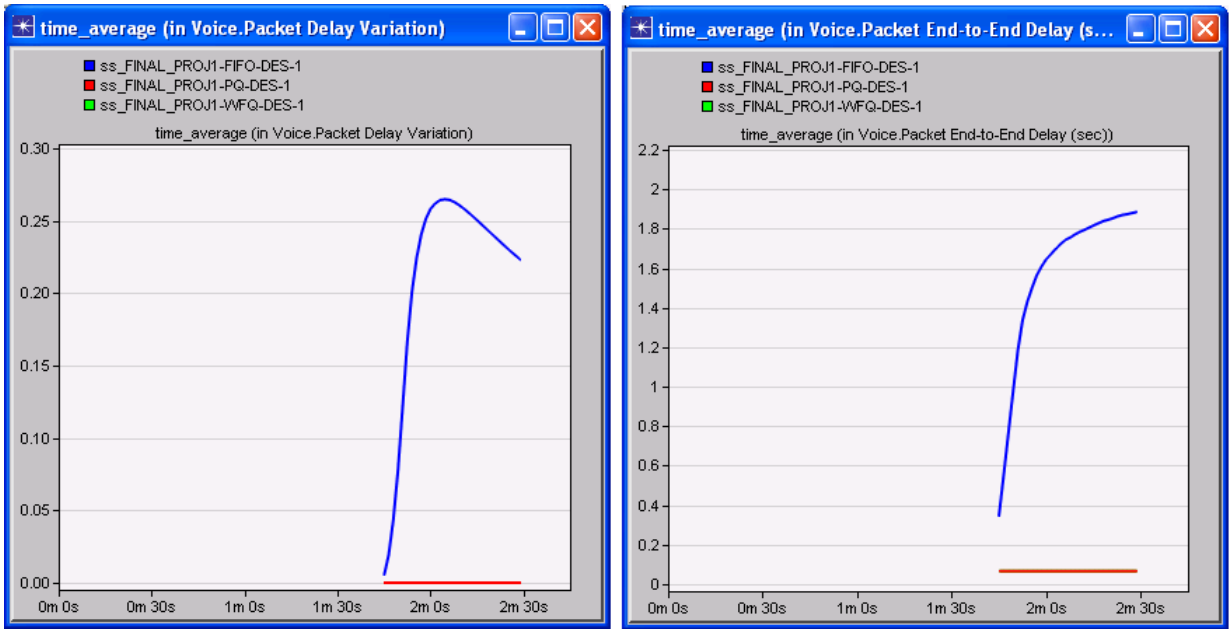

Figure 7.8: Delay variations (left) and actual packet delay in seconds (right). Blue line FIFO, Red LineL: PQ, Green Line: WFQ (time average)

Chapter 8

Conclusions and Scope of Future Work

In the present research work, we have developed a decentralized, hierarchical control scheme for stability enhancement of an interconnected power system. We have implemented methods for identification of loosely coupled subsystems, called 'control areas', in a large-scale power system. The techniques that allows us to identify these interconnected subsystems make use of the singular perturbation approach. Using Lyapunov's second method, we determine the necessary and sufficient conditions for achieving global asymptotic stability following large disturbances in such systems. We show that global asymptotic stability can be realized by damping oscillations based on control laws which only depend on local measurements. Furthermore, we infer by simulations on IEEE standard test beds that a better damping of oscillations is obtained if the control devices are installed on buses close to the boundaries of the control areas. Since the transmission line conductors have relatively high reactances as compared to the resistances, reactive power cannot be wheeled to large electrical distances in the network. This characteristic effects the controllability of voltage at various nodes in the power system, and we utilize this property to design decentralized control of voltage instability, following small disturbances in a large-scale power system. Furthermore, regression models are developed between the available reactive power in a region with its local voltage stability margin. We also identify the random effects in the model due to the uncertainty in the independent variables (the available reactive power in local generators). The decentralized control scheme is implemented under a multi-agent system framework. We observe by simulations that the hierarchical, decentralized control schemes require lesser communication bandwidth, have a system-wide situational awareness and still achieve the goal of global asymptotic stability. A communication network design has been discussed which performs efficiently in both normal and stressed operating conditions of he network.

The present research can be extended in several ways in the future. Currently, an energy function based approach has been applied to predict the local angular stability margins,

which has several shortcomings: (a) the system is considered lossless, assuming the ratio of the resistance to reactance in transmission lines to be negligible, (b) similarly dynamics in load model are ignored for simplicity, and only a reduced network model is used. While by using these approximations, the path dependent integration terms are removed from the model, the resulting model may lead to approximate control laws with large error probabilities. Hence, in future research work, models may be enhanced with the path-dependent terms included. Another direction of research that can be explored for the development of decentralized stability analysis is the application of subsystem-wise spectral analysis schemes, followed by data fusion, as proposed by Williams et.al. in [103]. Furthermore, current schemes are only implemented on IEEE standard test beds. A better approach consists in assessing the applicability of the method in a real utility power system by using the transmission system data of a large electric utility. The methods of uncertainty quantification of control decisions can be expanded to both local and global levels.

Chapter 9

Bibliography

[1] K. Morison, L. Wang, and P. Kundur, "Power system security assessment," *IEEE Power Energy Mag.*, vol. 2, no. 5, pp. 30-39, Sept.-Oct. 2004.

[2] P. Kundur *et al.*,"Definition and classification of power system stability IEEE/CIGRE joint task force on stability terms and definitions," *IEEE Trans. Power Syst.*, vol. 19, no. 3, pp. 1387-1401, Aug. 2004.

[3] K. Ziegler, and A. Oneal, "Balancing and Frequency Control," NERC, Princeton, NJ, Jan. 26, 2011. Available online at: `http://www.nerc.com/comm/oc/rslandingpagedl/relatedfiles/nercbalancingandfrequencycontrol040520111.pdf`

[4] M. Glavic, and T. Van Cutsem, "A short survey of methods for voltage instability detection," *IEEE PES General Meeting* , vol., no., pp.1-8, 24- 29, July 2011.

[5] N. Sandell, P. Varaiya, M. Athans, and M. Safonov, "Survey of decentralized control methods for large scale systems," *IEEE Trans. Autom. Control*, vol. 23, no. 2, pp. 108-128, April 1978.

[6] J. Swigart, and S. Lall, *Networked Control Systems*. London:Springer, 2010.

[7] S.D.J. McArthur, E.M. Davidson, V.M. Catterson, A.L. Dimeas, N.D.Hatziargyriou, F. Ponci, and T. Funabashi, "Multi-Agent Systems for Power Engineering Applications—Part I: Concepts, Approaches, and Technical Challenges," *IEEE Trans. Power Syst.* , vol.22, no.4, pp.1743-1752, Nov. 2007.

[8] –,"Multi-Agent Systems for Power Engineering Applications—Part II: Technologies, Standards, and Tools for Building Multi-agent Systems," *IEEE Trans. Power Syst.* , vol.22, no.4, pp.1753-1759, Nov. 2007.

[9] V.R. Saksena, J. O'Reilly, and P.V. Kokotovic, "Singular perturbations and time-scale methods in control theory: Survey 1976–1983," Automatica, vol. 20, no. 3, pp. 273-293, 1984.

[10] F.N.Bailey, "The Application of Lyapunov's Second Method to Interconnected Systems," *Jour. Soc. for Indus. and Appl. Math. Series A Control*, vol.3, no.3, pp. 443–462, 1965.

[11] P. Kokotovic, H.K. Khalil, and J. O'reilly, *Singular perturbation methods in control: analysis and design*. Philadelphia: Siam, 1999.

[12] J.N. Tsitsiklis, "Problems in Decentralized Decision making and Computation," MIT Cambridge Lab for Info. and Decision Syst., Rep. No. LIDS-TH-1424, 1984.

[13] R.R. Tenney, and N.R. Sandell Jr., "Detection with distributed sensors," *IEEE Trans. Aerosp. Electron. Syst*, vol. AES-17,no.4, pp. 501-510, Jul. 1981.

[14] J. F. Chamberland, and V. V. Veeravalli, "Wireless Sensors in Distributed Detection Applications," *IEEE Signal Process. Mag.*, vol. 24, no. 3, pp. 16-25, May 2007.

[15] R. Viswanathan and P. K. Varshney, "Distributed detection with multiple sensors I. Fundamentals," *Proc. IEEE*, vol. 85, no. 1, pp. 54-63, Jan 1997.

[16] S. A. Kassam, and H. V. Poor, "Robust techniques for signal processing: A survey," *Proc. IEEE*, vol. 73, no. 3, pp. 433-481, March 1985.

[17] S. A. Aldosari and J. M. F. Moura, "Detection in Sensor Networks: The Saddlepoint Approximation," *IEEE Trans. Signal Process.*, vol. 55, no. 1, pp. 327-340, Jan. 2007.

[18] N.R. Jennings, "Controlling cooperative problem solving in industrial multi-agent systems using joint intentions," *Artificial Intelligence*, vol. 75, no. 2, pp. 195-240, 1995.

[19] J. T. Feddema, C. Lewis, and D. A. Schoenwald, "Decentralized control of cooperative robotic vehicles: theory and application," *IEEE Trans. Robot. Autom.*, vol. 18, no. 5, pp. 852-864, Oct 2002.

[20] M. Di Santo, A. Vaccaro, D. Villacci, and E. Zimeo, "A distributed architecture for online power systems security analysis," *IEEE Trans. Ind. Electron.*, vol. 51, no. 6, pp. 1238-1248, Dec. 2004.

[21] M. Glavic, and T. Van Cutsem, "Wide-Area Detection of Voltage Instability From Synchronized Phasor Measurements. Part I: Principle," *IEEE Trans. Power Syst.*, vol. 24, no. 3, pp. 1408-1416, Aug. 2009.

[22] R. F. Nuqui, "State Estimation and Voltage Security Monitoring Using Synchronized Phasor Measurements," PhD Thesis, Virginia Polytechnic Institute and State University, Blacksburg, Virginia, 2001.

[23] R. Diao, K. Sun, V. Vittal, R. J. O'Keefe, M. R. Richardson, N. Bhatt, D. Stradford, S. K. Sarawgi, "Decision Tree-Based Online Voltage Security Assessment Using PMU Measurements,"*IEEE Trans. Power Syst.*, vol. 24, no. 2, pp. 832-839, May 2009.

[24] L. Bao, Z. Huang and W. Xu, "Online voltage stability monitoring using VAr reserves," *IEEE Trans. Power Syst.*, vol.18, no.4, pp.1461-1469, Nov. 2003.

[25] T. Van Cutsem, "A method to compute reactive power margins with respect to voltage collapse," *IEEE Trans. Power Syst.* , vol.6, no.1, pp.145-156, Feb 1991.

[26] B. Leonardi and V. Ajjarapu, "Development of Multilinear Regression Models for Online Voltage Stability Margin Estimation," *IEEE Trans. Power Syst.*, vol.26, no.1, pp.374-383, Feb. 2011.

[27] H. Lefebvre, D. Fragnier, J.Y. Boussion, P. Mallet, and M. Bulot, "Secondary coordinated voltage control system: feedback of EDF," *Proc. PES Summer Meeting*, Vol. 1, no., pp. 290-295, 2000.

[28] S. Corsi, M. Pozzi, C. Sabelli, and A. Serrani, "The coordinated automatic voltage control of the Italian transmission Grid-part I: reasons of the choice and overview of the consolidated hierarchical system," *IEEE Trans. Power Syst.*, vol.19, No.4, pp.1723-32, Nov. 2004.

[29] J.L. Sancha, J.L. Fernandez, and J.T. Abarca, "Secondary voltage control: analysis, solutions and simulation results for the Spanish transmission system," *IEEE Trans. Power Syst.*, vol.11, no.2, pp.630-638, May 1996.

[30] V. Venkatasubramanian, J. Guerrero, J. Su, H. Chun, X. Zhang, F. Habibi-Ashrafi, A. Salazar, and B. Abu-Jaradeh, "Hierarchical two-level voltage controller for large power systems," *IEEE Trans. Power Syst.* , vol.31, no.1, pp.397-411, Jan. 2016.

[31] H. Mehrjerdi, S. Lefebvre, M. Saad, and D. Asber, "A Decentralized Control of Partitioned Power Networks for Voltage Regulation and Prevention Against Disturbance Propagation," *IEEE Trans. Power Syst.*, vol.28, no.2, pp.1461-1469, May 2013.

[32] –,"Coordinated Control Strategy Considering Effect of Neighborhood Compensation for Voltage Improvement in Transmission Systems," *IEEE Trans. Power Syst.* , vol.28, no.4, pp.4507-4515, Nov. 2013.

[33] I. Kamwa, R. Grondin, and L.Loud, "Time-varying contingency screening for dynamic security assessment using intelligent-systems techniques," *IEEE Trans. Power Syst.*, Vol. 16, No. 3, pp. 526-536, Aug. 2001.

[34] Y. Guo, D. J. Hill, and Y. Wang, "Global transient stability and voltage regulation for power systems," *IEEE Trans. Power Syst.*, vol. 16, no. 4, pp. 678-688, Nov. 2001.

[35] M. Noroozian *et. al.*, "A robust control strategy for shunt and series reactive compensators to damp electromechanical oscillations," *IEEE Trans. Power Del.*, vol. 16, no. 4, pp. 812-817, Oct 2001.

[36] J.H. Chow, *Power system coherency and model reduction*. New York: Springer, 2013.

[37] A.M. Lyapunov, "The general problem of motion stability," *Annals Math. Studies*, 1892.

[38] C. P. Steinmetz,"Power control and stability of electric generating stations," *AIEE Trans.*, vol. XXXIX, Part II, pp. 1215–1287, July 1920.

[39] AIEE Subcommittee on Interconnections and Stability Factors,"First report of power system stability," *AIEE Trans.*, pp. 51–80, 1926.

[40] P. Kundur, *Power System Stability and Control*. New York: McGraw-Hill, 1994.

[41] P.W. Sauer, and M.A. Pai, *Power system dynamics and stability*. NJ: Prentice Hall, 1998.

[42] A.R.Bergen and D.J.Hill, "Structure Preserving Model for Power System Stability Analysis", *IEEE Trans. Power Appar. Syst.*, PAS-100, 1, Jan.1981.

[43] P.C. Magnusson,"Transient Energy Method of Calculating Stability," *AIEE Trans.*, vol.66, pp. 747-755, 1947.

[44] P.D.Aylett,"The energy-integral criterion of transient stability limits of power systems." *Proc. IEE-Part C: Monographs*, vol.105, no.8, pp. 527-536, 1958.

[45] A.H.El-Abiad, and K. Nagappan. "Transient stability regions of multimachine power systems." *IEEE Trans. Power Appar. Syst.*, vol. 2, no., pp. 169-179, 1966.

[46] Z.Artstein, "Stabilization with relaxed controls," *Nonlinear Anal.*, vol. 11, pp. 1163–1173, 1983.

[47] M. Ghandhari, "Control Lyapunov functions: A control strategy for damping of power oscillations in large power systems," PhD Dissertation, Royal Institute of Technology-KTH, Stockholm. 2000.

[48] J.D.Crawford, "Introduction to bifurcation theory," *Review Modern Phys.*, vol.63, no.4, pp. 991-1037, Oct. 1991.

[49] K. Vu, M. M. Begovic, D. Novosel, and M. M. Saha, "Use of Local Measurements to Estimate Voltage Stability Margin," *IEEE Trans. Power Syst.*, vol. 14, no. 3, pp. 1029-1035, Aug. 1999.

[50] I. Smon, G. Verbic, and F. Gubina, "Local Voltage-Stability Index Using Tellegen's Theorem," *IEEE Trans. Power Syst.*, vol. 21, no. 3, pp.1267-1275, Aug. 2006.

[51] T. Van Cutsem, L. Wehenkel, M. Pavella, B. Heilbronn, M. Goubin, "Decision tree approaches to voltage security assessment," *IEE Proc. Gen., Trans. and Dist.*, Vol. 140, No. 3, pp. 189-198, May 1993.

[52] R. A. Schlueter, I.-P. Hu, M. W. Chang, J. C. Lo and A. Costi, "Methods for determining proximity to voltage collapse," *IEEE Trans. Power Syst.*, vol.6, no.1, pp.285-292, Feb. 1991.

[53] P. Zhang, and S. T. Lee, "Probabilistic load flow computation using the method of combined cumulants and Gram-Charlier expansion," *IEEE Trans. Power Syst.*, vol. 19, no. 1, pp. 676-682, Feb. 2004.

[54] C.L. Su, "Probabilistic load-flow computation using point estimate method," *IEEE Trans. Power Syst.*, vol. 20, no. 4, pp. 1843-1851, Nov. 2005.

[55] H.E. Daniels, "Saddlepoint approximations in statistics," *Ann. Math. Statist.* vol.25, pp.631-650, 1954.

[56] N. Reid, Saddlepoint methods and statistical inference (with discussion). Statist. Sci., vol. 3, pp. 213-238, 1988.

[57] I. Kamwa, R. Grondin, and Y. Hebert, "Wide-area measurement based stabilizing control of large power systems-a decentralized/hierarchical approach," *IEEE Trans. Power Syst.*, vol. 16, no. 1, pp. 136-153, 2001.

[58] I. Kamwa, J. Béland, G. Trudel, R. Grondin, C. Lafond, and D. McNabb, "Wide-area monitoring and control at Hydro-Québec: Past, present and future," *Proc. IEEE/PES General Meeting, Panel Session PMU Prospective Applications*, Montreal, QC, Canada, Jun. 2006.

[59] K. Sun, S. Likhate, V. Vittal, V. S. Kolluri and S. Mandal, "An Online Dynamic Security Assessment Scheme Using Phasor Measurements and Decision Trees," *IEEE Trans. Power Syst.*, vol. 22, no. 4, pp. 1935-1943, Nov. 2007.

[60] T. Lie, R. A. Schlueter, P. A. E. Rusche and R. H. Rhoades, "Method of identifying weak transmission network stability boundaries," *IEEE Trans. Power Syst.*, vol. 8, no. 1, pp. 293-301, Feb 1993.

[61] A. G. Expósito, A. V. Jaén, C. G. Quiles, P. Rousseaux, T. V. Cutsem, "A taxonomy of multi-area state estimation methods," *Elec. Power Syst. Research*, vol. 81, no. 4, pp. 1060-1069, April 2011.

[62] J. Chen and A. Abur, "Placement of PMUs to enable bad data detection in state estimation," *IEEE Trans. Power Syst.*, vol. 21, no. 4, pp. 1608-1615, Nov. 2006.

[63] L. Mili, T. Baldwin, and R. Adapa, "Phasor measurement placement for voltage stability analysis of power systems," *Proc. of the 29th IEEE Conf. on Decision and Control* , pp. 3033-3038, 1990.

[64] T. J. Overbye, "Use of energy methods for on-line assessment of power system voltage security," *IEEE Trans. Power Syst.*, vol. 8, no. 2, pp. 452-458, May 1993.

[65] H. White, "A heteroskedasticity-consistent covariance matrix estimator and a direct test for heteroskedasticity." *Econometrica*,vol.,no.,pp. 817-838, 1980.

[66] E. M. Davidson, S. D. J. McArthur, J. R. McDonald, T. Cumming, and I. Watt, "Applying multi-agent system technology in practice: Automated management and analysis of SCADA and digital fault recorder data," *IEEE Trans. Power Syst.*, vol. 21, no. 2, pp. 559–567, May 2006.

[67] S. D. J. McArthur, S. M. Strachan, and G. Jahn, "The design of a multi-agent transformer condition monitoring system," *IEEE Trans. Power Syst.*, vol. 19, no. 4, pp. 1845–1852, Nov. 2004.

[68] T. Nagata and H. Sasaki, "A multi-agent approach to power system restoration," *IEEE Trans. Power Syst.*, vol. 17, no. 2, pp. 457–462, May 2002.

[69] S. E. Widergren, J. M. Roop, R. T. Guttromson, and Z. Huang, "Simu- lating the dynamic coupling of market and physical system operations," *IEEE Power Engineering Society General Meeting*, Jun. 2004, pp. 748–753.

[70] D. Koesrindartoto, S. Junjie, and L. Tesfatsion, "An agent-based com- putational laboratory for testing the economic reliability of wholesale power market designs," *IEEE Power Engineering Society General Meeting*,Jun. 2005, pp. 931–936.

[71] A. L. Dimeas and N. D. Hatziargyriou, "Operation of a multi-agent system for microgrid control," *IEEE Trans. Power Syst.* , vol. 20, no. 3, pp. 1447–1455, Aug. 2005.

[72] A. Korbik, S. D. J. McArthur, G. W. Ault, G. M. Burt, and J. R. McDonald, "Enabling active distribution networks through decentralized autonomous network management," *Proc. 18th International Conf. on Electricity Distribution (CIRED)* , Turin, Jun. 2005.

[73] D. P. Buse, P. Sun, Q. H. Wu, and J. Fitch, "Agent-based substation automation," *IEEE Power Energy Mag.*, vol. 1, no. 2, pp. 50–55, Mar./Apr. 2003.

[74] IEEE PESE Multi-Agent Systems Working group. `http://sites.ieee.org/pes-mas/`

[75] M. Wooldridge, *An introduction to multiagent systems*. John Wiley & Sons, 2009.

[76] R.E.Mackiewicz, "Overview of IEC 61850 and Benefits," *IEEE PES Power Syst. Conf. and Expo.*, vol., no., pp.623-630, Oct. 29 2006-Nov. 1 2006.

[77] J.P. Britton, and A.N. deVos, "CIM-based standards and CIM evolution," *IEEE Trans. Power Syst.* , vol.20, no.2, pp.758-764, May 2005.

[78] Foundation for Intelligent Physical Agents (FIPA), "Agent Management Specification," 2004, `http://www.fipa.org/specs/fipa00023/SC00023K.html`.

[79] J.Lopes, A., N. Hatziargyriou, J. Mutale, P. Djapic, and N. Jenkins."Integrating distributed generation into electric power systems: A review of drivers, challenges and opportunities." Elec. Power Syst. Research, vol. 77, no. pp. 1189-1203.

[80] K. Farid, R. Iravani, N. Hatziargyriou, and A. Dimeas. "Microgrids management," *IEEE Power and Energy Magazine*, vol.6, no. 3, pp. 54-65. 2008.

[81] V. C. Gungor and F. C. Lambert, "A survey on communication networks for electric system automation," *Int. Jour. Comp. and Telecom. Network*, Vol. 50 no. 7, Elsevier North-Holland, Inc. New York, NY, USA. 15 May 2006

[82] B.A. Akyol, H.Kirkham , S.L.Clements, M.D. Hadley, "A Survey of Wireless Communications for the Electric Power System," Pacific Northwest National Laboratory. Richland, Washi ngton. January 2010.

[83] T. Tran-Anh, P. Auriol, and T. Tran-Quoc, "Distribution network modeling for power line communication applications," *Int. Symp. on Power Line Communications and Its Applications*, pp. 361-365, 6-8 April 2005.

[84] X. Chunchun, B.J. Billian, L. Zhang , J.S.Tsai, R.W. Conners, V.A. Centeno, A.G, Phadke, and Y. Liu, "Power system frequency monitoring network (FNET) implementation," *IEEE Trans. Power Syst.*, vol. 20, no. 4, pp. 1914–1921, Nov.2005.

[85] E. Sortomme, S. S. Venkata, J. Mitra. "Microgrid protection using communication - assisted digital relays." *IEEE Trans. Power Del.*, 25, no. 4, pp. 2789-2796, 2010.

[86] A.G. Phadke., "Synchronized phasor measurements-a historical overview," *Proc. Transmission and Distribution Conf. and Exhibit. 2002: Asia Pacific.* IEEE/PES,vol.1, pp.476–479. 2002.

[87] Yi Deng; Hua Lin; Phadke, A.G.; Shukla, S.; Thorp, J.S.; Mili, L., "Communication network modeling and simulation for Wide Area Measurement applications," *Innovative Smart Grid Technologies (ISGT), 2012 IEEE PES* , 16-20 Jan. 2012.

[88] S.A. Rasheed, K. Masnoon, N. Thanthry, R.Pendse, "PCF vs DCF: a performance comparison," *Proc. Thirty-Sixth Southeastern Symposium on System Theory.* pp. 215–219. 2004.

[89] B.Carpenter and K.Nichols, "Differentiated services in the Internet." *Proc. of the IEEE* , vol. 90, pp.1479-1494,2002.

[90] C. Zhu, O. W. W. Yang, J. Aweya, M. Ouellette; D.Y. Montuno, "A Comparison of Active Queue Management Algorithms Using the OPNET Modeler," vol. 40, no. 6, pp. 158-167. 2002.

[91] S. Shukla, and L. Mili, "A hierarchical decentralized coordinated voltage instability detection scheme for SVC," *North American Power Symposium (NAPS)*, vol., no., pp.1-6, 4-6 Oct. 2015.

[92] S.Shukla, and L.Mili, "Hierarchical Decentralized Control for Enhanced Rotor Angle and Voltage Stability of Large-Scale Power Systems," under review, *IEEE Trans. Power Syst.*

[93] S. Shukla, Yi Deng, S. Shukla, and L. Mili, "Construction of a microgrid communication network," *IEEE ISGT 2014 conf.*, Washington, DC, 2014, pp. 1-5.

[94] H. Mehrjerdi, S. Lefebvre, M. Saad M, and D. Asber,,"Coordinated Control Strategy Considering Effect of Neighborhood Compensation for Voltage Improvement in Transmission Systems," *IEEE Trans. Power Syst.* , vol.28, no.4, pp.4507-4515, Nov. 2013.

[95] H.F.Wang, "Multi-agent co-ordination for the secondary voltage control in power-system contingencies," *Proc. IEE Generation, Transmission and Distribution*, vol.148, no.1, pp.61-66, Jan 2001.

[96] H. F. Wang, H. Li, and H. Chen, "Coordinated secondary voltage control to eliminate voltage violations in power system contingencies," *IEEE Trans. Power Syst.*, vol.18, no.2, pp.588-595, May 2003.

[97] D. Ernst, M. Glavic, and L. Wehenkel, "Power systems stability control: reinforcement learning framework," *IEEE Trans. Power Syst.* , vol.19, no.1, pp.427-435, Feb. 2004.

[98] J.O. Rawlings, S.G. Pantula, and D.A. Dickey, *Applied regression analysis: a research tool*, Springer Science & Business Media, NY, 2001 Apr 6.

[99] "Conjugate Families," available online at `https://fisher.osu.edu/~schroeder.9/AMIS900/ech6.pdf`

[100] Available online at: `https://www.mathworks.com/matlabcentral/fileexchange/52385-power-system-toolbox`

[101] H. Li, A. Bose, and V. M. Venkatasubramanian, "Wide-area voltage monitoring and optimization," *IEEE Trans. Smart Grid*, vol. 7, no. 2, pp. 785-793, March 2016.

[102] B.F.Green Jr., and J.W. Tukey, "Complex analyses of variance: general problems," *Psychometrika*, vol.25, no.2, pp. 127-152, Jun 1960.

[103] M.O. Williams, C.W. Rowley, I. Mezić, and I.G. Kevrekidis, "Data Fusion via Intrinsic Dynamic Variables: An Application of Data-Driven Koopman Spectral Analysis," *arXiv preprint arXiv*. 2014 Nov 20.